



HAL
open science

State of the art in large-scale soil moisture monitoring

E. Ochsner, M.H. Cosh, Richard Cuenca, H. Dorigo R., S. Draper C., Y. Hagimoto, Yann H. Kerr, M. Larson K., E.G. Njoku, E. Small E., et al.

► To cite this version:

E. Ochsner, M.H. Cosh, Richard Cuenca, H. Dorigo R., S. Draper C., et al.. State of the art in large-scale soil moisture monitoring. *Soil Science Society of America Journal*, 2013, pp.1-32. 10.2136/sssaj2013.03.0093 . ird-00913404

HAL Id: ird-00913404

<https://ird.hal.science/ird-00913404v1>

Submitted on 9 Dec 2013

HAL is a multi-disciplinary open access archive for the deposit and dissemination of scientific research documents, whether they are published or not. The documents may come from teaching and research institutions in France or abroad, or from public or private research centers.

L'archive ouverte pluridisciplinaire **HAL**, est destinée au dépôt et à la diffusion de documents scientifiques de niveau recherche, publiés ou non, émanant des établissements d'enseignement et de recherche français ou étrangers, des laboratoires publics ou privés.



**STATE OF THE ART IN LARGE-SCALE SOIL MOISTURE
MONITORING**

Journal:	<i>Soil Science Society of America Journal</i>
Manuscript ID:	S-2013-03-0093-IR.R1
Manuscript Type:	Invited Review
Keywords:	soil moisture, monitoring

SCHOLARONE™
Manuscripts

Review Only

STATE OF THE ART IN LARGE-SCALE SOIL MOISTURE MONITORING

Formatted: Indent: First line: 0.5"

ABSTRACT

Soil moisture is an essential climate variable influencing land-atmosphere interactions, an essential hydrologic variable impacting rainfall-runoff processes, an essential ecological variable regulating net ecosystem exchange, and an essential agricultural variable constraining food security. Large-scale soil moisture monitoring has advanced in recent years creating opportunities to transform scientific understanding of soil moisture and related processes. These advances are being driven by researchers from a broad range of disciplines, but this complicates collaboration and communication. And, for some applications, the science required to utilize large-scale soil moisture data is poorly developed. In this review, we describe the state of the art in large-scale soil moisture monitoring and identify some critical needs for research to optimize the use of increasingly available soil moisture data. We review representative examples of 1) emerging in situ and proximal sensing techniques, 2) dedicated soil moisture remote sensing missions, 3) soil moisture monitoring networks, and 4) applications of large-scale soil moisture measurements. Significant near-term progress seems possible in the use of large-scale soil moisture data for drought monitoring. Assimilation of soil moisture data for meteorological or hydrologic forecasting also shows promise, but significant challenges related to spatial variability and model structures ~~and model errors~~ remain. Little progress has been made ~~yet~~ in the use of large-scale soil moisture observations within the context of ecological or agricultural modeling. Opportunities abound to advance the science and practice of large-scale soil moisture monitoring for the sake of improved Earth system monitoring, modeling, and forecasting.

25 The science and practice of large-scale soil moisture monitoring has entered a stage of
26 unprecedented growth with the potential to transform scientific understanding of the patterns and
27 dynamics of soil moisture and soil moisture-related processes. Large-scale soil moisture
28 monitoring may lead to improved understanding of soil moisture controls on water, energy, and
29 carbon fluxes between the land and atmosphere, resulting in improved meteorological forecasts
30 and climate projections. Soil moisture measurements are also key in assessing flooding and
31 monitoring drought. Knowledge gained from large-scale soil moisture observations can help
32 mitigate these natural hazards, yielding potentially great economic and societal benefits. Here
33 large-scale refers to spatial support scales of $>1^2 \text{ m}^2$ for an in situ sensor or spatial extents of
34 $>100^2 \text{ km}^2$ for an in situ sensor network (Crow et al., 2012; Western and Blöschl, 1999). In this
35 review areas are often enumerated in the XX^2 format to indicate the length of one side of a
36 square of the given area, e.g. $10,000 \text{ km}^2 = 100^2 \text{ km}^2$. New developments continue within the
37 realm of in situ sensors which monitor soil moisture at the point-scale, i.e., $<1^2 \text{ m}^2$ support.
38 These point-scale sensors have been reviewed recently (Dobriyal et al., 2012; Robinson et al.,
39 2008) and will not be considered here except within the context of large-scale networks. Rather,
40 this review aims to broadly describe the state of the art in large-scale soil moisture monitoring.
41 Airborne and satellite remote sensing approaches for soil moisture are also considered large-
42 scale monitoring techniques in this review.

43 To provide context, it is helpful to begin with a brief historical overview of soil moisture
44 monitoring in general. The first major technological advance in modern soil moisture
45 monitoring can be traced to the development of the neutron probe after World War II (Evelt,
46 2001). The measurement of soil moisture based on neutron thermalization first appeared in peer-
47 reviewed literature in a paper by Iowa State College (now University) soil physicists, Gardner

Formatted: Superscript

Formatted: Superscript

Formatted: Superscript

Formatted: Superscript

48 and Kirkham (1952). This technology was soon commercialized under a contract between the US
49 Army Corps of Engineers and Nuclear-Chicago Corporation, and by 1960 hundreds of neutron
50 probes were in use around the world (Evetts, 2001). The neutron probe remained the de facto
51 standard for indirect soil moisture measurement until a soil physicist and two geophysicists
52 working for the Government of Canada made a key breakthrough in using dielectric properties to
53 measure soil water (Topp et al., 1980). Despite initial skepticism from the soil science and
54 remote sensing communities (Topp, 2006), the time domain reflectometry (TDR) approach of
55 Topp et al. (1980) eventually became a dominant technology for soil moisture monitoring, and
56 created for the first time, the possibility of automated, multiplexed, unattended, in situ
57 monitoring (Baker and Allmaras, 1990). By the 1990s, the TDR technology had proven the
58 value of electromagnetic methods for monitoring soil moisture, and an avalanche of impedance
59 or capacitance type probes followed (Robinson et al., 2008). These capacitance probes typically
60 operate at frequencies much lower than the effective frequency of TDR. As a result these probes
61 are simpler and less expensive, but also less accurate than TDR (Blonquist et al., 2005). Much
62 effort has also been devoted to the development of heat dissipation (Fredlund and Wong, 1989;
63 Phene et al., 1971; Reece, 1996) and heat pulse sensors (Bristow et al., 1993; Campbell et al.,
64 1991; Heitman et al., 2003; Ochsner et al., 2003; Song et al., 1999; Tarara and Ham, 1997) for
65 soil moisture measurement with reasonable success.

66 While Canadian researchers were beginning to develop the groundbreaking TDR method,
67 scientists in the US were pioneering remote sensing of soil moisture from tower, aircraft, and
68 satellite platforms using microwave radiometers (Schmugge et al., 1974), scatterometers (Dickey
69 et al., 1974), synthetic aperture radar (Chang et al., 1980), and combined radar/radiometer
70 systems (Ulaby et al., 1983). ~~A variety of~~ Various other techniques were also introduced during

71 the same time, including methods based on polarized visible light (Curran, 1978), thermal inertia
72 (Pratt and Ellyett, 1979), and terrestrial gamma radiation (Carroll, 1981). Satellite remote
73 sensing approaches in particular have engendered much enthusiasm and interest with their
74 promise of global data coverage, leading Vinnikov et al. (1999) to speculate that, in regards to
75 long-term soil moisture monitoring, “The future obviously belongs to remote sensing of soil
76 moisture from satellites.” And, in fact, the intervening decades of research on remote sensing of
77 soil moisture are now beginning to bear fruit in terms of operational satellites for large-scale soil
78 moisture monitoring.

79 Not everyone has been content to wait for the arrival of operational soil moisture
80 satellites; rather, some have envisioned and created large-scale in situ monitoring networks for
81 soil moisture. The earliest organized networks were in the Soviet Union and used repeated
82 gravimetric sampling (Robock et al., 2000). The Illinois Climate Network was the first large-
83 scale network to use a nondestructive measurement device, the neutron probe (Hollinger and
84 Isard, 1994), while the US [Department of Agriculture \(USDA\)](#) Natural Resources
85 Conservation Service [\(NRCS\)](#) Soil Climate Analysis Network [\(SCAN\)](#) (Schaefer et al., 2007)
86 and the Oklahoma Mesonet (McPherson et al., 2007) pioneered the use of automated, unattended
87 sensors in large-scale soil moisture networks during the 1990s. Since then numerous networks
88 have emerged around the world, and have come to play vital roles in the science and practice of
89 large-scale soil moisture monitoring, not the least of which is their role in calibrating and
90 validating satellite remote sensing techniques.

91 The past ten years have witnessed the emergence of potentially transformative new soil
92 moisture technologies which are beginning to fundamentally alter the possibilities for large-scale
93 monitoring. These new methods include the cosmic-ray soil moisture observing system

94 (COSMOS), global positioning system (GPS) based techniques, and fiber optic distributed
95 temperature sensing (DTS) approaches (Larson et al., 2008; Sayde et al., 2010; Steele-Dunne et
96 al., 2010; Zreda et al., 2008). Meanwhile, the number and scope of large-scale automated soil
97 moisture monitoring networks has been steadily increasing, both in the US and around the world.
98 And, in 2009, the European Space Agency ([ESA](#)) launched the Soil Moisture Ocean Salinity
99 (SMOS) satellite, the first one designed specifically for soil moisture monitoring ([Kerr et al.,
100 2010](#)).

101 Despite these developments, many challenges remain within the realm of large-scale soil
102 moisture monitoring. The recent progress in this field has been enabled by contributions from
103 many different disciplines, and future progress will likely be interdisciplinary, as well. But,
104 staying informed about new developments can be challenging when the research is spread across
105 a broad range of science disciplines from soil science to remote sensing to geodesy to
106 meteorology. Contemporary soil physicists, whose predecessors were instrumental in birthing
107 the modern era of soil moisture monitoring, have been largely focused on development and
108 testing of point-scale measurement techniques and have perhaps not been adequately engaged in
109 advancing the science of large-scale monitoring. [Great advances have been made in satellite
110 remote sensing approaches for estimating surface soil moisture, but the coarse horizontal
111 resolution and the shallow sensing depth are significant limitations for many applications
112 \(\[Wagner et al., 2007\]\(#\)\). ~~Most importantly~~ Furthermore, the ~~basic~~ science and technology required
113 to actually use large-scale soil moisture data is relatively under-developed. There has been a
114 dearth of research investment in developing modeling and forecasting tools ~~informed~~ driven by
115 ~~large-scale~~ soil moisture data, ~~especially data~~ from ~~large-scale~~ in situ networks. \[There has also
116 been little research on the use of remotely sensed soil moisture products for applications beyond\]\(#\)](#)

117 | weather forecasting or streamflow prediction.— This was understandable in previous decades
118 | when the widespread availability of such data was a distant prospect, but the circumstances have
119 | changed. Soil moisture data are now common and may be ubiquitous in the near future.

120 | In light of these circumstances, we seek to meet the need for a cross-disciplinary state of
121 | the art review for the sake of improving communication and collaboration. We further seek to
122 | engage and mobilize the expertise of the international soil science, and specifically soil physics,
123 | community in advancing the science and practice of large-scale soil moisture monitoring. Also,
124 | we seek to highlight the pressing need to accelerate the pace of progress in the area of using
125 | large-scale soil moisture observations for advanced Earth systems monitoring, modeling, and
126 | forecasting applications. Our objectives are 1) to succinctly review the state of the art in large-
127 | scale soil moisture monitoring and 2) to identify some critical needs for research to optimize the
128 | use of increasingly available soil moisture data.

129 | This review does not aim to be comprehensive. Rather we have selected specific topics
130 | which are illustrative of the opportunities and challenges ahead. This review is organized in four
131 | primary sections: 1) emerging in situ and proximal sensing techniques, 2) dedicated soil moisture
132 | remote sensing missions, 3) soil moisture monitoring networks, and 4) applications of large-scale
133 | soil moisture measurements. In this context, “in situ” techniques are those using sensors
134 | embedded in the soil, and “proximal” techniques are those using sensors which are in close
135 | proximity to the soil, but not embedded in it. Some observations regarding primary challenges
136 | and opportunities for large-scale soil moisture monitoring are provided at the end of the review.

137

138 | **EMERGING IN SITU AND PROXIMAL SENSING TECHNIQUES**

139 | **Soil Moisture Monitoring Using Cosmic Ray Neutrons**

140 Area-average soil moisture can be measured in the field using cosmic-ray neutron
141 background radiation whose intensity in air above the land surface depends primarily on soil
142 moisture. The cosmic-ray probe integrates soil moisture over an area hundreds of meters in
143 diameter, something that would require an entire network of point measurement devices.

144 Measurements can be made using stationary probes, which provide an hourly time series of soil
145 moisture, or mobile probes, which provide snapshots in time over an area or along a line.

146 Cosmic-ray protons that impinge on the top of the atmosphere create secondary neutrons
147 that in turn produce additional neutrons, thus forming a self-propagating nucleonic cascade
148 (Simpson, 2000; Desilets and Zreda, 2001). As the secondary neutrons travel through the
149 atmosphere and then through the top few meters of the biosphere, hydrosphere and lithosphere,
150 fast neutrons are created (Desilets et al., 2010). Because fast neutrons are strongly moderated by
151 hydrogen present in the environment (Zreda et al., 2008, 2012), their measured intensities reflect
152 variations in the soil moisture (Zreda et al., 2008) and other hydrogen present at and near the
153 Earth's surface (Zreda et al., 2012; Franz et al., 2013).

154 The process of neutron moderation depends on three factors that together define the
155 neutron stopping power of a material (Zreda et al., 2012): (1) the elemental scattering cross
156 section or probability of scattering; hydrogen has a high probability of scattering a neutron; (2)
157 the logarithmic decrement of energy per collision, which characterizes how efficient each
158 collision is; hydrogen is by far the most efficient element; and (3) the number of atoms of an
159 element per unit mass of material, which is proportional to the concentration of the element and
160 to the inverse of its mass number. Because of the abundance of water in soils and hydrogen's
161 low atomic mass, hydrogen, next to oxygen and silicon, makes up a significant fraction of all

162 atoms in many soils. The extraordinarily high stopping power of hydrogen makes the cosmic-
163 ray soil moisture method work.

164 The fast neutrons that are produced in air and soil travel in all directions within and
165 between air and soil and in this way an equilibrium concentration of neutrons is established. The
166 equilibrium is shifted in response to changes in the hydrogen content of the media, which in
167 practice means changes in the amount of water on or in the soil. Adding water to soil results in
168 more efficient moderation of neutrons by the soil, causing a decrease of fast neutron intensity
169 above the soil surface. Removing water from the soil has the opposite effect. Thus, by measuring
170 the fast neutron intensity in the air the moisture content of the soil can be inferred, for example
171 using the equation of Desilets et al. (2010):

$$\theta = \frac{a_0}{(N/N_0) - a_1} - a_2 \quad [1]$$

172
173
174 which is plotted in Fig. 1. In the equation θ is the neutron-derived moisture content, N is the
175 measured neutron intensity, N_0 is the neutron intensity in air above a dry soil (this is a calibration
176 parameter obtained from independent in situ soil moisture data), and a_0 , a_1 , and a_2 are fitted
177 constants that define the shape of the calibration function. Neutron transport modeling shows that
178 the shape of the calibration function is similar for different chemical compositions of soil and
179 soil textures (Zreda et al., 2008; Desilets et al., 2010) and in presence of hydrogen pools other
180 than pore water, for example vegetation or water vapor (Franz et al., 2013; Rosolem et al., 2012).
181 Therefore, the same function can be used under different field conditions once corrections are
182 made for all pools of hydrogen (Franz et al., 2013).

183 The probe senses all hydrogen present within the distance that fast neutrons can travel in
184 soils, water, air and other materials near the land surface. That distance varies with the chemical

185 composition and density of the material, from centimeters in water through decimeters in soils to
186 hectometers in air. The support volume can be visualized as a hemisphere above the soil surface
187 placed on top of a cylinder in the soil (Fig. 2). For soil moisture measurements the diameter and
188 height of the cylinder are important. The horizontal footprint, which is defined as the area
189 around the probe from which 86% ($1-e^{-2}$) of counted neutrons arise, is a circle with a diameter of
190 660 m at sea level (Zreda et al., 2008). It decreases slightly with increasing soil moisture content
191 and with increasing atmospheric water vapor content, and it increases with decreasing air density
192 (decreasing atmospheric pressure or increasing altitude)(Zreda et al., 2012). The horizontal
193 footprint has been verified by field measurements (Zweck et al., 2011).

194 The effective depth of measurement, which is defined as the thickness of soil from which
195 86% ($1-e^{-2}$) of counted neutrons arise, depends strongly on soil moisture (Zreda et al., 2008). It
196 decreases non-linearly from about 70 cm in soils with no water to about 12 cm in saturated soils
197 and is independent of air density. The effective depth of measurement decreases with increasing
198 amount of hydrogen in other reservoirs, such as lattice water, soil organic matter or vegetation.
199 The decrease in the vertical support volume is more significant at the dry end (on the order of 10
200 cm) than at the wet end (on the order of 1 cm). The vertical footprint has not been verified
201 empirically.

202 Neutrons react with any hydrogen present near the Earth's surface. Therefore, the
203 measured neutron intensity reflects the total reservoir of neutrons present within the sensing
204 distance of the probe (Fig. 2), and hence the probe can be viewed as the total surface moisture
205 probe. The greater the concentration of hydrogen, the greater is its impact on the neutron
206 intensity. Large near-surface reservoirs of hydrogen, roughly in order of decreasing size, are: (1)
207 surface water (including snow), (2) soils, (3) lattice water and water in soil organic matter; (4)

208 vegetation, and (5) atmospheric water vapor. Because the neutron signal integrates all these
209 factors, isolation of one of these components, for example soil moisture, requires that the others
210 be: (a) constant in time, (b) if not constant, assessed independently, or (c) negligibly small. In
211 addition, the support volume (or the measurement volume) will be affected by these other
212 sources of hydrogen.

213 Calibration requires simultaneous measurements of area-average soil moisture (θ) and
214 neutron intensity (N), and solving Eq. [1] for the calibration parameter N_θ . Area-average soil
215 moisture representative of the cosmic-ray footprint is obtained by collecting numerous soil
216 samples around the cosmic-ray probe and measuring moisture content by the oven-drying
217 method (Zreda et al., 2012); other methods, such as ~~time domain reflectometry~~TDR, can be used
218 as well. The measured neutron intensities must be corrected for atmospheric water vapor and
219 pressure variations. Soil samples must be analyzed for chemical composition to correct the
220 calibration function for any additional water in mineral grains (lattice water) and in organic
221 matter present in the soil (Zreda et al., 2012). The presence of that extra water shifts the position
222 of the calibration point to the left on the calibration function (Fig. 1), which results in steeper
223 curve and thus in reduced sensitivity of neutrons to changes in soil moisture. Other sources of
224 water have a similar effect on the calibration function.

225 Measurement precision of soil moisture determination is due to neutron counting
226 statistics. The counts follow the Poisson distribution (Knoll, 2000) in which for the total number
227 of counts, N , the standard deviation is $N^{0.5}$. Thus, more counts produce better precision (~~i.e.~~
228 lower coefficient of variation), provided that the neutron intensity remains stationary over the
229 counting time. High counting rates are expected under these conditions: (1) high altitude and
230 high latitude, because the incoming cosmic-ray intensity, which is the precursor to fast neutrons,

231 increases with both (Desilets and Zreda, 2003; Desilets et al., 2006); (2) dry soil, because of the
232 inverse relation between soil moisture and neutron intensity (Fig. 1); (3) dry atmosphere, because
233 of the inverse relation between atmospheric moisture and neutron intensity (Rosolem et al.,
234 2012); (4) no vegetation; (5) low lattice and organic matter content of soil. Opposite conditions
235 will result in lower counting rates and poorer precision.

236 The accuracy of soil moisture determination depends on a few factors related to
237 calibration and the presence of other pools of hydrogen within cosmic-ray probe support volume.
238 The calibration uncertainty is due to two factors: (1) the accuracy of the independent measure of
239 area-average soil moisture, which is usually below $0.01 \text{ m}^3 \text{ m}^{-3}$; (2) the accuracy of neutron
240 count rate at the time of calibration, which is usually around 2%. (These calibration data sets can
241 be viewed at cosmos.hwr.arizona.edu.) If these were the only contributing factors, the accuracy
242 would be better than $0.01 \text{ m}^3 \text{ m}^{-3}$. But there are a few complicating factors that may lead to an
243 increase of the uncertainty. They include atmospheric water vapor, infiltration fronts, changing
244 horizontal correlation scale of soil moisture, variable vegetation, and variations in the incoming
245 cosmic-ray intensity. Corrections have been developed for these factors, but their contributions
246 to the overall uncertainty of soil moisture determination have not been assessed rigorously. At a
247 desert site near Tucson, Arizona, Franz et al. (2012) found a root mean square error (RMSE) of
248 $0.017 \text{ m}^3 \text{ m}^{-3}$ between the soil moisture estimates from a well-calibrated cosmic-ray probe and
249 the depth-weighted soil moisture average from a network of point-scale sensors distributed
250 across the probe footprint.

251 Cosmic-ray soil moisture probes are used as stationary or roving devices. Stationary
252 probes are installed above the land surface to measure and transmit neutron intensity and
253 ancillary data at user-prescribed time intervals (Zreda et al., 2012). These measurements are then

Formatted: Superscript

Formatted: Superscript

254 used, together with cosmic-ray background intensity data, to compute soil moisture. A network
255 of stationary probes, called the COsmic-ray Soil Moisture Observing System (COSMOS), ~~is~~
256 ~~beinghas been~~ installed in the USA, with the main aim to provide area-average soil moisture data
257 for atmospheric applications (Zreda et al., 2012). Data are available with one hour latency at
258 <http://cosmos.hwr.arizona.edu>. Other networks or individual probes are being installed in
259 Australia (the network named CosmOz), Germany (Rivera Villarreyes et al., 2011) and
260 elsewhere around the globe.

261 A mobile version of the cosmic-ray soil moisture probe, called COSMOS rover, is under
262 development. Its main application is mapping soil moisture over large areas from a car or an
263 aircraft; a backpack version is possible as well. The vehicle-mounted instrument is
264 approximately ten times larger than the stationary cosmic-ray probe to provide more counts
265 (better statistics) in short time as the vehicle progresses along the route. The measured neutron
266 intensity is converted to soil moisture using the usual calibration equation (Desilets et al., 2010).
267 Transects (Desilets et al., 2010) or maps (Zreda et al., 2011) of soil moisture can be produced
268 within hours or days. Such maps ~~are may prove~~ useful for many applications, including
269 calibration and validation of satellite soil moisture missions ~~like SMOS. SMOS (Kerr et al.,~~
270 ~~2010) and SMAP (Entekhabi et al., 2010).~~

271 Soil Moisture Monitoring Using Global Positioning System Signals

272 While the cosmic ray probe utilizes an existing natural “signal”, the ambient fast neutron
273 intensity, to infer soil moisture, new methods employing ~~global positioning system (GPS)~~
274 receivers utilize existing anthropogenic signals. The GPS signals follow two types of paths
275 between the satellites that transmit GPS signals and the antennas that receive them (Fig. 3).
276 Some portion of GPS signals travel directly from satellites to antennas. These direct signals are

277 optimal for navigation and geodetic purposes. Antennas also receive GPS signals that reflect off
278 the land surface, referred to as multipath by the geodetic community (Georgiadou and
279 Kleusberg, 1988). GPS satellites transmit microwave (L-band) signals (1.57542 and 1.22760
280 GHz) that are optimal for sensing water in the environment (Entekhabi et al., 2010). For bare
281 soil conditions, the reflection coefficients depend on permittivity of the soil, surface roughness,
282 and elevation angle of the reflections. Therefore, reflected GPS signals can be used to estimate
283 soil moisture, as well as other environmental parameters. GPS antennas and receivers can also
284 be mounted on satellites (Lowe et al., 2002) or on planes (Katzberg et al., 2005). The data
285 collected by these instruments are considered remote sensing observations. Alternatively, GPS
286 reflections can also be measured using antennas mounted fairly close to the land surface (Larson
287 et al., 2008; Rodriguez-Alvarez et al., 2011a), yielding a hybrid remote sensing in situ
288 observation proximal sensing technique. Ground-based GPS studies use the interference of the
289 direct and reflected GPS signals, and thus the method is often called GPS interferometric
290 reflectometry (GPS-IR).

291 For GPS-IR systems, the sensing footprint depends on (1) the height of the antenna above
292 the ground and (2) the range of satellite elevation angles used in the analysis. As satellite
293 elevation angle (E) increases, the portion of the ground that yields specular (i.e., mirror-like)
294 reflections both shrinks and moves closer to the antenna. For the case of a typical geodetic
295 antenna height of 2 m, the center of the area sensed varies from 25 m at an elevation angle of
296 $E=5^\circ$ degrees to 5 m at an elevation angle of $E=30^\circ$ degrees. Larger sampling areas can be
297 achieved by raising the antenna to heights of ~ 100 m, above which observations are complicated
298 by the GPS code lengths (Rodriguez-Alvarez et al., 2011a). As GPS is a constellation of more
299 than 30 satellites, different GPS satellites rise and set above a GPS soil moisture site throughout

300 the day. These reflections are measured from different azimuths depending on the orbital
301 characteristics of each satellite. For the best sites, more than 60 soil moisture estimates can be
302 made per day. So, the soil moisture data estimated from GPS reflections should be considered as
303 daily in temporal frequency, once averaged over an area of $\sim 1000 \text{ m}^2$ for antenna heights of 2 m
304 (Larson et al., 2008).

305 | Two methods of GPS soil moisture sensing ~~are currently being~~ have been developed. The
306 first is based on using GPS instruments designed for geodesists and surveyors. These GPS
307 instruments traditionally measure the distance between the satellites and antenna in order to
308 estimate position. However these GPS instruments also measure signal power, or signal-to-noise
309 ratio (SNR). Embedded on the direct signal effect are interference fringes caused by the reflected
310 signal being in or out of phase with respect to the direct signal. The SNR frequency is primarily
311 driven by the height of the antenna above the ground. As permittivity of the soil changes, the
312 amplitude, phase, and frequency of the SNR interferogram varies. (Larson et al., 2010;
313 Zavorotny et al., 2010). Of the three parameters, the phase of the SNR interferogram is the most
314 useful for estimating soil moisture.

315 | Chew et al (2013) demonstrated theoretically that phase varies linearly with surface soil
316 moisture. For the soils described by Hallikainen et al. (2005), the slope of this relationship does
317 not vary with soil type. For most conditions, phase provides a good estimate of average soil
318 moisture in the top 5 cm. The exception is when very wet soil overlies dry soil, for example
319 immediately following short-duration rainstorms when the wetting front has not propagated to ~ 5
320 cm (Larson et al., 2010). Estimates of soil moisture from phase have been compared to in situ
321 soil moisture measurements (Fig. 4). At grass-dominated sites with relatively low vegetation
322 | water content ($< 0.5 \text{ kg m}^{-2}$), SNR phase varies linearly with in situ soil moisture ($r^2 > 0.876$)

323 | (Larson et al., 2008; ~~and unpublished data~~ Larson et al., 2010), consistent with the theoretical
324 | analysis by as predicted by Chew et al. (2013). The vegetation at these sites is typical of many
325 | rangeland areas in the western ~~U.S.~~ US. A SNR interferogram is also affected by higher water
326 | content vegetation, for example that which exists in irrigated agricultural fields (Small et al.,
327 | 2010). Methods are being developed to retrieve surface soil moisture from SNR interferograms
328 | under these conditions.

329 | One advantage to using geodetic GPS equipment to measure soil moisture is that existing
330 | geodetic networks can provide much needed hydrologic information. The National Science
331 | Foundation's Plate Boundary Observatory (~~PBO~~) network has more than 1100 stations with
332 | effectively identical GPS instrumentation. Many of the stations are located amidst complex
333 | topography, which does not facilitate estimation of soil moisture via GPS-IR. However, soil
334 | moisture is being estimated at 59 stations with relatively simple topography. The data ~~is~~ are
335 | updated daily and ~~is~~ are available at <http://xenon.colorado.edu/portal/>.

336 | A second GPS soil moisture sensing method is also under development (Rodriguez-
337 | Alvarez et al., 2009). Similar to Larson et al. (2008), this system measures the interference
338 | pattern resulting from the combination of direct and reflected GPS signals. A dual polarization
339 | antenna measures power of the vertically- and horizontally-polarized signals separately, which is
340 | not possible using standard geodetic instrumentation. The satellite elevation angle at which
341 | reflectivity of the vertically-polarized signal approaches zero, ~~i.e.~~ i.e., the Brewster angle, varies
342 | with soil moisture (Rodriguez-Alvarez et al., 2011a). The existence of this Brewster angle
343 | yields a notch in the interference pattern. The position of the notch is then used to infer soil
344 | moisture.

345 Over a bare soil field, this technique yielded 10 soil moisture estimates over a one month
346 period; they show good agreement with those measured in situ at a depth of 5 cm (RMSE_{error} <
347 0.03 $\text{m}^3 \text{m}^{-3}$) (Rodriguez-Alvarez et al., 2009). A vegetation canopy introduces additional
348 notches to the observed interference pattern. The position and amplitude of these notches can be
349 used to infer both vegetation height and soil moisture. This approach yielded excellent estimates
350 of corn height throughout a growing season (RMSE_{error} = 6.3 cm) (Rodriguez-Alvarez et al.,
351 2011b). Even beneath a 3-m tall corn canopy, soil moisture estimates typically differed by <0.04
352 $\text{m}^3 \text{m}^{-3}$ from those measured with in situ probes at 5 cm. The main difference between these two
353 approaches is that the approach of Larson et al. (2008) uses commercially-available geodetic
354 instrumentation – which typically already exists – and can be simultaneously used to measure
355 position. The approach of Rodriguez-Alvarez et al. (2009) uses a system specifically designed
356 for environmental sensing, but it is not yet commercially-available.

Formatted: Superscript

Formatted: Superscript

358 Soil Moisture Monitoring Using Distributed Temperature Sensing

359 Much as the Larson et al. (2008) GPS-IR method repurposes commercially available GPS
360 receivers to monitor soil moisture, other researchers have sought to develop new soil moisture
361 monitoring methods using commercially available distributed temperature sensing (DTS)
362 systems. In a DTS system, an optical instrument is used to observe temperature along a
363 continuum of points within an attached optical fiber cable, typically by the principle of Raman
364 scattering (Selker et al., 2006). The spatial location corresponding to each temperature
365 measurement is determined based on the travel time of light in the fiber in a manner analogous to
366 TDR. Weiss (2003) pioneered the use of DTS systems for soil moisture monitoring by
367 successfully demonstrating the potential use of fiber optics to detect the presence of moisture in a

368 landfill cover constructed from sandy loam soil. A 120-V generator supplied current to the
369 stainless steel sheath of a buried optical fiber cable for ~ 626 s at a rate of 18.7 W m^{-1} , and the
370 corresponding spatially variable temperature rise of the cable was observed at 40-s temporal
371 resolution and 1-m spatial resolution. Analysis of the temperature rise data using the single
372 probe method (Carslaw and Jaeger, 1959) resulted in satisfactory estimates of the spatial
373 variability of soil thermal conductivity along the cable, which in turn reflected the imposed
374 spatial variability of soil moisture. However, the temperature uncertainty achieved was $\sim 0.55^\circ\text{C}$,
375 and Weiss concluded that without improvements in signal-to-noise ratio, that system would not
376 be able to resolve small changes in soil moisture above $0.06 \text{ m}^3 \text{ m}^{-3}$ for the sandy loam soil used
377 in that study.

378 The potential of using passive (unheated) DTS methods for soil moisture estimation was
379 explored by Steele-Dunne et al. (2010). Optical fiber cable was installed in a tube on the soil
380 surface and at depths of 8 and 10 cm. The soil texture was loamy sand, and the vegetation cover
381 was sparse grass. With temperatures from the upper and lower cables as time-dependent
382 boundary conditions, the temperature at the middle cable was modeled by numerical solution of
383 the 1-D heat conduction equation. A numerical search routine was used to find the thermal
384 diffusivity which produced the best agreement between the simulated and observed temperatures
385 at the 8 cm depth. The results demonstrated that the passive DTS system could detect temporal
386 changes in thermal diffusivity associated with rainfall events, but the accuracy of the diffusivity
387 estimates was hindered by uncertainties about the exact cable depths and spacings. Furthermore,
388 deriving soil moisture estimates was complicated by uncertainty and nonuniqueness in the
389 diffusivity—soil moisture relationship.

390 Sayde et al. (2010) modified the active DTS approach of Weiss (2003) by interpreting the
391 temperature rise data in terms of cumulative temperature increase, i.e., the integral of the
392 temperature rise from the beginning of heating to some specified time limit. Based on a
393 laboratory sand column experiment with 2-min, 20 W m^{-1} heat pulses, they developed an
394 empirical calibration function which fit the observed cumulative temperature increase (0 to 120
395 s) versus soil moisture data. Based on that function and the observed uncertainty in the
396 cumulative temperature increase data, the uncertainty in the soil moisture estimates would
397 increase approximately linearly from $0.001 \text{ m}^3 \text{ m}^{-3}$ when soil moisture is $0.05 \text{ m}^3 \text{ m}^{-3}$ to 0.046 m^3
398 m^{-3} when soil moisture is $0.41 \text{ m}^3 \text{ m}^{-3}$. Gil-Rodríguez et al. (2012) used the approach of Sayde
399 et al. (2010) to satisfactorily monitor the dimensions and evolution of the wetted bulb during
400 infiltration beneath a drip emitter in a laboratory column of sandy loam soil.

401 Striegl and Loheide (2012) used an active DTS approach to monitor spatial and temporal
402 dynamics of soil moisture along a 130-m transect associated with a wetland reconstruction
403 project (Fig. 5). They used a 10-min, 3 W m^{-1} heat pulse, a lower heating rate than used in
404 previous active DTS studies. They followed Sayde et al. (2010) in adopting a primarily
405 empirical calibration approach, but rather than cumulative temperature increase, they related soil
406 moisture to the average temperature rise observed from 380 to 580 s after the onset of heating. A
407 calibration function was developed by relating the observed temperature rise data to independent
408 soil moisture measurements at three points along the transect, and the resulting function had a
409 $\text{RMSE} = 0.016 \text{ m}^3 \text{ m}^{-3}$ for soil moisture $< 0.31 \text{ m}^3 \text{ m}^{-3}$ but $\text{RMSE} = 0.05 \text{ m}^3 \text{ m}^{-3}$ for wetter
410 conditions. Their system successfully monitored field scale spatiotemporal dynamics of soil
411 moisture at 2-m and 4-h resolution across a 2-month period consisting of marked wetting and
412 drying cycles (Fig. 6).

413 The passive and active DTS methods for monitoring soil moisture offer the potential for
414 unmatched spatial resolution (<1 m) in long-term soil moisture monitoring on field scale (>100
415 m) transects. These methods may in the near future greatly impact our understanding of the fine-
416 scale spatiotemporal structure of soil moisture and shed new light on the factors influencing that
417 structure. Thus far, the active DTS methods have shown more promise than passive DTS, but
418 more sophisticated data assimilation approaches for interpreting passive DTS data are in
419 development. The active DTS method is still in its infancy, and many key issues remain to be
420 addressed. None of the active DTS methods developed to date involve spatial variability in the
421 soil moisture calibration function, so heterogeneity in soil texture and bulk density could give
422 rise to appreciable uncertainties in field settings. Field installation of the optical fiber cables at
423 the desired depths with good soil contact and minimal soil disturbance is also a significant
424 challenge. Custom designed cable plows (Steele-Dunne et al., 2010) and commercial vibratory
425 plows (Striegl and Loheide, 2012) have been used with some success. The active DTS methods
426 have demonstrated good precision for low to moderate soil moisture levels, but further
427 improvements in measurement precision are needed for wet conditions. Obtaining good quality
428 temperature measurements using a DTS instrument in the field requires that thermally-stable
429 calibration baths be included in the system design. The instrument itself must also be in a
430 thermally-stable environment because sizeable errors can result from sudden changes in the
431 instrument temperature (Striegl and Loheide, 2012). The measurement principles behind DTS
432 are discussed in more detail by Selker et al. (2006), and practical aspects of DTS, including key
433 limitations and uncertainties, are described by Tyler et al. (2009).

434

435 | **DEDICATED SOIL MOISTURE REMOTE SENSING MISSIONS**

436 Remote sensing approaches for soil moisture monitoring have been investigated since
437 the 1970s, although but the first dedicated soil moisture satellite mission, measuring in the L-
438 band range (1-2 GHz), SMOS, was not launched until 2009. However, sSoil moisture estimates
439 have been are also being, nonetheless, derived retrieved from other satellite instruments not
440 specifically designed for sensing soil moisture, most notably from microwave sensors operating
441 at sub-optimal frequencies not specifically optimized for soil moisture monitoring. The
442 Advanced Microwave Scanning Radiometer for EOS (AMSR-E) instrument was carried into
443 orbit aboard the US National Aeronautics and Space Administration (NASA) Aqua satellite in
444 2002 and provided passive measurements in the C band range (~4-8 GHz) at six dual-polarized
445 frequencies until October 2011 when a problem with the rotation of the antenna ended the data
446 stream (Njoku et al., 2003). Several different retrieval algorithms have been developed to
447 retrieve soil moisture from the lowest two frequencies (6.9, 10.6 GHz) observed by AMSR-E
448 (e.g., Owe et al, 2001; Njoku et al 2003). Soil moisture information is also being retrieved from
449 active microwave sensors, specifically from Following the launch of AMSR-E, the ESA's
450 launched the Advanced Scatterometer (ASCAT), which was launched in in 2006 aboard the
451 MetOp-A meteorological satellite (and before that from ASCAT's predecessors, the ERS
452 satellites). The ERS and The ASCAT instruments are is a C-band radar scatterometers designed
453 for measuring wind speed; however soil moisture retrievals have also been developed (Bartalis et
454 al., 2007 Wagner et al., 1999). An operationally-supported, remotely-sensed soil moisture
455 product derived from the ASCAT instrument is currently available (Wagner et al., 2013).
456 Wagner et al. (2007) provided an excellent review of then-existing satellite remote sensing
457 approaches for soil moisture; here we focus on two newer satellite approaches and one airborne
458 approach.

Formatted: Left

459

460

Soil Moisture and Ocean Salinity Mission (SMOS)

461

The Soil Moisture and Ocean Salinity mission (Kerr et al., 2010), an Earth Explorer

462

Opportunity mission, was ~~successfully~~ launched on November 2, 2009; and ~~successfully~~

463

~~e~~concluded its commissioning phase in May 2010. It was developed under the leadership of the

464

~~European Space Agency (ESA)~~ with the Centre National d'Etudes Spatiales (CNES) in France

465

and the Centro para el Desarrollo Tecnológico Industrial (~~CDTI~~) in Spain.

466

Microwave radiometry at low frequencies is an established technique for estimating

467

surface soil moisture with an adequate sensitivity. The choice of L-band as the spectral range in

468

which to operate was determined from a large number of studies that demonstrated L-band has

469

high sensitivity to changes of moisture in the soil (Schmugge and Jackson, 1994) and salinity in

470

the ocean (Lagerloef, 2001). Furthermore, observations at L-band are less susceptible to

471

attenuation due to the atmosphere or the vegetation than measurements at higher frequencies

472

(Jackson and Schmugge, 1989; Jackson and Schmugge, 1991). L-band also enables a larger

473

penetration depth into the surface soil layer than is possible with shorter wavelengths

474

(Escorihuela et al., 2010).

475

Even though the L-band radiometry concept was demonstrated early by a space

476

experiment (SKYLAB) back in the 1970's, no dedicated space mission followed because

477

achieving a ~~suitable~~ ground resolution ($\leq 50\text{-}60\text{ km}$) required a prohibitive antenna size (≥ 48

478

m). The so-called interferometry design, inspired from the very large baseline antenna concept

479

(radio astronomy), made such a venture possible. Interferometry was first put forward in the

480

1980's (Levine, 1988) and validated with an airborne prototype (Levine et al., 1994; Levine et

481

al., 1990). The idea consists of deploying an array of small receivers ~~in space (located~~

Formatted: Font: Not Bold, Not All caps

Formatted: Left

482 ~~on distributed along a deployable structure) that folds for launch then unfolds in orbit. This~~
483 ~~approach enables reconstruction of, then reconstructing~~ a brightness temperature (T_B) field with a
484 resolution corresponding to the spacing between the outmost receivers. The two-dimensional
485 interferometer allows measuring T_B at several incidence angles, with full polarization. Such an
486 instrument instantaneously records a whole scene; as the satellite moves, a given point within the
487 2D field of view is observed from different view angles. The series of independent
488 measurements allows retrieving surface parameters with much improved accuracy.

Formatted: Font: Italic

Formatted: Font: Italic

489 The baseline SMOS payload is thus an L-band (1.413 GHz, 21 cm - located within the
490 protected 1400-1427 MHz band) 2D interferometric radiometer designed to provide accurate soil
491 moisture data with moderate spatial resolution. The radiometer that is Y shaped with three 4.5 m
492 arms as shown in Figure 7. SMOS is on a sun-synchronous (6 a.m. ascending) circular orbit and
493 measures the ~~T_B brightness temperature~~ emitted from the Earth at L-band over a range of
494 incidence angles (0 to 55°) across a swath of approximately 1000 km (~~covering the globe twice~~
495 ~~in less than 3 days~~) with a spatial resolution of 35 to 50 km (average is 43 km) and a maximum
496 revisit time of three days for both ascending and descending passes (Kerr et al., 2001; Kerr et al.,
497 2010). A retrieval algorithm incorporating an L-band microwave emission forward model is
498 applied to the T_B data to estimate soil moisture (Kerr et al., 2012).

499 ~~The SMOS mission originated from recognition of the need for accurate, global, soil~~
500 ~~moisture monitoring from space. Short wave radiation instruments were quickly discarded~~
501 ~~because of poor sensitivity and the negative impact of cloud cover (Kerr, 2007). Use of thermal~~
502 ~~infra red also suffered complications due to the need for accurate knowledge of forcings (Kerr,~~
503 ~~2007). Radars and synthetic aperture radar (SAR) typically suffer from low temporal resolution,~~
504 ~~often compensated by a high spatial resolution. Another limitation of these active techniques is~~

505 ~~linked to the difficulty in separating the surface roughness contribution from that of soil~~
506 ~~moisture, often requiring the “change detection approach” (Moran et al., 1998; Moran et al.,~~
507 ~~2002). Another possibility is to use scatterometers which are characterized by a lower spatial~~
508 ~~resolution but higher temporal resolution adequate for water budget monitoring. The European~~
509 ~~Remote Sensing Satellite 1 (ERS 1), European Remote Sensing Satellite 2 (ERS 2), and then~~
510 ~~MetOp scatterometers offered such opportunities (Magagi and Kerr, 1997a; Magagi and Kerr,~~
511 ~~1997b; Magagi and Kerr, 2001; Wagner et al., 2007) relying on a change detection approach, and~~
512 ~~thus not delivering absolute values. Consequently, it seemed logical to investigate passive~~
513 ~~microwaves at low frequencies as the ultimate approach to infer soil moisture from space with~~
514 ~~the caveat of lower spatial resolution. Interferometry was first put forward by D. LeVine et al. in~~
515 ~~the 1980’s (the ESTAR project) and validated with an airborne prototype (Le Vine et al., 1994;~~
516 ~~Le Vine et al., 1990). In Europe, an improved concept was next proposed to the European Space~~
517 ~~Agency (ESA): the Microwave Imaging Radiometer using Aperture Synthesis (MIRAS) concept~~
518 ~~(Goutoule, 1995). This concept has now materialized into the SMOS mission.~~

519 The SMOS data ~~have demonstrated good sensitivity and stability.~~ The data quality was
520 sufficient to allow the production – from an interferometer – of prototype global surface soil
521 moisture maps within one year after launch. It was the first time ever such maps were obtained.
522 Initially, the accuracy was relatively poor and many retrievals were not satisfactory. The data
523 were much impaired by radio frequency interference (RFI) leading to degraded measurements in
524 several areas including parts of Europe and China (Oliva et al., 2012). ~~With the help of the~~
525 ~~SMOS team, ESA and CNES took actions to reduce RFI.~~ Actions have since been taken by ESA
526 and CNES to reduce RFI. Specific RFI sources are now identified and ~~localized then their~~
527 locations are provided to ESA personnel who interact directly with the appropriate national

528 agencies. These efforts have resulted in over 215 powerful and persistent RFI sources
529 disappearing, including the US Defense Early Warning System in Northern Canada and many
530 sources in Europe. Unfortunately, the remaining number of sources in some countries is large.

531 While RFI reduction and retrieval algorithm improvements ~~efforts~~ were ongoing, ~~first~~
532 ~~attempts to use SMOS data in a variety of applications were investigated. The first topic~~
533 ~~were efforts~~ to validate the SMOS soil moisture retrievals ~~began against in situ measurements,~~
534 ~~model outputs or other remote sensing platforms. In one of the first SMOS validation studies,~~
535 ~~locally-calibrated relationships between surface soil moisture and microwave T_B allowed~~
536 ~~estimation of surface soil moisture from SMOS T_B with RMSE values ranging from 0.03 to 0.12~~
537 ~~$m^3 m^{-3}$ when compared to the 5 cm soil moisture data from eleven stations of the SMOSMANIA~~
538 ~~in situ network in France (Albergel et al., 2011). A subsequent study using 16 stations in the~~
539 ~~SMOSMANIA network and a different SMOS soil moisture retrieval produced RMSE values~~
540 ~~ranging from 0.03 to 0.08 $m^3 m^{-3}$ (Parrens et al., 2012). Across four in situ networks in the US~~
541 ~~that are approximately the size of the SMOS footprint, Jackson et al. (2012) found RMSE values~~
542 ~~for SMOS ranging from 0.03 to 0.07 $m^3 m^{-3}$. Collow et al. (2012) evaluated SMOS soil moisture~~
543 ~~retrievals against in situ soil moisture observations in Oklahoma and in the northern US and~~
544 ~~found a consistent dry bias, with SMOS soil moisture values ranging from 0.00 to 0.12 $m^3 m^{-3}$~~
545 ~~lower than the in situ data from the 5 cm depth. In the northern US, RFI from the Defense Early~~
546 ~~Warning System contributed to the bias. A dry bias for SMOS was also found by Al Bitar et al.~~
547 ~~(2012) using data from NRCS SCAN and SNOTEL in situ networks and by Albergel et al.~~
548 ~~(2012a) using data from in situ stations around the world. Understanding the causes of the~~
549 ~~apparent underestimation of surface soil moisture by SMOS. These efforts showed that SMOS~~
550 ~~soil moisture retrievals equaled or surpassed the best techniques previously available with ample~~

Formatted: Superscript

Formatted: Superscript

Formatted: Superscript

Formatted: Superscript

Formatted: Highlight

551 room for improvements (Al Bitar et al., 2012; Albergel et al., 2012a; Bircher et al., 2012;
552 Jaackson et al., 2012; Kerr et al., 2012; Leroux et al., 2012; Mecklenburg et al., 2012; Rahmoune
553 et al., 2012; Schwank et al., 2012)-in these studies is an important area of ongoing research.

554 Floods in Pakistan occurring just after the end of the commissioning phase proved that
555 SMOS was able to track such events in spite of the complex topography. The floods in the US
556 during spring 2011 were clearly seen in the SMOS data, as well as the related human activities
557 such as levee bursting. Most of the large flood events occurring since launch have been
558 monitored, and SMOS has shown its ability to provide information quickly and regularly, not
559 being hindered by either cloud cover or revisit time, at the cost of a spatial resolution which is
560 lower than optimal for this application. In several cases, the arrival of intensive rains (Yasi
561 Hurricane in Australia for instance) SMOS data enabled anticipation of flooding risks as a
562 function of soil wetness prior to the rains.

563 Currently intensive work is underway to improveOne of the primary challenges in using
564 SMOS soil moisture data is that the spatial support volume, roughly 40 km X 40 km X 5 cm, is
565 not ideal for some applications. Significant horizontal spatial variability in soil moisture is likely
566 to occur within a SMOS footprint. This sub-footprint scale soil moisture variability can
567 significantly influence catchment runoff responses (e.g. Zehe et al., 2005) and simulation of
568 latent heat flux in a land surface model (e.g. Alavi et al., 2010; Li and Avissar, 1994). Some
569 progress has been made toward deriving accurate soil moisture estimates with higher spatial
570 resolution by using SMOS data together with other data sources. the spatial resolution of the
571 SMOS retrievals. By combining SMOS data with data from the Moderate Resolution Imaging
572 Spectroradiometer, surface soil moisture estimates with 4-km resolution (Merlin et al., 2010) and
573 1-km resolution (Merlin et al., 2012; Piles et al., 2011) have been developed. with good success

574 ~~using disaggregation techniques (Merlin et al., 2010; Merlin et al., 2012). Further work is~~
575 ~~needed to refine and validate these higher resolution surface soil moisture estimates and to~~
576 ~~expand their spatial coverage beyond limited test areas.~~
577 ~~Current activities are also devoted to the estimation of water in the entire root zone with some~~
578 ~~success, to inferring a drought index, as well as to the possibilities of using SMOS for routing~~
579 ~~modeling (Pauwels et al., 2012) and for correcting space estimates of rainfall over land. Work to~~
580 ~~address science challenges affecting the SMOS data is also ongoing (Kerr et al., 2012). One may~~
581 ~~cite for instance improving knowledge of water bodies and their temporal evolution, modeling of~~
582 ~~forests, improving knowledge of soil texture on a global basis and—of course—general~~
583 ~~instrument calibration issues. Other current efforts are devoted to improving the auxiliary data~~
584 ~~sets used in retrievals (e.g. snow and frozen soils) as well as improving underlying models (e.g.~~
585 ~~dielectric permittivity, forest emissions, etc...).~~
586 ~~Currently,~~ SMOS data is freely available from different sources, depending on the type (or
587 Level) of data required. Level 1 (~~T_b~~ brightness temperatures) and Level 2 (ocean salinity over
588 oceans or soil moisture/ vegetation opacity over land) data are available ~~from ESA. The data is~~
589 ~~provided in swath mode (half orbits from pole to pole) in BinHex format and on the ISEA-49H~~
590 ~~grid. These Levels are available~~ through the ESA ([https://earth.esa.int/web/guest/missions/esa-](https://earth.esa.int/web/guest/missions/esa-operational-eo-missions/SMOS)
591 ~~operational-eo-missions/SMOS~~). Level 3 data consist of composited data over either one day
592 (~~i.e.~~ all the Level 2 data of one day in the same file), three days, ten days, or one month and
593 over the globe (either morning or afternoon passes) for soil moisture and vegetation opacity.
594 Over oceans the sampling is either daily or monthly. Level 3 data are available from the Centre
595 Aval De Traitement des données SMOS (~~CATDS~~) through an ftp site
596 (<ftp://eftp.ifremer.fr/catds/cpdc>; write to support@catds.fr to get access). ~~The data is provided in~~

Formatted: Indent: First line: 0"

Formatted: Left

597 ~~NetCDF format on the EASE grid (25km sampling). Other soil moisture products (root zone soil~~
598 ~~moisture, drought indices, etc...) will soon be available from the same site. Finally, the~~
599 ~~implementation of these Level 3 products is expected to~~may bring significant improvements,
600 particularly in the vegetation opacity retrieval using temporal information (Jacquette et al.,
601 2010). Figure 8 shows a typical monthly Level 3 soil moisture product. Note that the SMOS
602 surface soil moisture maps are global in extent but contain gaps where no soil moisture retrieval
603 is currently possible. These gaps are associated with RFI, steep topography, dense vegetation,
604 snow cover, or frozen soils.

605
606 ~~After the successful launch of SMOS, Aquarius was successfully launched on June 10~~ ←
607 ~~2011 and SMAP (see below) is scheduled to launch in 2014. These NASA missions are in a way~~
608 ~~complementary to SMOS and should also bring their yield of good results. New breakthroughs~~
609 ~~are expected either using single instrument measurements or, more likely, through synergisms~~
610 ~~with other sensors either in the optical/thermal infra-red range or with active/ passive microwave~~
611 ~~sensors. But, a lingering challenge remains. How to achieve better temporal and spatial sampling~~
612 ~~of the globe for soil moisture? The simplest approach relies on disaggregation techniques.~~
613 ~~These techniques use data from high resolution sensors to distribute soil moisture as measured by~~
614 ~~an interferometer, and successful results have been already obtained (Merlin et al., 2010; Merlin~~
615 ~~et al., 2005; Merlin et al., 2012). Recognizing the challenge of improving spatial resolution,~~
616 ~~CNES has initiated research activities whose goal is to develop a new mission which would~~
617 ~~fulfill all the SMOS requirements but with a ten times better spatial resolution and an improved~~
618 ~~sensitivity (factor of three for salinity applications), paving the way to more applications in water~~
619 ~~resources management, coastal area monitoring, basin hydrology or even thin sea ice monitoring~~

Formatted: Centered

620 ~~(Kaleschke et al., 2012). The concept, named SMOSNEXT, is based of merging spatial and~~
621 ~~temporal 2D interferometry and is currently undergoing phase 0 at CNES with a proof of concept~~
622 ~~experiment funded by the R&D program.~~

623 **Soil Moisture Active/Passive Mission (SMAP)**

624 The NASA Soil Moisture Active Passive (SMAP) mission (Entekhabi et al., 2010) is
625 scheduled to launch in October 2014. Like SMOS, the SMAP mission will utilize L-band
626 measurements to determine surface soil moisture conditions, but SMAP will feature both active
627 and passive L-band instruments, unlike SMOS which relies on passive measurements alone. The
628 SMAP measurement objective is to provide frequent, high-resolution global maps of near-
629 surface soil moisture and freeze/thaw state. These ~~measurements~~ will greatly improve ~~play a~~
630 role in improving estimates of water, energy and carbon fluxes between the land and
631 atmosphere. Observations of the timing of freeze/thaw transitions over boreal latitudes will may
632 help reduce major uncertainties in quantifying the global carbon balance. The SMAP soil
633 moisture mission requirement is to provide estimates of soil moisture at 10 km spatial resolution
634 in the top 5 cm of soil with an error of no greater than $0.04 \text{ cm}^3 \text{ cm}^{-3}$ at three-day average
635 intervals over the global land area, excluding regions of snow and ice, frozen ground,
636 mountainous topography, open water, urban areas, and vegetation with water content greater
637 than 5 kg m^{-2} (averaged over the spatial resolution scale). This level of performance will enable
638 SMAP to meet the needs of hydrometeorology and hydroclimate applications.

639 The SMAP spacecraft (Fig. 9) will carry two L-band microwave instruments: a non-
640 imaging synthetic aperture radar operating at 1.26 GHz and a digital radiometer operating at 1.41
641 GHz. The instruments share a rotating 6-meter offset-fed mesh reflector antenna that sweeps out
642 a 1000 km-wide swath. The spacecraft will operate in a 685-km polar orbit with an 8-day

643 | repeating ground track. The instrument is designed to provide ~~high resolution and high accuracy~~
644 | global maps of soil moisture ~~at 10 km resolution~~ and freeze/thaw state ~~at 3 km resolution, every~~
645 | ~~two to~~ with a maximum revisit time of three days using combined active (radar) and passive
646 | (radiometer) instruments. The radiometer incorporates ~~radio frequency interference (RFI)~~
647 | mitigation features to protect against RFI from man-made transmitters. The radiometer is
648 | designed to provide ~~high accurate~~ soil moisture ~~data accuracy~~ at moderate spatial resolutions
649 | (40 km) by measuring microwave emission from the surface. The emission is relatively
650 | insensitive to surface roughness and vegetation ~~as compared to the radar~~. The radar measures
651 | backscatter from the surface with high spatial resolution (1–3 km in high resolution mode), but is
652 | more influenced by roughness and vegetation than the radiometer. The combined radar and
653 | radiometer measurements are expected to provide soil moisture accuracy approaching
654 | radiometer-based retrievals but with intermediate spatial resolution approaching radar-based
655 | resolutions. Thus, the driving aspects of SMAP's measurement requirements include
656 | simultaneous measurement of L-band ~~T_B brightness temperature~~ and backscatter with a three-day
657 | revisit and high spatial resolution (40 km and 3 km, respectively). The combined SMAP soil
658 | moisture product will be ~~produced at 10 km resolution~~ output on a 9-km grid. Significant
659 | progress has been made towards developing a suitable soil moisture retrieval algorithm for
660 | merging the SMAP radiometer and radar data (Das et al., 2011).

661 | The planned data products for SMAP are being developed by the SMAP project and
662 | Science Definition Team and include: Level 1B and 1C instrument data (calibrated and
663 | geolocated radar backscatter cross sections and radiometer ~~T_B brightness temperatures~~); Level 2
664 | geophysical retrievals of soil moisture; Level 3 daily composites of Level 2 surface soil moisture
665 | and freeze/thaw state data; and Level 4 value-added data products that are based on assimilation

666 of SMAP data into land surface models. The SMAP Level 1 radar data products will be archived
667 and made available to the public by the Alaska Satellite Facility in Fairbanks, AK, while the
668 Level 1 radiometer and all higher level products will be made available by the National Snow
669 and Ice Data Center in Boulder, CO.

670 The Level 4 products will support key SMAP applications and address more directly the
671 driving science questions of the SMAP mission. SMAP L-band microwave measurements will
672 provide direct sensing of surface soil moisture in the top 5 cm of the soil column. However,
673 several of the key applications targeted by SMAP require knowledge of root zone soil moisture
674 (RZSM) in the top 1 m of the soil column, which is not directly measured by SMAP. The SMAP
675 Level 4 data products are designed to fill this gap and provide model-based estimates of ~~root~~
676 ~~zone soil moisture~~RZSM that are informed by and consistent with assimilated SMAP surface
677 observations. The Level 4 algorithm will use an ensemble Kalman filter to merge SMAP data
678 with soil moisture estimates from the NASA Catchment land surface model (Reichle et al.,
679 2012). Error estimates for the Level 4 soil moisture product will be generated as a by-product of
680 the data assimilation system. A Level 4 carbon product will also be produced that utilizes daily
681 soil moisture and temperature inputs with ancillary land cover classification and vegetation gross
682 primary productivity (~~GPP~~) inputs to compute the net ecosystem exchange (NEE) of carbon
683 dioxide with the atmosphere over northern (> 45°N latitude) vegetated land areas. ~~The NEE of~~
684 ~~carbon dioxide with the atmosphere is a fundamental measure of the balance between carbon~~
685 ~~uptake by vegetation GPP and carbon losses through autotrophic and heterotrophic respiration.~~
686 The SMAP Level 4 carbon product will provide regional mapped measures of NEE and
687 component carbon fluxes that are within the accuracy range of tower-based eddy covariance
688 measurement approaches.

689 **Airborne Microwave Observatory of Subcanopy and Subsurface Mission (AirMOSS)**

690 Current estimates of NEE at regional and continental scales contain such important
691 uncertainties that amongst the 11 or so models tested there could be differences of 100 percent or
692 more, and it is not always clear whether the North American ecosystem is a net sink or source for
693 carbon (Denning et al., 2005; Friedlingstein et al., 2006). Root zone soil moisture (~~RZSM~~) is
694 widely accepted to have a first-order effect on NEE (e.g. ~~Law et al., 2002~~[Suyker et al., 2003](#)), yet
695 RZSM measurements are not often available with spatial or temporal extent necessary for input
696 into regional or continental scale NEE models. Unlike the L-band missions, SMOS and SMAP,
697 which measure surface soil moisture, the AirMOSS mission is designed to measure RZSM
698 directly. The hypothesis of the NASA-funded AirMOSS project is that integrating spatially and
699 temporally resolved observations of ~~root zone soil moisture~~[RZSM](#) into ecosystem dynamics
700 models can significantly reduce the uncertainty of NEE estimates and carbon balance estimates.

701 The AirMOSS plan is to provide measurements to estimate RZSM using an ultra-high
702 frequency (UHF – also referred to as P-band) airborne radar, over representative sites of the nine
703 major North American biomes (Fig. 10). These include: boreal forest (Biome 1); temperate
704 grassland and savanna shrublands (Biome 5); temperate broadleaf and mixed forest (Biome 2);
705 temperate conifer forest east (Biome 3); temperate conifer forest west (Biome 4); Mediterranean
706 woodlands and shrublands (Biome 6); arid and xeric shrublands (Biome 7); tropical and
707 subtropical dry forest (Biome 8); and tropical and subtropical moist forest (Biome 9). These
708 radar observations will be used to retrieve ~~root zone soil moisture~~[RZSM](#), which along with other
709 ancillary data, such as topography, land cover, and various in-situ flux and soil moisture
710 observations, will provide the first comprehensive data set for understanding the processes that

711 control regional carbon and water fluxes. The public access web site for the AirMOSS project is
712 <http://airmoss.jpl.nasa.gov/>.

713 The airborne P-band radar system, flown on a NASA Gulfstream III aircraft, has a flight
714 configuration over the experimental sites of typically 100 km by 25 km made up of four flight
715 lines (Fig. 11). This represents an intermediate footprint between the flux tower observations (on
716 the order of 1 km) and regional to continental scale model simulations. ~~It should be noted that~~
717 ~~each~~ Each AirMOSS flux site also has a hydrologic modeling domain of on the order of 100 km
718 by 100 km that will be populated with the corresponding ancillary data sets to allow flexibility in
719 the flight line design. The hydrologic simulation domain is determined based on maximizing the
720 overlap of full watersheds with the actual flight domain. These watersheds are to be simulated
721 using the fully distributed, physically-based finite element model PIHM (Penn State Integrated
722 Hydrologic Model) (Qu and Duffy, 2007; Kumar et al., 2010). Carbon dioxide modeling will be
723 performed using the Ecosystem Demography (ED2) model (Moorcroft et al., 2001). Each
724 AirMOSS site has flux tower measurements for water vapor and carbon dioxide made using an
725 eddy covariance system.

726 The P-band radar operates in the 420 to 440 MHz frequency range (70 cm), with a longer
727 wavelength than typically used in the L-band missions such as SMOS or the upcoming U.S. US
728 SMAP mission ~~(next section)~~. Previous studies using similar wavelengths have shown that
729 RZSM can be computed with an absolute accuracy of better than $0.05 \text{ m}^3 \text{ m}^{-3}$ and relative
730 accuracy of 0.01 to 0.02 $\text{m}^3 \text{ m}^{-3}$ through a canopy of up to 120 Mg ha^{-1} and to soil depths of 50 to
731 100 cm, depending on the vegetation and soil water content (Moghaddam et al., 2000;
732 Moghaddam 2009). This P-band radar system has evolved from the existing Uninhabited Aerial
733 Vehicle Synthetic Aperture Radar ~~(UAVSAR)~~ subsystems, including the radio frequency

734 | electronics subsystem (~~RFES~~), the digital electronics subsystem (~~DES~~), the power subsystem,
735 | and the differential GPS subsystem. ~~In fact, the P-band radar system is mounted within the~~
736 | ~~UAVSAR platform pod on the NASA Gulfstream III thereby negating the requirement for~~
737 | ~~additional air-worthiness trials.~~ The radar backscatter coefficients are available at both 0.5 arc-
738 | second (approximately 15 m, close to the fundamental spatial resolution of the radar) and at 3
739 | arc-second (approximately 100 m), and the retrieved ~~root-zone soil moisture~~ RZSM maps will be
740 | at 3 arc-second resolution.

741 | AirMOSS flight operations began in Fall of 2012, and all sites in North America except
742 | the tropical sites (Chamela, Mexico and La Selva, Costa Rica) and the woody Savanna site
743 | (Tonzi Ranch, CA) were flown. ~~These P-band data are currently undergoing initial calibration.~~
744 | ~~However, a~~ three-band raw data image showing the spatial variation of soil moisture over the
745 | Metolius, Oregon site, along with soil roughness and vegetation effects which have not yet been
746 | removed, is shown in Fig. 12.

747

748 | **LARGE-SCALE SOIL MOISTURE MONITORING NETWORKS**

749 | Soil moisture networks with spatial extents of $>100^2$ km² are well-suited for monitoring
750 | the meteorological scale of soil moisture spatial variability as defined by Vinnikov et al. (1999)
751 | because atmospheric forcings often exhibit spatial autocorrelation lengths of 100s of km. These
752 | large-scale networks are also appropriate for studies related to basin-scale hydrology and meso-
753 | scale meteorology. Numerous smaller networks exist worldwide with spatial extents $<100^2$ km²,
754 | both within and outside the US. For example, the USDA Agricultural Research Service (~~ARS~~)
755 | has developed several soil moisture networks to enhance their experimental watershed program.
756 | Locations include the Little Washita in Oklahoma, Walnut Gulch in Arizona, Reynolds Creek in

757 Idaho, and Little River in Georgia (Jackson et al., 2010). The smaller scale networks are often
758 well-suited for watershed-scale hydrologic studies. A recent surge in the creation of these
759 smaller-scale networks has been driven by the need to validate soil moisture estimates from
760 satellites such as SMOS and SMAP. A partial list of current and planned soil moisture networks
761 with spatial extents $<100^2$ km² was provided by Crow et al. (2012).

762 **Large-Scale Soil Moisture Networks in the United States**

763 | Large-scale soil moisture networks in the U.S.-US are ~~currently~~ currently operating in a
764 variety of configurations at both national and state levels (Fig. 13, Table 1). In 1981, the Illinois
765 Water Survey began a long term program to monitor soil moisture in situ (Hollinger and Isard,
766 1994; Scott et al., 2010). This network was limited by its use of neutron probes, which required
767 significant resources to operate and maintain. These neutron probes were used to measure soil
768 moisture as frequently as twice a month. These stations were collocated with the Illinois Climate
769 Network stations as the Water and Atmospheric Resources Monitoring Program and ultimately
770 totaled 19 stations with measurements from the surface to a depth of 2 m. Beginning in 1998,
771 these stations were converted to continuously monitor soil moisture using dielectric sensors
772 (Hydra Probe, Stevens Water Monitoring Systems, Inc., Portland, OR), providing regular
773 statewide estimates of soil moisture.

774 | The next network to develop was in Oklahoma, which has become ~~an epicenter of a focal~~
775 point for mesoscale weather and climate research. The Oklahoma Mesonet was launched in 1991
776 and became fully operational in 1994, now consisting of 120 stations, with at least one station in
777 each county of Oklahoma (Brock et al., 1995; McPherson et al., 2007). Each station hosts a suite
778 of meteorological measurements, including air temperature, wind speed and direction, air
779 pressure, precipitation, and soil temperature. These stations monitor soil matric potential using

780 heat dissipation sensors (CS-229, Campbell Scientific, Inc., Logan, UT) at the 5 cm, 25 cm, and
 781 60 cm depths, with archived data from the 75 cm depth available for some sites. These matric
 782 potentials can be converted to soil moisture estimates via site- and depth-specific water retention
 783 curves (Illston et al., 2008). Recent improvement in the accuracy of the water retention curve
 784 parameters resulted in a field-validated, network-wide accuracy for the soil moisture data of
 785 $\pm 0.053 \text{ m}^3 \text{ m}^{-3}$ (Scott et al., in review). Also distributed through Oklahoma is a network of
 786 stations belonging to the Southern Great Plains (SGP) site of the US Department of Energy
 787 Atmospheric Radiation Measurement (ARM) Program (Schneider et al., 2003). This network
 788 uses the same type of sensor as the Oklahoma Mesonet. This network began in 1996 and spans
 789 portions of Oklahoma and Kansas. There are a variety of facilities administered by the ARM-
 790 SGP site including a large central facility, as well as extended and boundary facilities, hosting a
 791 variety of meteorological, surface, and soil profile measurements.

792 While the Oklahoma Mesonet was being developed, the USDA Natural Resource
 793 Conservation Service (NRCS) began a pilot soil moisture/soil temperature project to monitor
 794 these parameters on a national scale. This project developed into the Soil Climate Analysis
 795 Network (SCAN network), which now numbers approximately 180 stations across the U.S.
 796 (Schaefer et al., 2007). This network has a standardized depth profile of Hydra Probe sensors at
 797 5, 10, 20, 50, and 100 cm. A similar network to SCAN is the Climate Reference Network
 798 (CRN), operated by the National Oceanic and Atmospheric Administration (NOAA) National
 799 Climatic Data Center (Palecki and Groisman, 2011). This network commissioned 114 stations to
 800 provide a national scale weather and climate monitoring network. Soil moisture sensors are
 801 being added to these stations currently based on the SCAN configuration (Hydra Probes at 5, 10,
 802 20, 50, and 100 cm), but three profiles of sensors are installed at each site providing data in

Formatted: Not Highlight

Formatted: Not Highlight

Formatted: Not Highlight

Formatted: Superscript, Not Highlight

Formatted: Not Highlight

Formatted: Superscript, Not Highlight

Formatted: Not Highlight

803 triplicate for each depth. In addition to soil moisture, standard weather variables such as air
804 temperature, solar radiation, precipitation, and wind speed are also collected.

805 A number of other state-wide or large-scale networks have been developed since the mid
806 1990s. In 1998, the High Plains Regional Climate Center added soil moisture sensors to 14
807 Automated Weather Data Network (AWDN) stations in Nebraska. Since then sensors have been
808 added to other stations, so now there are 53 stations throughout the state monitoring soil moisture
809 on an hourly basis. These stations monitor soil moisture using impedance sensors (Theta Probe
810 ML2x, Delta-T Devices, Ltd., Cambridge, UK) at depths of 10 cm, 25 cm, 50 cm, and 100 cm
811 (Hubbard et al., 2009).

812 The North Carolina Environment and Climate Observing Network (ECONet) has been in
813 operation since 1999 when 27 stations were instrumented with Decagon ECHO probes (Weinan
814 et al., 2012). In 2003, these stations were converted to Theta Probe sensors and the network was
815 expanded to 37. Unlike most other networks, this network does not have a near-surface
816 measurement depth as these data are collected only at a 20 cm depth. The West Texas Mesonet
817 was initiated by Texas Tech University in 1999 and currently monitors soil moisture at 53
818 stations at depths of 5 cm, 20 cm, 60 cm, and 75 cm using water content reflectometers (615,
819 Campbell Scientific, Inc., Logan, UT) (Schroeder et al., 2005). In addition the network monitors
820 wind information, atmospheric pressure, solar radiation, soil temperature, precipitation, and leaf
821 wetness. The Georgia Automated Environmental Monitoring Network began in 1991
822 (Hoogenboom, 1993) and has since grown to include 81 stations. Soil moisture sensors have
823 been added to these stations at a depth of 30 cm for the purpose of agricultural and
824 meteorological monitoring. The newest large-scale soil moisture networks in the US are the
825 COSMOS and GPS-IR networks described in preceding sections of this manuscript. Additional

826 networks are on the horizon as well, including the National Ecological Observatory Network
827 (NEON) which will operate study sites in 20 eco-climatic domains throughout the U.S. in the
828 coming years (Keller et al., 2008).

829 **Large-Scale Soil Moisture Networks Outside the United States**

830 In recent years, several large-scale soil moisture monitoring networks have been
831 established outside of the US, either serving research purposes, supporting natural hazard
832 forecasting, or being an integrative part of meteorological observing systems (e.g., Calvet et al.,
833 2007). Table 1 gives an overview of known large-scale networks that are currently measuring
834 soil moisture on an operational or quasi-operational basis. No active network outside the US has
835 a spatial extent as large as that of the US national networks, but several have spatial extents and
836 densities comparable to the state level networks in the US. ~~Worth mentioning are the~~Some
837 networks, such as those in France and Mongolia, ~~that~~ were installed for validating satellite soil
838 moisture missions, and thus have a setup that allows for representing as accurately as possible
839 soil moisture variations at the spatial scale of a satellite footprint.

840 The networks described in the previous section have each been designed to meet different
841 research and operational objectives, and this has resulted in a large variety of measurement
842 setups and techniques, available metadata, data access points, and distribution policies. The first
843 action to offer a centralized access point for multiple, globally available in-situ soil moisture data
844 sets was the Global Soil Moisture Data Bank (GSMDB; Robock et al., 2000; Robock et al.,
845 2005). The GSMDB collected data sets existing at that time but did not perform any
846 harmonization of variables or data formats. The first international initiative addressing the latter
847 has been FLUXNET (Baldocchi et al., 2001), a “network of networks” dedicated to monitor
848 land-atmosphere exchange of carbon, energy, and water. Unfortunately, within FLUXNET soil

849 moisture is not measured at all sites while, more importantly, practical use of soil moisture data
850 from FLUXNET is severely hampered by restricted accessibility and the large time gap between
851 acquisition of the data and making them available to the science community.

852 In 2009, the International Soil Moisture Network (ISMN; <http://ismn.geo.tuwien.ac.at/>)
853 was initiated to overcome the issues of timeliness in data delivery, accessibility, and
854 heterogeneity of data (Dorigo et al., 2011a; Dorigo et al., 2011b). This international initiative is a
855 result of the coordinated efforts of the Global Energy and Water Cycle Experiment (~~GEWEX~~) in
856 cooperation with the Group of Earth Observation (~~GEO~~) and the Committee on Earth
857 Observation Satellites (~~CEOS~~) to support calibration and validation of soil moisture products
858 from remote sensing and land surface models, and to advance studies on the behavior of soil
859 moisture over space and time. The decisive financial incentive was given by the ~~European Space~~
860 ~~Agency (ESA)~~ who considered the establishment of the ISMN critical for optimizing the soil
861 moisture products from the SMOS mission.

862 The ISMN collects and harmonizes ground-based soil moisture data sets from a large
863 variety of individually operating networks and makes them available through a centralized data
864 portal. Currently, the database contains almost ~~6000-7000~~ soil moisture data sets from ~~almost~~
865 ~~+500~~ more than 1600 sites, distributed among ~~37-40~~ networks worldwide (Fig. 14). Not all the
866 networks are still active. Also, the data sets contained in the former GSMDB were harmonized
867 and transferred into the ISMN. ~~It should be noted that not all networks are still active.~~

868 Recently, several updates of the ISMN system were performed to keep up with the
869 increasing data amount and traffic, and to meet the requirements of advanced users. Many
870 datasets from operational networks (e.g., SCAN, the US Climate Reference Network, ~~SWEX~~
871 ~~Poland~~, and ARM) are now assimilated and processed in the ISMN on a fully automated basis in

872 | near-real time. In addition, an enhanced quality control system is ~~currently~~ being implemented
 873 | (Dorigo et al., 2013) while novel methods are being explored to obtain objective measures of
 874 | reliability and spatial representativeness of the various sites (Gruber et al., 2013).

875 | Challenges and Opportunities Related to Large-Scale Soil Moisture Networks

876 | The steadily increasing number of soil moisture monitoring stations goes hand in hand
 877 | with the growing awareness of the role of soil moisture in the climate system. Nevertheless, Figs.
 878 | 14 and 15 show that the current stations are concentrated geographically and mainly represent a
 879 | limited number of climate classes in temperate regions. The number of permanent soil moisture
 880 | stations is still very limited in the tropics (A category), dry areas (Bw classes), and in high
 881 | latitude areas (Dfc and E classes). Especially in the latter the hydrological cycle is not yet well
 882 | understood, and these regions are expected to be particularly sensitive to climate change. Thus,
 883 | international efforts should concentrate on expanding networks in these areas.

884 | However, the major challenge is not only to setup new networks but also to keep them
 885 | operational in the future. Since many networks heavily rely on project funding, their continuation
 886 | is typically only guaranteed for the lifetime of the project. Thus, internationally coordinated
 887 | effort should focus on developing mechanisms for continued financial and logistical support.

888 | One ~~of such mechanisms may be the development of a soil moisture component as part of~~ the
 889 | integration of the ISMN into the Global Terrestrial Network for Hydrology (GTN-H)
 890 | envisaged by the GCOS-Global Climate Observing System (GCOS, 2010). ~~The task of such a~~
 891 | ~~network should go beyond the achievements of the ISMN and also define standards for the~~
 892 | ~~measurements themselves in order to guarantee the consistency between sites.~~ Alternatively,
 893 | the integration of soil moisture monitoring sensors into existing operational meteorological
 894 | stations ~~would~~ may increase the probability for continued operation.

Formatted: Font: Bold

Formatted: Centered, Indent: First line: 0"

Formatted: Font: Bold

895 —Another significant challenge for in situ networks is defining standards for the
896 measurements themselves in order to enhance the consistency between sites. Best practices for
897 sensor calibration, installation, and in situ validation, as well as data quality control procedures
898 and data archiving and retrieval standards need to be developed. The Automated Weather Data
899 Network in Nebraska (Hubbard et al., 2009), the Oklahoma Mesonet (Illston et al., 2008), and
900 the ISMN (Dorigo et al., 2013) have documented, automated quality control procedures in place
901 which may prove useful for other networks. The Oklahoma Mesonet soil moisture network has
902 also been subjected to in situ validation by soil sampling (Illston et al., 2008; Scott et al. in
903 review), allowing quantitative estimates of the accuracy of the soil moisture data. Calibration
904 and validation are two separate and necessary steps in measurement. Calibration here means
905 developing a relationship between the sensor output and the true soil moisture value. Validation
906 here means collecting independent soil moisture data in situ after sensor installation to quantify
907 the accuracy of the calibrated and installed sensor. Such in situ validation is needed for all
908 networks.

Formatted: Indent: First line: 0.5"

910 APPLICATIONS OF LARGE-SCALE SOIL MOISTURE MEASUREMENTS

911 Drought Monitoring

912 Droughts are typically classified as ~~either~~ meteorological, agricultural, or hydrological
913 (Mishra and Singh, 2010). Meteorological drought is indicated by a lack of precipitation over a
914 specified region during a particular period of time. Agricultural drought occurs when declining
915 soil moisture levels negatively impact agricultural production. Some have used the term
916 “ecological drought” to designate similar conditions which reduce primary productivity in
917 natural ecosystems (Le Houérou, 1996). These two drought concepts are closely related and

918 | should perhaps be represented by the composite term “agro-ecological drought.” A third
919 | common drought classification is hydrological drought, which is a period of inadequate surface
920 | and subsurface water resources to support established water uses. Soil moisture is most directly
921 | related to agro-ecological drought, which is often preceded by meteorological drought and comes
922 | before hydrological drought. This places soil moisture squarely in the center of the spectrum of
923 | drought classifications and drought indicators, but soil moisture measurements have been largely
924 | neglected in the science and practice of drought monitoring to date.

925 | In earlier decades this deficiency was unavoidable because sufficient soil moisture data
926 | were simply not available to enable their use in operational drought monitoring. That situation
927 | began to change dramatically in the 1990s with the rise of large-scale soil moisture monitoring
928 | networks in the US (Hollinger and Isard, 1994; McPherson et al., 2007; Schaefer et al., 2007), a
929 | change now spreading around the world. Even more recently, global maps of surface soil
930 | moisture based on satellite remote sensing have become available, and these could be useful in
931 | drought monitoring. The primary impediment to the use of soil moisture measurements in
932 | operational drought monitoring is no longer a lack of data, but rather a lack of scientific
933 | understanding regarding how soil moisture measurements quantitatively indicate agro-ecological
934 | drought. Strong and transparent conceptual models are needed to link soil moisture
935 | measurements with vegetation impacts in agricultural and ecological systems.

936 | The first known attempt to use large-scale soil moisture measurements in drought
937 | monitoring was the Soil Moisture Index (SMI) introduced by Sridhar et al. (2008) based on data
938 | from the Automated Weather Data Network (AWDN) in Nebraska. Their results demonstrated
939 | that continuous soil moisture data-measurements at 10, 25, 50, and 100 cm depths from 37

940 stations in Nebraska ~~provided~~ formed the basis for a strong quantitative drought indicator. The
 941 SMI was subsequently revised by Hunt et al. (2009) who proposed the following relationship

$$942 \quad SMI = -5 + 10F_{AW} \quad [2]$$

943 where F_{AW} is the fraction of available water. Fraction of available water is calculated by

$$944 \quad F_{AW} = (\theta - \theta_{wp}) / (\theta_{fc} - \theta_{wp}) \quad [3]$$

945 where θ is the volumetric water content at a specified depth, θ_{fc} is the volumetric water content
 946 corresponding to field capacity, and θ_{wp} is the volumetric water content corresponding to

947 permanent wilting point. Hunt et al. (2009) calculated SMI using data from sensors at 10, 25,
 948 and 50 cm depths, and then calculated the average SMI across depths.

949 The use of F_{AW} as the basis for SMI is substantiated by current scientific understanding
 950 of plant water stress because water stress is more strongly related to the relative amount of plant
 951 available water in the soil than to the absolute amount of soil moisture (Allen et al., 1998).

952 Values of F_{AW} are typically between 0 and 1, however both higher and lower values are possible.

953 The scaling relationship in Eq. [2] thus causes SMI values to typically fall in the range from -5 to

954 +5. This scaling was ~~perhaps~~ chosen to make the range of SMI comparable to the range of other

955 drought indicators (e.g., Drought Monitor, Palmer Drought Severity Index; Svoboda et al.,

956 2002, Palmer, 1965). Although stress thresholds vary somewhat with plant species and weather

957 conditions, generally F_{AW} values < 0.5 result in water stress (Allen et al., 1998). When F_{AW} is

958 0.5, the SMI value is 0, the transition between stressed and non-stressed conditions. Again using

959 data from the Nebraska AWDN, Hunt et al. (2009) found that the modified SMI was effective for

960 identifying drought onset as well as soil recharge from rainfall events following significant dry

961 periods.

Formatted: Indent: First line: 0.5"

962 Recently, the SMI was applied using ~~data~~ [daily measurements of soil moisture in the 0-50](#)
963 [cm depth layer](#) from a network of six monitoring stations in the Czech Republic (Mozny et al.,
964 2012). That study supported the drought intensity scheme proposed by Sridhar et al. (Sridhar et
965 al., 2008) in which SMI values < -3 signify severe or extreme drought. Mozny et al. (Mozny et
966 al., 2012) related the concept of “flash drought” to SMI, specifying that a flash drought occurs
967 when SMI values decrease by at least 5 units during a period of 3 weeks. Thus, the SMI concept
968 has shown good potential as a quantitative drought indicator based on soil moisture
969 measurements, but some key uncertainties remain. The indicator is sensitive to the site- and
970 depth-specific values chosen for θ_{fc} and θ_{wp} . These critical water contents can be estimated from
971 the in situ soil moisture time series in some cases (Hunt et al., 2009), measured directly in the
972 laboratory, calculated using pedotransfer function models (Schaap et al., 2001), or estimated
973 from literature values (Sridhar et al., 2008), but best practices for determining these parameters
974 in the SMI context need to be developed.

975 Recently, Torres et al. (2013) introduced a method for using long-term measurements of
976 soil water deficits (SWD) from a large-scale monitoring network to compute site-specific
977 drought probabilities as a function of day of year. Improved quantification of seasonal patterns
978 in drought probability may allow crop cycles to be better matched with periods when drought is
979 less likely to occur; therefore, yield losses due to drought may be reduced. Soil water deficit for
980 each soil layer (D) is defined as

$$981 \quad D = (\theta_{fc} - \theta)\Delta z \quad [4]$$

982 where Δz is the thickness of the soil layer, and SWD is calculated by summing D over the
983 desired soil layers. Soil moisture data from eight stations of the Oklahoma Mesonet spanning 15
984 years were used to calculate deficits for the 0-10 cm, 10-40 cm, and 40-80 cm layers. Drought

985 was defined in this context as a period when SWD is sufficient to cause plant water stress,
 986 i.e., SWD exceeds a predetermined threshold. The threshold was set for each site and layer as
 987 0.5TAW, where TAW is the total available water calculated by substituting θ_{wp} for θ in Eq. [4].
 988 Values of SWD calculated from 0-40 cm (SWD₄₀) were similar to 7-d cumulative atmospheric
 989 water deficits (AWD), calculated as reference evapotranspiration minus precipitation, during
 990 much of the spring and fall, but the soil and atmospheric deficits diverged in the winter and
 991 summer months (Fig. 16).

992 Historical drought probabilities estimated for each day of the year using the SWD data
 993 were consistent between depths and agreed with general knowledge about the climate of the
 994 region (Fig. 17), while probabilities estimated using AWD data (Purcell et al., 2003) were
 995 substantially lower and inconsistent with general knowledge about the region and with prior
 996 drought probability estimates in nearby states. Torres et al. (2013) proposed modifications to the
 997 AWD method, either lowering the AWD threshold used to define drought or extending the
 998 summation period from 7 to 15 days, both of which resulted in drought probability estimates
 999 more consistent with the estimates from SWD method. They concluded that the new SWD
 1000 method gave plausible and consistent results when applied to both the 0- to 40- and 0- to 80-cm
 1001 soil layers and should be utilized when long-term soil moisture data are available.

1002 The first known operational use of large-scale soil moisture measurements for drought
 1003 monitoring involves, not SMI or SWD, but a related measure, plant available water (PAW).

1004 Plant available water is defined as

$$1005 \quad PAW = \sum_{i=1}^n (\theta_i - \theta_{wp_i}) dz_i \quad [5]$$

1006 for soil layers $i=1 \dots n$ of thickness dz_i . In 2012, the Oklahoma Mesonet (McPherson et al., 2007)
 1007 introduced daily-updated PAW maps based on its network of >100 stations monitoring soil

1008 moisture at standard depths of 5, 25, and 60 cm. These maps are intended for use in drought
1009 monitoring and show PAW for the 0-10 cm (4-inch), 0-40 cm (16-inch), and 0-80 cm (32-inch)
1010 soil layers (http://www.mesonet.org/index.php/weather/category/soil_moisture_temperature).

1011 The depth units (e.g., mm or inches) of PAW make it compatible with familiar hydrologic
1012 measurements such as precipitation and evapotranspiration (ET). Figure 18 shows maps of
1013 departure from average PAW for the 0-16 inch (40 cm) soil layer across Oklahoma for the
1014 months of May 2012 and May 2013. The maps show that significantly drier than average PAW
1015 conditions prevailed across large areas of central and eastern Oklahoma in May 2012 but
1016 significantly wetter than average PAW conditions covered much of the State in May 2013.
1017 These soil moisture patterns bear little resemblance to US Drought Monitor (Svoboda et al.,
1018 2002) maps from the same time periods (Fig. 18c,d), which suggest that drought conditions were
1019 substantially worse in May 2013 than May 2012 across the entire State. These maps illustrate
1020 that a drought indicator based on large-scale soil moisture monitoring can provide a dramatically
1021 different assessment of drought severity than the Drought Monitor, which blends information
1022 from meteorological indicators, streamflow percentiles, a soil moisture model, and expert
1023 opinion.

1024 ~~total rainfall, total short-crop reference ET based on the FAO-56 procedure (Allen et al., 1998),~~
1025 ~~and average PAW across the state of Oklahoma during May 2012. Dry conditions prevailed~~
1026 ~~across the state with reference ET exceeding rainfall at all measured locations. The PAW map~~
1027 ~~reflects the influence of rainfall and ET with relatively high PAW values in eastern, northeastern,~~
1028 ~~and central OK corresponding to regions with relatively high rainfall and/or relatively low~~
1029 ~~reference ET. However, the PAW maps also suggest more complex influences of vegetation,~~
1030 ~~soil type, and landscape “memory”. For example, note that PAW values were generally lower in~~

1031 ~~the southwest portion of the state than in the Panhandle region even though the Panhandle region~~
1032 ~~experienced lower rainfall totals and comparable reference ET. This illustrates the challenges~~
1033 ~~with using atmospheric data alone to monitor agro-ecological drought and suggests a unique and~~
1034 ~~complementary role for soil moisture measurements.~~

1035 These recent developments in the use of soil moisture measurements for drought
1036 monitoring are encouraging; however the research needs in this area are significant. As yet, little
1037 is known regarding how soil moisture-based drought indicators relate to other widely-accepted
1038 drought indicators like the Standardized Precipitation Index (Guttman, 1999) or the Palmer
1039 Drought Severity Index. Likewise, we do not know how soil moisture-based drought indicators
1040 are related to actual drought impacts in agricultural or ecological systems. Already SMI, SWD,
1041 and PAW have demonstrated potential as soil moisture-based drought indicators driven by in situ
1042 measurements, ~~but these three indicators all address the question, “How dry is it?” rather than the~~
1043 ~~equally important question, “How much drier than average is it?”~~. Other soil moisture-based
1044 indicators have been proposed on the basis of numerical modeling studies. These include the
1045 model-based Normalized Soil Moisture index (Peled et al., 2010) and the Soil Moisture Deficit
1046 Index (Narasimhan and Srinivasan, 2005), neither of which has been evaluated using actual soil
1047 moisture measurements.

1048 Furthermore, most in situ soil moisture measurements are made under grassland
1049 vegetation because of problems with establishing long-term meteorological stations in cropland
1050 or forest. There is a dearth of research on how to estimate soil moisture under contrasting land
1051 use/land cover combinations based on in situ observations under grassland vegetation. This
1052 deficiency complicates the interpretation of agro-ecological drought indicators based on in situ
1053 soil moisture measurements. Clearly, there should be a role for satellite remote sensing of soil

1054 moisture to assist in overcoming some of the deficiencies of drought monitoring by in situ soil
1055 moisture observations. Bolten et al. (2010) showed that ~~AMSR-E~~ ~~AMSR-E~~ surface soil
1056 moisture retrievals could add significant value to ~~root zone soil moisture~~ RZSM predictions in an
1057 operational drought modeling framework. Soil moisture data from AMSR-E have also shown
1058 potential as part of an integrated drought monitoring system for East Africa (Anderson et al.,
1059 2012)-. However, there are as yet no operational systems for drought monitoring that utilize
1060 satellite soil moisture measurements. We anticipate a surge in this type of research in the near
1061 future.

1062 1063 **Meteorological Modeling and Forecasting**

1064 Drought provides a clear example of the interaction between the atmosphere and the land
1065 surface, an interaction strongly influenced by the soil moisture conditions. A schematic of
1066 atmospheric boundary layer (ABL) interactions with the land surface is presented in Fig. 19.
1067 Daytime growth of the ABL is directly affected by soil and vegetation states and processes, and
1068 these processes play a role in partitioning the energy balance which relates net radiation to soil
1069 heat flux, sensible heat flux, and latent heat flux, i.e., evapotranspiration. Root-zone soil
1070 moisture can influence the ~~atmospheric boundary layer~~ ABL by controlling land surface energy
1071 and moisture fluxes. -For example, Basara and Crawford (2002) found that soil water content in
1072 the root-zone, particularly the 20 to 60 cm depths, during the summer was linearly correlated
1073 with daytime evaporative fraction and daily-maximum values of sensible heat flux and latent
1074 heat flux on days with strong radiative forcing and weak shear in the lower troposphere. Root-
1075 zone soil moisture was also linearly related to key parameters in the ABL such as the daily
1076 maximum air temperature at 1.5 m.

1077 Numerous large-scale hydrologic-atmospheric-remote sensing experiments have been
1078 conducted to better understand the soil moisture-moderated interactions of the soil-vegetation
1079 system with the diurnal ~~atmospheric boundary layer~~ABL. Improved parameterization of general
1080 circulation models (~~GCMs~~) was one of the initial objectives of the experiments. Table 2 gives a
1081 concise overview of a few of these experiments, including HAPEX-MOBILHY which was the
1082 first experiment conducted on this scale (André et al, 1986; André et al., 1988). ~~It should be~~
1083 ~~noted in~~Most of the experiments listed cover large geographic areas which play a significant
1084 roles in the general circulation system of the planet.

1085 The strong linkage of surface soil moisture and parameterization of soil hydraulic
1086 processes with ABL response was demonstrated by Ek and Cuenca (1994), based on data from
1087 the HAPEX-MOBILHY. This study found that variations in soil hydraulic process
1088 parameterization could have a clear impact on the simulated surface energy budget and
1089 ~~atmospheric boundary layer~~ABL development. This impact was accentuated for dry to moderate
1090 soil moisture conditions with bare soils. Ek continued to do considerable work in the area of
1091 simulation of the ABL and the influence of soil moisture conditions, often using data from
1092 regional experiments such as HAPEX-MOBILHY and the Cabauw data set from the Netherlands
1093 (Monna and van der Vliet, 1987). Data from HAPEX-MOBILHY ~~were~~ used to evaluate the
1094 evolution of the relative humidity profile in the ABL in Ek and Mahrt (1994). The relationships
1095 between canopy conductance, root density, soil moisture and soil heat flux with simulation of the
1096 ABL using the Cabauw data set was investigated in Ek and Holtslag (2004). ~~It should be noted~~
1097 ~~that~~The ABL simulation evolved from the Oregon State University 1-D planetary boundary-
1098 layer model (OSU1DPBL) (Mahrt and Pan, 1984; Pan and Mahrt, 1987) to the Coupled
1099 Atmospheric boundary layer-Plant-Soil (CAPS) model. These models in turn are the basis for

1100 the Noah land-surface model (Chen and Dudhia, 2001; Ek et al., 2003) which plays a major role
1101 in the Medium-Range Forecast Model for numerical weather prediction (NWP) at the NOAA
1102 National Center for Environmental Prediction.

1103 Given its influence on ABL development, ~~root-zone soil moisture~~RZSM can have a
1104 strong influence on weather forecasts. If not suitably constrained, the ~~root-zone soil~~
1105 ~~moisture~~RZSM in ~~a an atmospheric~~NWP model will drift from the true climate, resulting in
1106 erroneous boundary layer forecasts (Drusch and Viterbo, 2007). ~~Root-zone soil moisture cannot~~
1107 ~~currently be observed at the spatial scales required by NWP, and~~ ~~S~~since the mid 1990s, many
1108 NWP centers have been indirectly constraining their model soil moisture using methods that
1109 minimize the errors in measured screen-level (1.5-2.0 m) temperature and humidity (Best et al
1110 2007; Hess, 2001; Mahfouf 1991; Mahfouf et al 2009). While this approach reduces boundary
1111 layer forecast errors, it does not generate realistic soil moisture since the latter is often adjusted
1112 to compensate for model errors unrelated to soil moisture (Douville et al., 2000; Drusch and
1113 Viterbo, 2007; Hess, 2001). Ultimately a model with inaccurate soil moisture cannot accurately
1114 describe the atmosphere across the full range of forecast lengths produced from NWP models.

1115 Hence, the NWP community has been working towards improving model soil moisture
1116 by assimilating remotely sensed near-surface soil moisture. Near-surface soil moisture is more
1117 directly related to ~~root-zone soil moisture~~RZSM than screen-level variables, and assimilating
1118 near-surface soil moisture data (0 to 5 cm) has been shown to improve model ~~root-zone soil~~
1119 ~~moisture~~RZSM (Calvet et al., 1998; Hoeben and Troch, 2000; Montaldo et al., 2001). Figure 20
1120 compares several experiments constraining model ~~root-zone soil moisture~~RZSM by assimilating
1121 observations of near-surface soil moisture and screen-level temperature and relative humidity,
1122 highlighting the fundamental difference between these two approaches. These experiments were

1123 conducted with Météo-France's NWP land surface model using an ~~Extended-extended~~ Kalman
1124 ~~Filter-filter~~ and the ~~Advanced Microwave Scanning Radiometer for the Earth Observing System~~
1125 ~~(AMSR-E)~~ Land Parameter Retrieval Model near-surface soil moisture data (Owe et al.,
1126 ~~2008~~2001). Refer to Draper et al. (2011) for further details.

1127 In general, assimilating the screen-level observations (~~black dashed line~~) improved the fit
1128 between the mean forecast and observed screen-level variables, compared to the open loop (~~no~~
1129 ~~assimilation, solid black line~~). However, the assimilation had a slight negative impact on the fit
1130 between the mean forecast and observed near-surface soil moisture. In contrast, assimilating the
1131 AMSR-E soil moisture (~~grey solid line~~) improved the fit between the mean forecast and observed
1132 near-surface soil moisture, while degrading the fit between the modeled and observed screen-
1133 level variables. This result is consistent with previous studies showing that adjusting model soil
1134 moisture to improve screen-level forecasts does not necessarily improve soil moisture (Douville
1135 et al, 2000; Drusch and Viterbo, 2007; -Seuffert et al 2004), and conversely improving the model
1136 soil moisture does not necessarily improve atmospheric forecasts (Seuffert et al 2004).
1137 Consequently, in the foreseeable future it is unlikely that remotely sensed near-surface soil
1138 moisture will be used in NWP in place of screen-level observations. However, combining the
1139 assimilation of both observation types can reduce errors in both model soil moisture and low-
1140 level atmospheric forecasts. For example, when both data types were assimilated together (~~Fig.~~
1141 ~~20~~) (~~grey dashed line~~) in Fig. 20, the fit between the model and both observation types was
1142 improved, although the mean soil moisture improvements were very small (see also Seuffert et
1143 al, 2004).

1144 Currently near-surface soil moisture observations are assimilated operationally at the UK
1145 Met Office (UKMO) and the European Centre for Medium Range Weather Forecasting

1146 (ECMWF). While the development of soil moisture assimilation in NWP is motivated by the
1147 eventual use of L-band observations (e.g., SMOS and SMAP), both centers are currently
1148 assimilating ~~Advanced Scatterometer (ASCAT)~~ Surface Degree of Saturation (SDS) data
1149 (Bartalis et al, 2007), and since this is currently the only operationally-supported remotely sensed
1150 soil moisture product with global coverage. At ~~the~~ UKMO the screen-level observation based
1151 soil moisture analysis was amended in July 2010, to also constrain the near-surface soil moisture
1152 by nudging it with ASCAT SDS data (Dharssi et al, 2011). Compared to nudging with only
1153 screen-level observations, adding the ASCAT data very slightly improved near-surface soil
1154 moisture forecasts over selected sites in the US, while also improving screen level temperature
1155 and relative humidity forecasts over the tropics and Australia (with neutral impact elsewhere).
1156 At ~~ECMWF~~ the NWP ~~land surface~~ analysis was updated in November 2010, to an extended
1157 Kalman filter based scheme, enabling the assimilation of remotely sensed data (de Rosnay et al
1158 2012, Drusch et al 2009). The ASCAT SDS are not used in their weather forecasting model, but
1159 are assimilated together with screen-level observations in an offline land surface analysis system.
1160 Including the ASCAT data in this system has had a neutral impact on near-surface soil moisture
1161 and screen-level forecasts (Albergel et al 2012b; de Rosnay et al, 2012).

1162 The above examples highlight some challenges of land data assimilation specific to NWP
1163 applications. For example, the computation cost of the assimilation is a major limitation in NWP
1164 (de Rosnay et al 2012, Drusch et al 2009), hence the assimilation methods applied must be
1165 relatively simple. Further work is required to improve the land surface analysis schemes used in
1166 NWP, and in particular to propagate the surface soil moisture information into the root-zone (not
1167 currently achieved by the schemes in place at the UKMO or ECMWF). Additionally, Dharssi et
1168 al. (2011) and de Rosnay et al. (2012) identified the observation bias correction strategy, i.e.

1169 the method by which satellite derived surface soil moisture values are adjusted to be consistent
1170 with the model used for assimilation, as a likely cause of the limited impact of assimilating the
1171 ASCAT data. Bias correction of remotely sensed soil moisture is difficult in NWP, since the long
1172 data records required to estimate statistics of the model climatology are not available from NWP
1173 models, due to frequent model updates and the prohibitive cost of rerunning models.

1174 However, the greatest challenge faced by soil moisture assimilation in NWP is that
1175 improving the model soil moisture may not immediately improve atmospheric forecasts, due to
1176 errors in the model physics. It is likely that the greatest contribution of using remotely sensed
1177 near-surface soil moisture observations in NWP will be in helping to identify and address these
1178 physics errors. Already, the availability of remotely sensed soil moisture and efforts to
1179 assimilate that data have stimulated improvements in modeling soil moisture processes. For
1180 example, in response to discrepancies between modeled and SMOS observed $T_{B, \text{brightness}}$
1181 ~~temperatures~~, ECMWF recently improved their bare soil evaporation parameterization, resulting
1182 in improved model near-surface soil moisture and $T_{B, \text{brightness temperature}}$ (Albergel et al,
1183 2012b). As soil moisture data is used more extensively in NWP models, this should also help to
1184 expose and eventually address other errors in the model surface flux processes.

1185 **Ecological Modeling and Forecasting**

1186 Ecological modeling is another area which could logically benefit from increased
1187 availability of large-scale soil moisture monitoring. Soil moisture is a key parameter in the
1188 control of plant growth, soil respiration, and distribution of plant functional types in terrestrial
1189 ecosystems (Blyth et al. 2010; Ren et al. 2008; Pan et al. 1998; Neilson 1995). Plant growth
1190 (~~i.e.~~, assimilation of CO_2 through photosynthesis) is coupled with water loss through
1191 transpiration which is regulated by soil water availability (Yang et al. 2011; Sellers et al. 1997;

Formatted: Subscript

1192 Field et al., 1995). Decomposition of soil organic carbon is also sensitive to soil moisture
1193 content via microbial activity and other processes (Ise and Moorcroft 2006; Xu et al. 2004;
1194 Orchard and Cook 1983). Furthermore, temporal and spatial availability of soil moisture content
1195 constrains distribution and properties of plant functional types (Bremond, Boom, and Favier
1196 2012; Seneviratne et al. 2010; Gerten et al. 2004; Breshears and Barnes 1999).

1197 A striking example of the interactions between vegetation and soil moisture conditions is
1198 provided by the Tiger Bush sites in the HAPEX-Sahel experiment. The Tiger Bush is made up
1199 of relatively long and narrow patches of vegetation approximately 40-m wide separated by
1200 nearly cemented patches of bare soil approximately 60-m wide and these sites are characteristic
1201 of certain regions in the Sahel. One can note in the >3-m deep profile in Fig. 21 (monitored by
1202 neutron probe) that there is limited variation in soil moisture content and only in the upper 50 cm
1203 of the bare soil profile, while there are appreciable soil moisture changes even past 300-cm in the
1204 vegetated strip. The result is that nearly all of the high intensity rainfall during the rainy season
1205 in this environment runs off the bare soil into the vegetated strip which thereby receives on the
1206 order of ~~two hundred percent~~ 200% of the precipitation. Verhoef (1995) noted this effect and that
1207 the result was a well-watered vegetation strip adjacent to a very dry bare soil strip in this
1208 environment. Verhoef (1995) was able to show that in the generally hot and dry conditions of
1209 the Sahel, advective conditions for sensible heat flux from the bare soil resulted such that the
1210 ~~evapotranspiration (ET)~~ from the vegetated strip clearly exceeded the potential, or reference, ET
1211 rate (Verhoef et al., 1999; Verhoef and Allen, 2000). Carbon fluxes would obviously be affected
1212 by the heterogeneity in the Tiger Bush system, as well.

1213 To better understand and predict ecosystem dynamics such as these, different classes of
1214 ecological models have been developed for various scales and emphases. For example,

1215 | biogeography models such as MAPSS (Neilson, 1995) and BIOMEs (Prentice et al., 1992;
1216 | Haxeltine and Prentice, 1996) focus on the distribution of species and ecosystems in space.
1217 | Biogeochemistry models such as CENTURY/DAYCENT (Parton et al., 1987, 1998), RothC
1218 | (Jenkinson and Coleman, 1994) and DNDC (Li et al., 1992) place emphasis on the carbon and
1219 | nutrient cycles within ecosystems. Biophysics models based on soil-vegetation-atmosphere
1220 | transfer (SVAT) schemes (SiB: Sellers et al. 1986; BATS: Dickinson et al. 1986) have been
1221 | developed to support regional and global climate modeling to provide accurate information for
1222 | the fluxes of water, radiation, heat and momentum between the atmosphere and the various land
1223 | surfaces. Recently developed dynamic global vegetation models (~~DGVM~~) such as LPJ (Sitch et
1224 | al., 2003), IBIS (Foley et al., 1996) and MC1 (Bachelet et al., 2001), generally incorporate above
1225 | classes of models and schemes to simulate dynamics of potential vegetation and its associated
1226 | biogeochemical and hydrological cycles.

1227 | These models estimate soil moisture content or its proxy using different schemes such as
1228 | the bucket method (Robock et al. 1995; Manabe 1969), the precipitation to potential
1229 | evapotranspiration ratio method (Scheffer et al., 2005), and the water balance model (Law et al.
1230 | 2002). Details of these and other schemes are discussed in Shao and Henderson-Sellers (1996)
1231 | and Ren et al. (2008). These schemes often use simple algorithms to reduce computational
1232 | demand and are less reliable compared to schemes used in hydrologic models [e.g., the Richards
1233 | equation (Richards, 1931)]. Also, especially in cases of large scale ecological models, a more
1234 | realistic parameterization of soil moisture content at subgrid-scale as related to topography is
1235 | often desirable (Gordon et al. 2004). Optimization of the degree of the simplification and the
1236 | spatial resolution is necessary due to computational restrictions, but is difficult to judge due to

1237 lack of adequate observational data with which to verify the performance of the models (Ren et
1238 al.2008).

1239 Traditionally, ecological models have been tested through intercomparison studies such
1240 as the Vegetation/Ecosystem Modeling and Analysis Project (~~VEMAP~~; VEMAP Members
1241 1995), the Carbon Land Model Project (~~CLAMP~~; Randerson et al. 2009), the Project for
1242 Intercomparison of Land-surface Parameterization Schemes (~~PLPS~~; Henderson-Sellers et al.
1243 1996; 1995), and the Global Soil Wetness Projects (~~GSWP/GSWP2~~; Dirmeyer et al. 2006;
1244 Dirmeyer 1999) because evaluating the model performance, especially at larger scales, has been
1245 difficult due to the incompleteness of observation data sets. However, these models are not
1246 independent because they have integrated the same theories and relied on similar data sets as
1247 they evolved (Reichstein et al. 2003). Therefore, while model intercomparison is an important
1248 task, extreme care must be exercised to derive any conclusions.

1249 Future research advances in this area will require use of ~~newly available~~ observation data
1250 at suitable spatial and temporal scales.-(Seneviratne et al. 2010). Observation data from large-
1251 scale soil moisture monitoring in particular should be valuable to validate the simplification and
1252 scaling of ecological models. Wagner et al. (2003) found that modeled 0 to 50 cm monthly
1253 average soil moisture from the Lund-Potsdam-Jena (LPJ) dynamic global vegetation model
1254 agreed “reasonably well” over tropical and temperate locations with values derived from satellite
1255 microwave scatterometer, yielding Pearson correlation coefficients >0.6. The agreement was
1256 poorer over drier and colder climatic regions. However, few studies have used large-scale soil
1257 moisture data to improve the structure or parameterizations of ecological models or to improve
1258 model predictions through data assimilation.

1259 Furthermore, the relationship between soil moisture and terrestrial ecosystem is dynamic
1260 and interdependent: soil moisture constrains the properties of the ecosystem as described earlier,
1261 which in turn, modifies hydrology through evapotranspiration, LAI, and surface roughness
1262 (Breshears and Barnes 1999). Newer generations of ecological models, especially dynamic
1263 global vegetation models, include these important feedback processes to simulate the effects of
1264 future climate change on natural vegetation and associated carbon and hydrologic cycles.
1265 Validation of these models ~~studies will~~may reveal an increased need for data from large-scale
1266 soil moisture observations across various ecosystems and for continuous expansion of
1267 observation networks.

1268 Hydrologic Modeling and Forecasting

1269 One motivation underlying many large-scale soil moisture monitoring efforts is the desire
1270 to more accurately model and forecast watershed dynamics, especially streamflow and flood
1271 events. Pauwels et al. (2001) demonstrated the possibility of improved stream discharge
1272 estimates through assimilation of surface soil moisture estimates derived using data from the
1273 ESA satellites ERS1 and ERS2 into a land atmosphere transfer scheme. The study was limited
1274 to bare soil conditions and small catchments (<20 km²). The assimilation improved discharge
1275 estimates 20-50% in seven out of 12 cases considered, but degraded model accuracy by up to
1276 10% in the remaining five cases. Francois et al. (2003) showed that assimilation of ERS1 ~~SAR~~
1277 data into a simple two-layer land surface scheme through an extended Kalman filter approach
1278 improved the Nash-Sutcliffe efficiency (NSE) for streamflow from 70% to 85%. Their study
1279 involved a larger catchment (104 km²) than that of Pauwels et al. (2001) and included vegetation
1280 cover. The sensitivity of simulated flow to soil moisture was highest when soil moisture itself

1281 was high. The assimilation scheme was also able to correct for 5-10% errors in the input data,
1282 e.g., potential evapotranspiration or precipitation.

1283 More recent applications of large-scale soil moisture data for hydrologic modeling and
1284 forecasting have focused on newer satellite remote sensing datasets. Brocca et al. (2010) used a
1285 simple nudging scheme to assimilate the ASCAT surface soil wetness index into a rainfall—
1286 runoff model for five catchments ($<700 \text{ km}^2$) in the Upper Tiber River basin in Italy.
1287 Assimilation increased the NSE for streamflow prediction during flood events in all five
1288 catchments, with increases ranging from 2 to 17% (Fig. 22). In a subsequent study, ~~root-zone~~
1289 ~~soil moisture~~RZSM was estimated from the ASCAT surface soil moisture data through
1290 application of an exponential filter, and both data types were then assimilated into a two-layer
1291 rainfall—runoff model using an ensemble Kalman filter approach (Brocca et al., 2012).
1292 Assimilation of the ~~root-zone soil moisture~~RZSM estimates produced a clear improvement in
1293 discharge prediction for a 137 km^2 catchment (NSE improved from 76% to 86%), while
1294 assimilation of surface soil moisture had only a small effect.

1295 Thus far only a few studies have evaluated methods for using soil moisture data to
1296 improve hydrologic forecasting in catchments of $>1000 \text{ km}^2$. One example is the work of Meier
1297 et al. (2011) in which the ERS1 and ERS2 soil water index was used, along with rainfall data, to
1298 drive a conceptual rainfall—runoff model in an ensemble Kalman filter framework assimilating
1299 observed discharge every 10 days. The method was applied to three catchments in the Zambezi
1300 River basin in southern Africa. The catchments ranged in size from $95,300$ to $281,000 \text{ km}^2$. The
1301 catchment average soil water index correlated well with measured discharge when the data were
1302 shifted by a catchment-specific time lag. This time lag allowed 40-d lead time streamflow
1303 forecasts with a NSE value of 85% for the largest watershed, but in a catchment with steep

1304 slopes and little soil water storage the lead time was as short as 10 d. Gains in streamflow
1305 forecast accuracy, ~~especially during flood events~~, have even been demonstrated by using
1306 assimilating point soil moisture observations from a single location within a catchment of 1120
1307 km² together with streamflow data, suggesting that even sparse observations networks in large
1308 catchments can be quite useful (Fig. 22; Aubert et al., 2003). The effectiveness of the
1309 assimilation process was dominated by streamflow assimilation when considering the entire
1310 period, but the effectiveness of the assimilation process was dominated by soil moisture
1311 assimilation during flood events.

1312 That large-scale soil moisture monitoring can benefit hydrologic modeling and
1313 forecasting is now well-established with gains in forecast efficiency of 10-20% being typical;
1314 however, significant challenges and uncertainties remain. Most of the research to date in this
1315 area has focused on the use of satellite derived surface soil moisture products, with few studies
1316 using in situ soil moisture measurements within a data assimilation framework (Aubert et al.,
1317 2003; Chen et al., 2011). Thus, the world's growing in situ soil moisture monitoring
1318 infrastructure (Table 1) is a virtually unexplored resource in this context, and many opportunities
1319 exist to develop hydrologic forecasting tools which utilize that infrastructure.

1320 A key challenge associated with assimilation of soil moisture data, regardless of the
1321 source, is to identify and overcome structural deficiencies in the hydrologic models themselves.
1322 For example, a data assimilation experiment using in situ soil moisture measurements in
1323 Oklahoma was generally unsuccessful in improving streamflow predictions from the widely used
1324 Soil and Water Assessment Tool (SWAT) model (Chen et al., 2011). The calibrated SWAT
1325 model significantly underestimated the vertical coupling of soil moisture between upper and
1326 lower soil layers, and the inadequate coupling was apparently a structural, rather than parametric,

1327 problem in the model. Thus, the ensemble Kalman filter assimilation approach was not effective
1328 in improving estimates of deep soil moisture or streamflow. This particular challenge of correctly
1329 representing linkages between soil moisture across two or more soil layers has been identified as
1330 a key concern in studies with other models as well (Brocca et al., 2012). Further research is
1331 needed to optimize the structure of SWAT and other hydrologic models in order to maximize the
1332 benefits from assimilating increasingly available large-scale soil moisture observations (Brocca
1333 et al., 2012).

1334 Another challenge which has been encountered in this arena is uncertainty regarding
1335 proper characterization of model errors and observation errors within the assimilation procedure
1336 (Francois et al., 2003; Brocca et al., 2012). Statistical representations of model errors must often
1337 be made in a somewhat arbitrary or subjective fashion, and pre-existing biases in either the
1338 observations or the model can be particularly problematic (Chen et al., 2011; Brocca et al.,
1339 2012). Nevertheless, research in this area appears to be gaining momentum, and opportunities
1340 abound to advance hydrologic modeling and forecasting with the help of existing and emerging
1341 large-scale soil moisture datasets.

1342

1343 **PRIMARY CHALLENGES AND OPPORTUNITIES**

1344 In this review, we have attempted to describe the state of the art in large-scale soil
1345 moisture monitoring and to identify some critical needs for research to optimize the use of
1346 increasingly available soil moisture data. We have considered: 1) emerging in situ and proximal
1347 sensing techniques, 2) dedicated soil moisture remote sensing missions, 3) soil moisture
1348 monitoring networks, and 4) applications of large-scale soil moisture measurements. The
1349 primary challenges and opportunities in these topic areas can be summarized as follows. For

1350 | emerging in situ and proximal sensing techniques (e.g., COSMOS and GPS) empirical
1351 | confirmations of theoretical predictions regarding the variable measurement depths are needed.
1352 | Calibration procedures for these methods, as well as the DTS methods, need to be further refined
1353 | and standardized with due accounting for site-specific factors such as soil and vegetation
1354 | characteristics which influence instrument performance. Spatial and temporal heterogeneity in
1355 | these site-specific factors must also be considered in some instances, creating additional
1356 | challenges. Also, the community of expertise for these methods, that is the number of
1357 | researchers with the capability to advance these technologies, needs to be expanded.

1358 | Probably the largest share of scientific resources in this general topic area is currently
1359 | devoted to the advancement of satellite remote sensing approaches for soil moisture monitoring.
1360 | These investments are bearing fruit, but challenges and opportunities remain. One significant
1361 | challenge is to further improve methods for estimating ~~root zone soil moisture~~RZSM, the
1362 | information we often need, using surface soil moisture observations, the information satellites
1363 | provide. Progress has been made towards this goal, by using data assimilation into numerical
1364 | models to retrieve ~~root zone soil moisture~~RZSM from near-surface observations. ~~Continued~~
1365 | ~~improvements are also needed in~~ downscaling relatively coarse resolution calibration and
1366 | ~~validation of~~ remotely-sensed soil moisture products to describe sub-footprint spatial variability
1367 | which plays an important role in many applications, because the relatively coarse resolution of
1368 | ~~these products is not well matched with most in situ observations.~~ Coarse resolution, satellite-
1369 | derived soil moisture products are challenging to validate (Reichle et al., 2004), so continuing
1370 | efforts to effectively use these products for modeling and forecasting will likely play an
1371 | important role in their evaluation. Although not primarily a scientific challenge, more work is
1372 | needed to reduce problems associated with RFI. Similarly, continuity of missions is a necessity

1373 if remotely sensed soil moisture data are to be adopted for operational applications like
1374 numerical weather prediction.

1375 In contrast with remote sensing approaches, relatively few resources are currently
1376 devoted toward large-scale in situ soil moisture monitoring networks. Although the number of
1377 networks is growing steadily, the lack of standardization of procedures across networks is a
1378 significant challenge. There is a need for rigorous guidelines and standards to be developed and
1379 adopted worldwide for in situ soil moisture monitoring networks, similar to guidelines for
1380 measurement of other meteorological variables. Best practice standards for sensor selection,
1381 calibration, installation, validation, and maintenance are needed, as well as standards for site
1382 selection, data quality assurance and quality control, data delivery, metadata delivery, and data
1383 archives. The recent recognition of soil moisture as an “Essential Climate Variable” by the
1384 Global Climate Observing System, and the development of the [International Soil Moisture](#)
1385 [Network ISMN](#) are positive steps in this direction, but much more is needed.

1386 For both in situ networks and remote sensing approaches, sustainability is a significant
1387 challenge, perhaps underestimated. Societal and scientific needs for soil moisture data would
1388 seem to justify that our monitoring systems be designed to function without interruption for
1389 many decades. Current realities within science and society at large typically result in monitoring
1390 systems which are designed to function for only a few years. Researchers are rewarded for
1391 developing new systems and technologies, not for ensuring their long-term viability. Successful
1392 long-term operation of monitoring systems generally requires substantial state or federal support.
1393 Securing such long-term support for soil moisture monitoring systems is often difficult. Thus,
1394 determining effective pathways to transition monitoring systems from research mode to
1395 operational mode remains a key challenge.

1396 In closing, we again note the growing need to develop the science necessary to make
1397 effective use of the rising number of large-scale soil moisture datasets. One area where
1398 significant progress seems possible in the near term is the use of large-scale soil moisture data
1399 for drought monitoring. Already some progress has been made using in situ data for this purpose
1400 and approaches using remote sensing data seem sure to follow. Significant efforts have been
1401 devoted to the use of soil moisture observations within the area of numerical weather prediction.
1402 In general, assimilation of soil moisture data has resulted in only modest improvements in
1403 forecast skill. The primary problem is that the current model structures are not well suited for
1404 assimilation of these data, and the model physics may not be properly parameterized to allow for
1405 accurate soil moisture values. A smaller effort, but arguably greater progress, has been made in
1406 the assimilation of soil moisture data into models designed primarily for hydrologic prediction,
1407 especially rainfall—runoff models. Here gains in forecast efficiency of 10-20% are not
1408 uncommon. Nonetheless, as with numerical weather prediction, a key challenge is to identify or
1409 create models that are structured in a way that is optimal for assimilation of soil moisture data.
1410 To date little or no progress has been made in using large-scale soil moisture observations to
1411 improve the structure, parameters, or forecasts of ecological models, and perhaps surprisingly,
1412 the same can be said for crop models. These topic areas are ripe with opportunity-opportunities
1413 and challenges yet to be uncovered. Another frontier where the potential is great but the workers
1414 are few is the use of soil moisture observations in socio-economic modeling and forecasting to
1415 address issues such as drought impacts and food security (Simelton et al., 2012). We are
1416 optimistic that these challenges and opportunities can be addressed by improved communication
1417 and collaboration across the relevant disciplines. The international soil science community has
1418 much to contribute in this context. Hopefully this review will be a small step towards further

1419 engaging that community in advancing the science and practice of large-scale soil moisture
1420 monitoring for the sake of improved Earth system monitoring, modeling, and forecasting.

1421

1422

1423

1424

REFERENCES

[Alavi, N., A.A. Berg, J.S. Warland, G. Parkin, D. Verseghy and P. Bartlett. 2010. Evaluating the Impact of Assimilating Soil Moisture Variability Data on Latent Heat Flux Estimation in a Land Surface Model. Canadian Water Resources Journal 35: 157-172. doi:10.4296/cwrj3502157.](#)

Al Bitar, A., D. Leroux, Y.H. Kerr, O. Merlin, P. Richaume, A. Sahoo, and E.F. Wood. 2012. Evaluation of SMOS soil moisture products over continental US using the SCAN/SNOTEL network. IEEE Trans. Geosci. Remote Sensing 50:1572-1586.

Albergel C., G. Balsamo, P. de Rosnay, J. Muñoz-Sabater, and S. Boussetta. 2012b. A bare ground evaporation revision in the ECMWF land-surface scheme: evaluation of its impact using ground soil moisture and satellite microwave data. Hydrol. Earth Syst. Sci. 16:3607-3620.

Albergel, C., P. de Rosnay, C. Gruhier, J. Munoz-Sabater, S. Hasenauer, L. Isaksen, Y. Kerr, and W. Wagner. 2012a. Evaluation of remotely sensed and modeled soil moisture products using global ground-based in situ observations. Remote Sens. Environ. 118:215-226.

[Albergel, C., C. Rüdiger, D. Carrer, J. Calvet, N. Fritz, V. Naeimi, Z. Bartalis and S. Hasenauer. 2009. An evaluation of ASCAT surface soil moisture products with in-situ observations in Southwestern France. Hyrdol. Earth Syst. Sci. 13: 115.](#)

[Albergel, C., E. Zakharova, J.-C. Calvet, M. Zribi, M. Pardé, J.-P. Wigneron, N. Novello, Y.](#)

[Kerr, A. Mialon and N.-e.-D. Fritz. 2011. A first assessment of the SMOS data in southwestern France using in situ and airborne soil moisture estimates: The CAROLS airborne campaign. Remote Sensing of Environment 115: 2718-2728.](#)

[doi:http://dx.doi.org/10.1016/j.rse.2011.06.012](http://dx.doi.org/10.1016/j.rse.2011.06.012)

Allen, R.G., L.S. Pereira, D. Raes, and M. Smith. 1998. Crop evapotranspiration: Guidelines for computing crop water requirements, Vol. FAO Irrigation and Drainage Paper No. 56. Rome.

[Anderson, W., B. Zaitchik, C. Hain, M. Anderson, M. Yilmaz, J. Mecikalski and L. Schultz.](#)

[2012. Towards an integrated soil moisture drought monitor for East Africa. Hydrol. Earth Syst. Sci. Discuss 9: 4587-4631.](#)

André, J- C., J- P. Goutorbe, A. Perrier, F. Becker, P. Bessemoulin, P. Bougeault, Y. Brunet, W. Brutsaert, T. Carlson, R. Cuenca, J. Gash, J. Gelpe, P. Hilderbrand, J-P. Lagouarde, C. Lloyd, L. Mahrt, P. Mascart, C. Mazaudier, J. Noilhan, C. Ottlé, M. Payen, T. Phulpin, R. Stull, J. Shuttleworth, T. Schmugge, O. Taconet, C. Tarrieu, R-M. Thepenier, C. Valencogne, D. Vidal-Madjar and A. Weill. 1988. Evaporation Over Land-Surfaces: First Results from HAPEX-MOBILHY Special Observing Period. *Annales Geophysicae*, Vol. 6, No. 5. pp. 477 - 492.

André, J-C., J-P. Goutorbe and A. Perrier. 1986. HAPEX-MOBILY: A hydrologic atmospheric experiment for the study of water budget and evaporation flux at the climatic scale. *Bulletin of the American Meteorological Society*, vol. 67, pp. 138-144.

Aubert, D., C. Loumagne, and L. Oudin. 2003. Sequential assimilation of soil moisture and streamflow data in a conceptual rainfall-runoff model. *J. Hydrol.* 280:145-161.

- Bachelet, D., J.M. Lenihan, C. Daly, R.P. Neilson, D.S. Ojima, and W.J. Parton. 2001. MC1: a dynamic vegetation model for estimating the distribution of vegetation and associated carbon, nutrients, and water—technical documentation. Version 1.0.
- Baker, J.M., and R.R. Allmaras. 1990. System for automating and multiplexing soil moisture measurement by time-domain reflectometry. *Soil Sci. Soc. Am. J.* 54:1-6.
- Baldocchi, D., Falge, E., Gu, L., Olson, R., Hollinger, D., Running, S., Anthoni, P., Bernhofer, C., Davis, K., Evans, R., Fuentes, J., Goldstein, A., Katul, G., Law, B., Lee, X., Malhi, Y., Meyers, T., Munger, W., Oechel, W., Paw, K. T., Pilegaard, K., Schmid, H. P., Valentini, R., Verma, S., Vesala, T., Wilson, K., and Wofsy, S.: FLUXNET: A New Tool to Study the Temporal and Spatial Variability of Ecosystem-Scale Carbon Dioxide, Water Vapor, and Energy Flux Densities, *Bull. Am. met. Soc.*, 82, 2415-2434, doi:10.1175/1520-0477, 2001.
- Bartalis, Z., Wagner, W., Naeimi, V., Hasenauer, S., Scipal, K., Bonekamp, H., Figa, J. and Anderson, C. 2007. Initial soil moisture retrievals from the METOP-A Advanced Scatterometer (ASCAT), *Geophysical Research Letters*, 34, L20401
- Basara, J.B., and K.C. Crawford. 2002. Linear relationships between root-zone soil moisture and atmospheric processes in the planetary boundary layer. *J. Geophys. Res.* 107:4274.
- Best, M., C. Jones, I. Dharssi, and R. Quaggin. 2007. A physically based soil moisture nudging scheme for the global model. MetOffice Technical Note.
- Best, M. and Maisey, P. 2002. A physically based soil moisture nudging scheme, Hadley Centre Technical Note 35, 22 pp., Met Office Hadley Centre, Exeter, UK.
- Bircher, S., J.E. Balling, N. Skou, and Y.H. Kerr. 2012. Validation of SMOS brightness temperatures during the HOBE airborne campaign, western Denmark. *IEEE Trans. Geosci.*

Remote Sensing 50:1468-1482.

Blonquist, J.M., S.B. Jones, and D.A. Robinson. 2005. Standardizing characterization of electromagnetic water content sensors: Part 2. Evaluation of seven sensing systems.

Vadose Zone J. 4:1059-1069.

Blyth, E., D. B. Clark, R. Ellis, C. Huntingford, S. Los, M. Pryor, M. Best, and S. Sitch. 2010.

A Comprehensive Set of Benchmark Tests for a Land Surface Model of Simultaneous Fluxes of Water and Carbon at Both the Global and Seasonal Scale. Geoscientific Model Development Discussions 3 (4) (October 26): 1829–1859. doi:10.5194/gmdd-3-1829-2010.

Bolten, J.D., W.T. Crow, Z. Xiwu, T.J. Jackson, and C.A. Reynolds. 2010. Evaluating the

utility of remotely sensed soil moisture retrievals for operational agricultural drought monitoring. IEEE J. of Selected Topics in Applied Earth Observations and Remote Sensing 3:57-66.10.1109/jstars.2009.2037163.

Bremond, Laurent, Arnoud Boom, and Charly Favier. 2012. Neotropical C3/C4 Grass

Distributions – Present, Past and Future. Global Change Biology 18 (7): 2324–2334. doi:10.1111/j.1365-2486.2012.02690.x.

Breshears, David D., and Fairley J. Barnes. 1999. Interrelationships Between Plant Functional

Types and Soil Moisture Heterogeneity for Semiarid Landscapes Within the Grassland/forest Continuum: a Unified Conceptual Model. Landscape Ecology 14 (5): 465–478. doi:10.1023/A:1008040327508.

Bristow, K.L., G.S. Campbell, and K. Calissendorff. 1993. Test of a heat-pulse probe for measuring changes in soil water content. Soil Sci. Soc. Am. J. 57:930-934.

Brocca, L., Hasenauer, S., Lacava, T., Melone, F., Moramarco, T., Wagner, W., Dorigo, W.,

Matgen, P., Martínez-Fernández, J., Ilorens, P., Latron, J., Martin, C., and Bittelli, M.: Soil

- moisture estimation through ASCAT and AMSR-E sensors: An intercomparison and validation study across Europe, *Remote Sensing Envir.*, 115, 3390-3408, 10.1016/j.rse.2011.08.003, 2011.
- Brocca, L., F. Melone, T. Moramarco, W. Wagner, V. Naeimi, Z. Bartalis, and S. Hasenauer. 2010. Improving runoff prediction through the assimilation of the ascats soil moisture product. *Hydro. Earth Syst. Sci.* 14:1881-1893.
- Brocca, L., T. Moramarco, F. Melone, W. Wagner, S. Hasenauer, and S. Hahn. 2012. Assimilation of surface- and root-zone ascats soil moisture products into rainfall-runoff modeling. *Geoscience and Remote Sensing, IEEE Transactions on* 50:2542-2555.
- Brock F.V., Crawford K.C., Elliott R.L., Cuperus G.W., Stadler S.J., Johnson H.L., Eilts M.D. 1995. The Oklahoma Mesonet: A technical Overview. *Journal of Atmospheric and Oceanic Technology* 12:5-19.
- Calvet, J. C., Fritz, N., Froissard, F., Suquia, D., Petitpa, A., and Pignatelli, B. 2007. In situ soil moisture observations for the CAL/VAL of SMOS: The SMOSMANIA network, *International Geoscience and Remote Sensing Symposium, 2007. IGARSS, Barcelona, Spain*, p. 1196-1199.
- Campbell, G.S., C. Calissendorff, and J.H. Williams. 1991. Probe for measuring soil specific heat using a heat-pulse method. *Soil Sci. Soc. Am. J.* 55:291-293.
- Carroll, T.R. 1981. Airborne soil moisture measurement using natural terrestrial gamma radiation. *Soil Sci.* 132:358-366.
- Carslaw, H.S., and J.C. Jaeger. 1959. *Conduction of heat in solids*. Second ed. Oxford University Press, Oxford.
- Chang, A.T.C., S.G. Atwater, V.V. Salomonson, J.E. Estes, D.S. Simonett, and M.L. Bryan.

1980. L-band radar sensing of soil moisture. *Geoscience and Remote Sensing, IEEE Transactions on* GE-18:303-310.

Chen, F., W.T. Crow, P.J. Starks, and D.N. Moriasi. 2011. Improving hydrologic predictions of a catchment model via assimilation of surface soil moisture. *Advances in Water Resources* 34:526-536.

Chen, F. and J. Dudhia. 2001. Coupling an advanced land surface hydrology model with the Penn State–NCAR MM5 modeling system. Part I: Model implementation and sensitivity. *Monthly Weather Review*, Vol. 129, pp. 569–585.

Chew, C., E. Small, K. Larson, and V. Zavorotny, in press. Effects of Near-Surface Soil Moisture on GPS SNR Data: Development of a Retrieval Algorithm for Volumetric Soil Moisture, *IEEE Trans. Geosci. Remote Sens.*

[Collow, T.W., A. Robock, J.B. Basara and B.G. Illston. 2012. Evaluation of SMOS retrievals of soil moisture over the central United States with currently available in situ observations. Journal of Geophysical Research: Atmospheres 117: D09113. doi:10.1029/2011jd017095.](#)

Curran, P.J. 1978. A photographic method for the recording of polarised visible light for soil surface moisture indications. *Remote Sensing of Environment* 7:305-322.

Crow, W.T., A.A. Berg, M.H. Cosh, A. Loew, B.P. Mohanty, R. Panciera, P. de Rosnay, D. Ryu, and J.P. Walker. 2012. Upscaling sparse ground-based soil moisture observations for the validation of coarse-resolution satellite soil moisture products. *Reviews of Geophysics* 50:RG2002 [DOI: 10.1029/2011RG000372.](#)

[Das, N.N., D. Entekhabi and E.G. Njoku. 2011. An Algorithm for Merging SMAP Radiometer and Radar Data for High-Resolution Soil-Moisture Retrieval. Geoscience and Remote Sensing, IEEE Transactions on 49: 1504-1512. doi:10.1109/TGRS.2010.2089526.](#)

- de Rosnay P., M. Drusch, D. Vasiljevic, G. Balsamo, C. Albergel and L. Isaksen. 2012. A simplified Extended Kalman Filter for the global operational soil moisture analysis at ECMWF, in press, Q. J. R. Meteorol. Soc.
- de Rosnay, P., C. Gruhier, F. Timouk, F. Baup, E. Mougin, P. Hiernaux, L. Kergoat, and V. LeDantec. 2009. Multi-scale soil moisture measurements at the Gourma Meso-scale Site in Mali. *J. Hydrol.* 375:241-252.
- Denning, A.S., R. Oren, D. McGuire, C. Sabine, S. Doney, K. Paustian, M. Torn, L. Dilling, L. Heath, and P. Tans. 2005. Science implementation strategy for the north american carbon program. US Global Change Research Program.
- Desilets, D. and Zreda, M., 2001. On scaling cosmogenic nuclide production rates for altitude and latitude using cosmic-ray measurements. *Earth and Planetary Science Letters*, 193, 213-225.
- Desilets, D. and Zreda, M., 2003. Spatial and temporal distribution of secondary cosmic-ray nucleon intensities and applications to in-situ cosmogenic dating. *Earth and Planetary Science Letters*, 206, 21-42.
- Desilets, D., Zreda, M. and Ferre, T., 2010. Nature's neutron probe: Land-surface hydrology at an elusive scale with cosmic rays. *Water Resources Research*, 46, W11505.
- Desilets, D., Zreda, M. and Prabu, T., 2006. Extended scaling factors for in situ cosmogenic nuclides: New measurements at low latitude. *Earth and Planetary Science Letters*, 246, 265-276.
- Dharssi, I. Bovis, K., Macpherson, B. and C. Jones: Operational assimilation of ASCAT surface soil wetness at the Met Office, *Hydrol. Earth Syst. Sci.*, 15, 2729-2746, 2011
- Dickey, F.M., C. King, J.C. Holtzman, and R.K. Moore. 1974. Moisture dependency of radar

- backscatter from irrigated and non-irrigated fields at 400 Mhz and 13.3 Ghz. *Geoscience Electronics, IEEE Transactions on* 12:19-22.
- Dickinson, R.E., A. Henderson-Sellers, P.J. Kennedy, and M.F. Wilson. 1986. Biosphere-Atmosphere Transfer Scheme (BATS) for the NCAR CCM. National Center for Atmospheric Research, Boulder, Colorado.
- Dirmeyer, P. 1999. Assessing GCM Sensitivity to Soil Wetness Using GSWP Data. *J Meteorol Soc Jpn* 77 (1B): 367–385.
- Dirmeyer, Paul A., Xiang Gao, Mei Zhao, Zhichang Guo, Taikan Oki, and Naota Hanasaki. 2006. GSWP-2: Multimodel analysis and implications for our perception of the land surface. *Bulletin of the American Meteorological Society* 87 (10): 1381–1397.
- Dobriyal, P., A. Qureshi, R. Badola, and S.A. Hussain. 2012. A review of the methods available for estimating soil moisture and its implications for water resource management. *J. Hydrol.* 458–459:110-117.
- Dorigo, W. A., Wagner, W., Hohensinn, R., Hahn, S., Paulik, C., Xaver, A., Gruber, A., Drusch, M., Mecklenburg, S., van Oevelen, P., Robock, A., and Jackson, T.: The International Soil Moisture Network: a data hosting facility for global in situ soil moisture measurements, *Hydrol. Earth Syst. Sci.*, 15, 1675-1698, 10.5194/hess-15-1675-2011, 2011b.
- Dorigo, W. A., Xaver, A., Vreugdenhil, M., Gruber, A., Hegyiová, A., Sanchis-Dufau, A. D., Wagner, W., and Drusch, M. 2013. Global automated quality control of in situ soil moisture data from the International Soil Moisture Network. *Vadose Zone Journal*. doi:10.2136/vzj2012.0097.
- Dorigo, W., Van Oevelen, P., Wagner, W., Drusch, M., Mecklenburg, S., Robock, A., and

- Jackson, T.: A New International Network for in Situ Soil Moisture Data, EOS Transactions, American Geophysical Union, 92, 141-142, 2011a.
- Douville, H., Viterbo, P., Mahfouf, J.-F. and Beljaars, A. 2000. Evaluation of the optimum interpolation and nudging techniques for soil moisture analysis using FIFE data, Monthly Weather Review, 128, 1733-1756.
- Draper, C., Mahfouf, J.-F. and Walker, J. 2011. Root-zone soil moisture from the assimilation of screen-level variables and remotely sensed soil moisture, Journal of Geophysical Research, 116, D02127.
- Drusch, M. and Viterbo, P. 2007. Assimilation of screen-level variables in ECMWF's Integrated Forecast System: A study on the impact on the forecast quality and analyzed soil moisture, Monthly Weather Review, 135, 300-314.
- Drusch, M., Scipal, K., de Rosnay, P., Balsamo, G., Andersson, E., Bougeault, P. and Viterbo, P. 2009. Towards a Kalman Filter based soil moisture analysis system for the operational ECMWF Integrated Forecast System, Geophysical Research Letters, 36, L10401.
- Ek, M.B. and R. H. Cuenca. 1994. Variation in Soil Parameters: Implications for Modeling Surface Fluxes and Atmospheric Boundary-Layer Development. Boundary-Layer Meteorology, Vol. 70, pp. 369 - 383.
- Ek, M. B. and A. A. M. Holstag. 2004. Influence of soil moisture on boundary layer cloud development. Journal of Hydrometeorology, Vol. 5, pp. 86-99.
- Ek, M.B. and L. Mahrt. 1994. Daytime evolution of relative humidity at the boundary-layer top. Monthly Weather Review, Vol. 122, pp. 2709-2721.
- Ek, M. B., K. E. Mitchell, Y. Lin, E. Rogers, P. Grummann, V. Koren, G. Gayno, and J. D. Tarpley. 2003. Implementation of Noah land surface model advances in the National

- Centers for Environmental Prediction operational mesoscale Eta model. *Journal of Geophysical Research*, Vol. 108, 8851, doi:10.1029/2002JD003296.
- Entekhabi, D., E.G. Njoku, P.E. O'Neill, K.H. Kellogg, W.T. Crow, W.N. Edelstein, J.K. Entin, S.D. Goodman, T.J. Jackson, and J. Johnson. 2010. The soil moisture active passive (SMAP) mission. *Proceedings of the IEEE* 98:704-716.
- Escorihuela, M.J., A. Chanzy, J.P. Wigneron, and Y.H. Kerr. 2010. Effective soil moisture sampling depth of L-band radiometry: A case study. *Remote Sens. Environ.* 114:995-1001.
- Evelt, S.R. 2001. Exploits and endeavors in soil water management and conservation using nuclear techniques. *International Symposium on Nuclear Techniques in Integrated Plant Nutrient, Water, and Soil Management*. Vienna, Austria. 16-20 October 2000.
- Field, C. B., R. B. Jackson, and H. A. Mooney. 1995. Stomatal Responses to Increased CO₂: Implications from the Plant to the Global Scale. *Plant, Cell & Environment* 18 (10): 1214–1225. doi:10.1111/j.1365-3040.1995.tb00630.x.
- Foley, J.A., I.C. Prentice, N. Ramankutty, S. Levis, D. Pollard, S. Sitch, and A. Haxeltine. 1996. An integrated biosphere model of land surface processes, terrestrial carbon balance, and vegetation dynamics. *Global Biogeochemical Cycles*. 10(4): 603–628.
- Francois, C., A. Quesney, and C. Ottlé. 2003. Sequential assimilation of ers-1 SAR data into a coupled land surface–hydrological model using an extended kalman filter. *Journal of Hydrometeorology* 4:473-487.
- [Franz, T.E., M. Zreda, R. Rosolem and T.P.A. Ferre. 2012. Field Validation of a Cosmic-Ray Neutron Sensor Using a Distributed Sensor Network. *Vadose Zone J.* 11: doi:10.2136/vzj2012.0046.](#)
- Franz, T.E., Zreda, M., Rosolem, R. and Ferre, T.P.A., 2013. A universal calibration function

- for determination of soil moisture with cosmic-ray neutrons. *Hydrology and Earth System Sciences*, 17:453-460.
- Fredlund, D.G., and D.K.H. Wong. 1989. Calibration of thermal conductivity sensors for measuring soil suction. *Geotechnical Testing J.* 12:188-194.
- Friedlingstein et al. 2006. Climate–Carbon Cycle Feedback Analysis: Results from the C4MIP Model Intercomparison. *Journal of Climate*, Vol. 19: pp. 3337–3353.
- Gardner, W., and D. Kirkham. 1952. Determination of soil moisture by neutron scattering. *Soil Sci.* 73:391-402.
- GCOS: Implementation Plan for the Global Observing System for Climate in support of the UNFCCC - 2010 Update, World Meteorological Organization, 2010.
- Georgiadou, Y., and A. Kleusberg 1988, On carrier signal multipath effects in relative GPS positioning, *Manuser. Geod.*, 13, 172– 179.
- Gerten, Dieter, Sibyll Schaphoff, Uwe Haberlandt, Wolfgang Lucht, and Stephen Sitch. 2004. Terrestrial Vegetation and Water Balance—hydrological Evaluation of a Dynamic Global Vegetation Model. *Journal of Hydrology* 286 (1–4) (January 30): 249–270. doi:10.1016/j.jhydrol.2003.09.029.
- Gil-Rodríguez, M., L. Rodríguez-Sinobas, J. Benítez-Buelga, and R. Sánchez-Calvo. in press. Application of active heat pulse method with fiber optic temperature sensing for estimation of wetting bulbs and water distribution in drip emitters. *Agricultural Water Management*
- Gordon, W. S., J. S. Famiglietti, N. L. Fowler, T. G. F. Kittel, and K. A. Hibbard. 2004. Validation of simulated runoff from six terrestrial ecosystem models: Results from VEMAP. *Ecological Applications* 14: ~~(2) (April 1)~~: 527–545. doi:10.1890/02-5287.
- Goutoule, J. M. 1995. MIRAS spaceborne instrument and its airborne demonstrator.

- Proceedings of the Consultative Meeting on Soil Moisture and Ocean Salinity (SMOS), ESA WPP-87, ESTEC, Noordwijk, Netherlands, April 20-21.
- Gruber, A., Dorigo, W., Zwieback, S., Xaver, A., and Wagner, W. 2013. Characterizing coarse-scale representativeness of in situ soil moisture measurements from the International Soil Moisture Network. *Vadose Zone Journal*. [12: - doi:10.2136/vzj2012.0170](https://doi.org/10.2136/vzj2012.0170)
- Guttman, N.B. 1999. Accepting the standardized precipitation index: A calculation algorithm. *Journal of the American Water Resources Association* 35:311-322.
- Haxeltine, A., and I.C. Prentice. 1996. BIOME3: An equilibrium terrestrial biosphere model based on ecophysiological constraints, resource availability, and competition among plant functional types. *Global Biogeochemical Cycles*. 10(4): 693–709.
- Hallikainen, M., F. Ulaby, M. Dobson, M. El-Rayes, and L. Wu, Microwave Dielectric Behavior of Wet Soil—Part I: Empirical Models and Experimental Observations, *IEEE Trans. Geosci. Remote Sens.*, vol. 23, no. 1, pp. 25-34, Jan. 1985.
- Heitman, J.L., J.M. Basinger, G.J. Kluitenberg, J.M. Ham, J.M. Frank, and P.L. Barnes. 2003. Field evaluation of the dual-probe heat-pulse method for measuring soil water content. *Vadose Zone J.* 2:552-560.
- Henderson-Sellers, A., A. J. Pitman, P. K. Love, P. Irannejad, and T. H. Chen. 1995. The project for intercomparison of land surface parameterization schemes (PILPS): phases 2 and 3. *Bulletin of the American Meteorological Society* 76 (4): 489–503.
- Henderson-Sellers, A., K. McGuffie, and A. J. Pitman. 1996. The Project for Intercomparison of Land-surface Parametrization Schemes (PILPS): 1992 to 1995. *Climate Dynamics* 12 (12): 849–859. doi:10.1007/s003820050147.
- Hess, H. 2001. Assimilation of screen-level observations by variational soil moisture analysis,

- Meteorology and Atmospheric Physics, 77, 145:154.
- Hoeben, R., and P.A. Troch. 2000. Assimilation of active microwave observation data for soil moisture profile estimation. *Water Resour. Res.* 36:2805-2819.
- Hoeffner, M., T. Lebel and B. Monteny (editors). 1996. Interactions surface continental/atmosphere: L'Expérience HAPEX-Sahel, OSTROM Éditions, Paris, 763 pp.
- Hollinger, S.E., and S.A. Isard. 1994. A soil moisture climatology of illinois. *Journal of Climate* 7:822-833.
- Hoogenboom, G., 1993. The Georgia automated environmental monitoring network. *Southeastern Climate Review* 4 (1), 12–18.
- Hubbard, K. G., J. You, V. Sridhar, E. Hunt, S. Korner, and G. Roebke. 2009. Near-surface soil-water monitoring for water resources management on a wide-area basis in the Great Plains. *Great Plains Res.* 19:45-54.
- Hunt, E.D., K.G. Hubbard, D.A. Willhite, T.J. Arkebauer, and A.L. Dutcher. 2009. The development and evaluation of a soil moisture index. *International Journal of Climatology* 29:747-759.
- Illston B.G., Basara J., Fischer D.K., Elliott R.L., Fiebrich C., Crawford K.C., Humes K.S., Hunt E., 2008, Mesoscale monitoring of soil moisture across a statewide network. *J. Atmospheric and Oceanic Technology* 25:167-182.
- Ise, Takeshi, and Paul R. Moorcroft. 2006. The Global-scale Temperature and Moisture Dependencies of Soil Organic Carbon Decomposition: An Analysis Using a Mechanistic Decomposition Model. *Biogeochemistry* 80 (3): 217–231. doi:10.1007/s10533-006-9019-5.
- Jackson T.J., Cosh M.H., Bindlish R., Starks P.J., Bosch D.D., Seyfried M.S., Goodrich D.C., Moran M.S., Du J. 2010. Validation of Advanced Microwave Scanning Radiometer Soil

- Moisture Products. *IEEE Transactions of Geoscience and Remote Sensing* 48:4256-4272.
- Jackson, T.J., and T.J. Schmugge. 1989. Passive microwave remote-sensing system for soil-moisture - some supporting research. *IEEE Transactions on Geoscience and Remote Sensing* 27:225-235.
- Jackson, T.J., and T.J. Schmugge. 1991. Vegetation effects on the microwave emission of soils. *Remote Sensing of Environment* 36:203-212.
- Jackson, T.J., R. Bindlish, M.H. Cosh, T.J. Zhao, P.J. Starks, D.D. Bosch, M. Seyfried, M.S. Moran, D.C. Goodrich, Y.H. Kerr, and D. Leroux. 2012. Validation of soil moisture and ocean salinity (SMOS) soil moisture over watershed networks in the U.S. *IEEE Trans. Geosci. Remote Sensing* 50:1530-1543.
- Jacquette, E., A. Al Bitar, A. Mialon, Y. Kerr, A. Quesney, F. Cabot, and P. Richaume. 2010. SMOS CATDS level 3 global products over land. In C. M. U. Neale and A. Maltese, eds. *In Remote sensing for Agriculture, Ecosystems, and Hydrology xii*, Vol. 7824.
- Jenkinson, D.S., and K. Coleman. 1994. Calculating the annual input of organic matter to soil from measurements of total organic carbon and radiocarbon. *European Journal of Soil Science*. 45: 167-174.
- Kaleschke, L., X. Tian-Kunze, N. Maaß, M. Mäkynen, and M. Drusch. 2012. Sea ice thickness retrieval from SMOS brightness temperatures during the arctic freeze-up period. *Geophysical Research Letters* 39:L05501.
- Katzberg, S., O. Torres, M. Grant, D. Masters, Utilizing calibrated GPS reflected signals to estimate soil reflectivity and dielectric constant: Results from SMEX02, *Geosci. Remote Sens.*, vol. 49, no. 1, pp. 71-84, Jan. 2005.

Keller, M., Schimel, D. S., Hargrove, W. W., and Hoffman, F. M., 2008, A continental strategy for the National Ecological Observatory Network, *Frontiers in Ecology*, 6, 282-287

Kerr, Y.H. 2007. Soil moisture from space: Where are we? *Hydrogeol. J.* 15:117-120.

~~Kerr, Y.H., P. Waldteufel, P. Richaume, J.P. Wigneron, P. Ferrazzoli, A. Mahmoodi, A. Al Bitar, F. Cabot, C. Gruhier and S.E. Juglea. 2012. The SMOS soil moisture retrieval algorithm. *Geoscience and Remote Sensing, IEEE Transactions on* 50: 1384-1403.~~

~~Kerr, Y.H., P. Waldteufel, J.P. Wigneron, S. Delwart, F. Cabot, J. Boutin, M.J. Escorihuela, J. Font, N. Reul, C. Gruhier, S.E. Juglea, M.R. Drinkwater, A. Hahne, M. Martin-Neira, and S. Mecklenburg. 2010. The SMOS mission: New tool for monitoring key elements of the global water cycle. *Proc. IEEE* 98:666-687.~~

Kerr, Y.H., P. Waldteufel, J.-P. Wigneron, J.-M. Martinuzzi, J. Font, and M. Berger. 2001. Soil moisture retrieval from space: The soil moisture and ocean salinity (SMOS) mission. *IEEE Trans. Geosci. Rem. Sens.* 39:1729-1735.

~~Kerr, Y.H., P. Waldteufel, J.P. Wigneron, S. Delwart, F. Cabot, J. Boutin, M.J. Escorihuela, J. Font, N. Reul, C. Gruhier, S.E. Juglea, M.R. Drinkwater, A. Hahne, M. Martin Neira, and S. Mecklenburg. 2010. The SMOS mission: New tool for monitoring key elements of the global water cycle. *Proc. IEEE* 98:666-687.~~

~~Kerr, Y.H., P. Waldteufel, P. Richaume, J.P. Wigneron, P. Ferrazzoli, A. Mahmoodi, A. Al Bitar, F. Cabot, C. Gruhier, S.E. Juglea, D. Leroux, A. Mialon, and S. Delwart. 2012. The SMOS soil moisture retrieval algorithm. *IEEE Trans. Geosci. Remote Sensing* 50:1384-1403.~~

Knoll, G.F., 2000. Radiation detection and measurement. Wiley, New York, 802 pp.

Formatted Table

- Kumar, Mukesh, Gopal Bhatt, Christopher Duffy. 2010. The Role of Physical, Numerical and Data Coupling in a Mesoscale Watershed Model (PIHM).
http://www.pihm.psu.edu/tab_publication.html
- Lagerloef, G.S.E. 2001. Satellite measurements of salinity. p. 2511-2516. In S. T. J. Steele, and K. Turekian, ed. In Encyclopedia of Ocean Sciences. Academic Press, London.
- Larson, K. M., Braun, J. J., Small, E. E., Zavorotny, V. U., Gutmann, E. D., and Bilich, A. L., 2010. GPS Multipath and its relation to near-surface soil moisture content, IEEE Journal of Selected Topics in Applied Earth Observations and Remote Sensing, 3, 1, 91-99.
- Larson, K.M., E.E. Small, E.D. Gutmann, A.L. Bilich, J.J. Braun, and V.U. Zavorotny. 2008. Use of GPS receivers as a soil moisture network for water cycle studies. Geophys. Res. Lett. 35:L24405.
- Larson, K.M., E. E. Small, E. Gutmann, A. Bilich, P. Axelrad, and J. Braun, Using GPS multipath to measure soil moisture fluctuations: initial results, GPS Solutions, vol. 12(3), pp. 173-177, 2008.
- Law, B.E, E Falge, L Gu, D.D Baldocchi, P Bakwin, P Berbigier, K Davis, et al. 2002. Environmental Controls over Carbon Dioxide and Water Vapor Exchange of Terrestrial Vegetation. Agricultural and Forest Meteorology, 113 (1-4): 97-120. doi:10.1016/S0168-1923(02)00104-1.
- Le Houérou, H.N. 1996. Climate change, drought and desertification. Journal of Arid Environments 34:133-185.
- [Levine, D. 1988. Synthetic aperture microwave radiometer. Laboratory for Oceans 1: 237-238.](#)
- Levine, D.M., A.J. Griffis, C.T. Swift, and T.J. Jackson. 1994. ESTAR: A synthetic aperture microwave radiometer for remote sensing applications. Proc. IEEE 82

- LeVine, D.M., M. Kao, A.B. Tanner, C.T. Swift, and A. Griffis. 1990. Initial results in the development of a synthetic aperture microwave radiometer. *IEEE Trans. Geosci. Remote Sens.*:614-619.
- Leroux, D. J., Y. H. Kerr, R. A. M. de Jeu and A. Mialon 2012. Simplified algorithm for SMOS: Adaptation of the land parameter retrieval model. EGU General assembly 2012, Wien Austria.
- [Li, B. and R. Avissar. 1994. The impact of spatial variability of land-surface characteristics on land-surface heat fluxes. *Journal of Climate* 7: 527-537.](#)
- Li, C., S. Frolking, and T.A. Frolking. 1992. A model of nitrous oxide evolution from soil driven by rainfall events: 1. Model structure and sensitivity. *Journal of Geophysical Research: Atmospheres*. 97(D9): 9759–9776.
- Lowe, S.T., J. L. LaBrecque, C. Zuffada, L. J. Romans, L. E. Young, and G. A. Hajj, 37, 1, doi:10.1029/2000RS002539, 2002
- Magagi, R.D., and Y.H. Kerr. 1997a. Retrieval of soil moisture and vegetation characteristics by use of ERS-1 wind scatterometer over arid and semi-arid areas. *J. Hydrol.* 189:361-384.
- Magagi, R.D., and Y.H. Kerr. 1997b. Characterization of surface parameters over arid and semi-arid areas by use of ERS-1 windscatterometer. *Remote Sensing Reviews* 15:133-155.
- Magagi, R.D., and Y.H. Kerr. 2001. Estimating surface soil moisture and soil roughness from ERS-1 winscatterometer data over semi-arid area: Use of the co-polarisation ratio. *Remote Sens. Environ.*:432-445.
- Mahfouf, J.-F. 1991. Analysis of soil moisture from near-surface parameters: A feasibility study, *Journal of Applied Meteorology*, 30, 1534-1547.
- Mahfouf, J.-F., Bergaoui, K., Draper, C., Bouyssel, C., Taillefer, F. and Taseva, L. 2009. A

- comparison of two off-line soil analysis schemes for assimilation of screen-level observations, *Journal of Geophysical Research*, 114, D08105.
- Mahrt, L. and H-L. Pan. 1984. A two-layer model of soil hydrology, *Boundary-Layer Meteorology*, Vol. 29, pp. 1-20.
- Manabe, Syukuro. 1969. Climate and the Ocean Circulation. *Monthly Weather Review* 97: 739. doi: 10.1175/1520-0493.
- McPherson, R.A., C.A. Fiebrich, K.C. Crawford, J.R. Kilby, D.L. Grimsley, J.E. Martinez, J.B. Basara, B.G. Illston, D.A. Morris, K.A. Kloesel, A.D. Melvin, H. Shrivastava, J.M. Wolfenbarger, J.P. Bostic, D.B. Demko, R.L. Elliott, S.J. Stadler, J.D. Carlson, and A.J. Sutherland. 2007. Statewide monitoring of the mesoscale environment: A technical update on the Oklahoma mesonet. *J. Atmos. Ocean. Tech.* 24:301-321.
- Mecklenburg, S., M. Drusch, Y.H. Kerr, J. Font, M. Martin-Neira, S. Delwart, G. Buenadicha, N. Reul, E. Daganzo-Eusebio, R. Oliva, and R. Crapolicchio. 2012. Esa's soil moisture and ocean salinity mission: Mission performance and operations. *IEEE Trans. Geosci. Remote Sensing* 50:1354-1366.
- Meier, P., A. Frömelt, and W. Kinzelbach. 2011. Hydrological real-time modelling in the zambezi river basin using satellite-based soil moisture and rainfall data. *Hyrdol. Earth Syst. Sci.* 15:999-1008.
- Merlin, O., A. Al Bitar, J.P. Walker, and Y. Kerr. 2010. An improved algorithm for disaggregating microwave-derived soil moisture based on red, near-infrared and thermal-infrared data. *Remote Sens. Environ.* 114:2305-2316.
- Merlin, O., A.G. Chehbouni, Y.H. Kerr, E.G. Njoku, and D. Entekhabi. 2005. A combined modeling and multi-spectral/multi-resolution remote sensing approach for disaggregation

- of surface soil moisture: Application to SMOS configuration IEEE Trans. Geosc. Remote Sens. 43:2036-2050.
- Merlin, O., C. Rudiger, A. Al Bitar, P. Richaume, J.P. Walker, and Y.H. Kerr. 2012. Disaggregation of SMOS soil moisture in southeastern Australia. IEEE Trans. Geosci. Remote Sensing 50:1556-1571.
- Mishra, A.K., and V.P. Singh. 2010. A review of drought concepts. J. Hydrol. 391:202-216.
- Moghaddam, M. 2009. Polarimetric SAR Phenomenology and Inversion Techniques for Vegetated Terrain, in SAGE Remote Sensing Handbook, T. Warner, Ed., Sage Publications, London.
- Moghaddam, M., S. Saatchi, and R. Cuenca. 2000. Estimating subcanopy soil moisture with radar. J. Geophysical Research - Atmospheres, Vol. 105, No. D11, pp. 14899-14911.
- Monna, W. A. A. and J. G. van der Vliet. 1987. Facilities for research and weather observations on the 213-m tower at Cabauw and at remote locations. KNMI Scientific Report WP-87-5, Royal Netherlands Meteorological Institute (KNMI), De Bilt, Netherlands.
- Montaldo, N., J.D. Albertson, M. Mancini, and G. Kiely. 2001. Robust simulation of root zone soil moisture with assimilation of surface soil moisture data. Water Resour. Res. 37:2889-2900.
- Moorcroft, P. R, G. C. Hurtt, S. W. Pacala. 2001. A method for scaling vegetation dynamics: the ecosystem demography model (ED), Ecological Monographs, 71, 557-585.
- Moran, M.S., D.C. Hymer, J. Qi, and Y. Kerr. 1998. Radar imagery for precision crop and soil management. Modern Agriculture 2:21-23.
- Moran, M.S., D.C. Hymer, J.G. Qi, and Y. Kerr. 2002. Comparison of ERS-2 SAR and

- LANDSAT TM imagery for monitoring agricultural crop and soil conditions. *Remote Sens. Environ.* 79:243-252.
- Mozny, M., M. Trnka, Z. Zalud, P. Hlavinka, J. Nekovar, V. Potop, and M. Virag. 2012. Use of a soil moisture network for drought monitoring in the Czech Republic. *Theoretical and Applied Climatology* 107:99-111.
- Narasimhan, B., and R. Srinivasan. 2005. Development and evaluation of soil moisture deficit index (SMDI) and evapotranspiration deficit index (ETDI) for agricultural drought monitoring. *Agr. Forest Meteorol.* 133:69-88.
- Neilson, Ronald P. 1995. A Model for Predicting Continental-Scale Vegetation Distribution and Water Balance. *Ecological Applications* 5 (2) (May 1): 362–385.
doi:10.2307/1942028.
- [Njoku, E.G., T.J. Jackson, V. Lakshmi, T.K. Chan and S.V. Nghiem. 2003. Soil moisture retrieval from AMSR-E. *Geoscience and Remote Sensing, IEEE Transactions on* 41: 215-229.](#)
- NRC. 2007. *Earth Science and Applications from Space: National Imperatives for the Next Decade and Beyond*. Washington DC: National Academies Press.
- Ochsner, T.E., R. Horton, and T. Ren. 2003. Use of the dual-probe heat-pulse technique to monitor soil water content in the vadose zone. *Vadose Zone J.* 2:572-579.
- Oliva, R., E. Daganzo, Y. Kerr, S. Mecklenburg, S. Nieto, P. Richaume, and C. Gruhier. 2012. SMOS RF interference scenario: Status and actions taken to improve the RFI environment in the 1400-1427 Mhz passive band. *IEEE Geosci. Remote Sens.* 50:1427-1439.
- Orchard, Valerie A., and F.J. Cook. 1983. Relationship Between Soil Respiration and Soil Moisture. *Soil Biology and Biochemistry* 15 (4): 447–453. doi:10.1016/0038-

0717(83)90010-X.

~~Owe, M., R. de Jeu, and T. Holmes. 2008. Multisensor historical climatology of satellite-derived global land surface moisture. *Journal of Geophysical Research* 113:F01002.~~

~~Owe, M., R. A. M. de Jeu, and J. P. Walker. 2001. A methodology for surface soil moisture and vegetation optical depth retrieval using the microwave polarization difference index. *IEEE Trans. Geosci. Remote Sens.*, 39, 1643–1654, doi:10.1109/36.942542.~~

Palecki, M.A., and P.Ya. Groisman, 2011. Observing climate at high elevations using United States Climate Reference Network Approaches. *J. Hydrometeor.* 12, 1137-1143, doi:10.1175/2011JHM1335.1.

Palmer, W.C. 1965. Meteorological drought. Research Paper No. 45. U.S. Weather Bureau, Washington, DC.

Pan, H-L. and L. Mahrt. 1987. Interaction between soil hydrology and boundary-layer development, *Boundary-Layer Meteorology*, Vol. 38, pp. 185-202.

Pan, Y., J.M. Melillo, A.D. McGuire, D.W. Kicklighter, L.F. Pitelka, K. Hibbard, L.L. Pierce, S.W. Running, D.S. Ojima, and W.J. Parton. 1998. Modeled responses of terrestrial ecosystems to elevated atmospheric CO₂: A comparison of simulations by the biogeochemistry models of the vegetation/ecosystem modeling and analysis project (VEMAP). *Oecologia* 114:389-404.

Parton, W.J., M. Hartman, D. Ojima, and D. Schimel. 1998. DAYCENT and its land surface submodel: description and testing. *Global and Planetary Change*. 19(1-4): 35–48.

Parton, W.J., D.S. Schimel, C.V. Cole, and D.S. Ojima. 1987. Analysis of Factors Controlling Soil Organic Matter Levels in Great Plains Grasslands. *Soil Science Society of America Journal*. 51(5): 1173.

Parrens, M., E. Zakharova, S. Lafont, J.-C. Calvet, Y. Kerr, W. Wagner and J.-P. Wigneron. 2012. Comparing soil moisture retrievals from SMOS and ASCAT over France. *Hydrology and Earth System Sciences*. 16: 423-440.

Pauwels, V.R.N., R. Hoeben, N.E.C. Verhoest, and F.P. De Troch. 2001. The importance of the spatial patterns of remotely sensed soil moisture in the improvement of discharge predictions for small-scale basins through data assimilation. *J. Hydrol.* 251:88-102.

Pauwels, V. R., H. Lievens, N. E. Verhoest, G. De Lannoy, D. Plaza Guingla, M. J. van den Berg, Y. Kerr, A. Al Bitar, O. Merlin, F. Cabot, S. Gascoin, E. Wood, M. Pan, A. Sahoo, J. Walker, G. Dumedah and M. Drusch 2012. Assimilation of SMOS data into a coupled land surface and radiative transfer model for improving surface water management. AGU Chapman Conference on Remote Sensing of the Terrestrial Water Cycle, Kona, Hawaii, US, AGU.

Peel, M. C., B.L. Finlayson, B.L., and T.A. McMahon. 2007, T.A. Updated world map of the Köppen-Geiger climate classification, *Hydrology and Earth System Sciences*, 11:1633-1644. doi: +10.5194/hess-11-1633-2007, 2007.

Peled, E., E. Dutra, P. Viterbo, and A. Angert. 2010. Technical note: Comparing and ranking soil-moisture indices performance over Europe, through remote-sensing of vegetation. *Hydrology and Earth System Sciences Discussions* 6:6247-6264.

Phene, C.J., G.J. Hoffman, and S.L. Rawlins. 1971. Measuring soil matric potential in situ by sensing heat dissipation within a porous body: I. Theory and sensor construction1. *Soil Science Society of America Journal*. 35:27-33.

Piles, M., A. Camps, M. Vall-Llossera, I. Corbella, R. Panciera, C. Rudiger, Y.H. Kerr and J. Walker. 2011. Downscaling SMOS-derived soil moisture using MODIS visible/infrared

[data. Geoscience and Remote Sensing, IEEE Transactions on 49: 3156-3166.](#)

Pratt, D.A., and C.D. Ellyett. 1979. The thermal inertia approach to mapping of soil moisture and geology. *Remote Sensing of Environment* 8:151-168.

Prentice, I., W. Cramer, S. Harrison, R. Leemans, R. Monserud, and A. Solomon. 1992. A global biome model based on plant physiology and dominance, soil properties and climate. *Journal Of Biogeography*. 19: 117–134.

Qu, Yizhong and Christopher J. Duffy. 2007. A semidiscrete finite volume formulation for multiprocess watershed simulation. *Water Resources Research*, Vol. 43, pp. 1 – 18.

Rahmoune, R., P. Ferrazoli, Y.H. Kerr , and P. Richaume. 2012. Analysis of SMOS signatures over forests and application of l2 algorithm. *IEEE Geosci. Remote Sens.* in press

Randerson, James T., Forrest M. Hoffman, Peter E. Thornton, Natalie M. Mahowald, Keith Lindsay, Yen-Huei Lee, Cynthia D. Nevison, et al. 2009. Systematic Assessment of Terrestrial Biogeochemistry in Coupled Climate–carbon Models. *Global Change Biology* 15 (10): 2462–2484. doi:10.1111/j.1365-2486.2009.01912.x.

Reece, C.F. 1996. Evaluation of a line heat dissipation sensor for measuring soil matric potential. *Soil Sci. Soc. Am. J.* 60:1022-1028.

[Reichle, R.H., W.T. Crow, R.D. Koster, J.S. Kimball and G.J.M. De Lannoy. 2012. SMAP](#)

[Level 4 Surface and Root Zone Soil Moisture \(L4_SM\) Data Product Algorithm](#)

[Theoretical Basis Document. Global Modeling and Assimilation Office. NASA Goddard Space Flight Center. Greenbelt, MD.](#)

http://smap.jpl.nasa.gov/files/smap2/L4_SM_InitRel_v1.pdf. Accessed June 11, 2013.

[Reichle, R.H., R.D. Koster, J. Dong and A.A. Berg. 2004. Global Soil Moisture from Satellite Observations, Land Surface Models, and Ground Data: Implications for Data Assimilation.](#)

[Journal of Hydrometeorology 5: 430-442. doi:10.1175/1525-7541](#)

- Reichstein, Markus, Ana Rey, Annette Freibauer, John Tenhunen, Riccardo Valentini, Joao Banza, Pere Casals, et al. 2003. Modeling temporal and large-scale spatial variability of soil respiration from soil water availability, temperature and vegetation productivity indices. *Global Biogeochemical Cycles* 17 (4) (November 22): 1104.
doi:10.1029/2003GB002035.
- Ren, D., L. M. Leslie, and D. J. Karoly. 2008. Sensitivity of an Ecological Model to Soil Moisture Simulations from Two Different Hydrological Models. *Meteorology and Atmospheric Physics* 100 (1): 87–99. doi:10.1007/s00703-008-0297-4.
- Richards, L. A. 1931. Capillary conduction of liquids through porous mediums. *Physics* 1, 318-333.
- Rivera Villarreyes, C.A., Baroni, G. and Oswald, S.E., 2011. Integral quantification of seasonal soil moisture changes in farmland by cosmic-ray neutrons. *Hydrology and Earth System Sciences* 15, 3843-3859.
- Robinson, D.A., C.S. Campbell, J.W. Hopmans, B.K. Hornbuckle, S.B. Jones, R. Knight, F. Ogden, J. Selker, and O. Wendroth. 2008. Soil moisture measurement for ecological and hydrological watershed-scale observatories: A review. *Vadose Zone J.* 7:358-389.
- Robock, A., K. Ya Vinnikov, C. A. Schlosser, N. A. Speranskaya, and Y. Xue. 1995. Use of midlatitude soil moisture and meteorological observations to validate soil moisture simulations with biosphere and bucket models. *Journal of Climate* 8 (1): 15–35.
- Robock, A., K.Y. Vinnikov, G. Srinivasan, J.K. Entin, S.E. Hollinger, N.A. Speranskaya, S. Liu, and A. Namkhai. 2000. The global soil moisture data bank. *Bulletin of the American Meteorological Society* 81:1281-1299.

- Robock, A., Mu, M., Vinnikov, K., Trofimova, I. V., and Adamenko, T. I.: Forty-five years of observed soil moisture in the Ukraine: No summer desiccation (yet), *Geophys. Res. Lett.*, 32, 1-5, 10.1029/2004GL021914, 2005.
- Rodell, M., Houser, P.R., Jambor, U., Gottschalck, J., Mitchell, K., Meng, C.-J., Arsenault, K., Cosgrove, B., Radakovich, J., Bosilovich, M., Entin, J.K., Walker, J.P., Lohmann, D., & Toll, D. 2004. The Global Land Data Assimilation System. *Bulletin of the American Meteorological Society*, 85: 381-394.
- Rodriguez-Alvarez, N., X. Bosch-Lluis, A. Camps, M. Vall-Ilossera, E. Valencia, J.F. Marchan-Hernandez, and I. Ramos-Perez. 2009. Soil Moisture Retrieval Using GNSS-R Techniques: Experimental Results Over a Bare Soil Field, *IEEE Trans. Geosci. Remote Sens.*, vol. 47, no. 11, pp. 3616-3624.
- Rodriguez-Alvarez, N., X. Bosch-Lluis, A. Camps, A. Aguasca, M. Vall-Ilossera, E. Valencia, I. Ramos-Perez, and H. Park. 2011a. Review of crop growth and soil moisture monitoring from a ground-based instrument implementing the interference pattern GNSS-R technique. *Radio Sci.* 46:RS0C03.10.1029/2011rs004680.
- Rodriguez-Alvarez, N., A. Camps, M. Vall-Ilossera, X. Bosch-Lluis, A. Monerris, I. Ramos-Perez, E. Valencia, J.F. Marchan-Hernandez, J. Martinez-Fernandez, G. Baroncini-Turricchia, C. Pérez-Gutiérrez, and N. Sánchez. 2011b. Land Geophysical Parameters Retrieval Using Interference Pattern GNSS-R Technique. *IEEE Trans. Geosci. Remote Sens.* 49: 71-84.
- Rosolem, R., Shuttleworth, W.J., Zreda, M., Franz, T.E., Zeng, X. and Kurc, S.A., 2012. The effect of atmospheric water vapor on the cosmic-ray soil moisture signal. *Journal of Hydrometeorology* (in revisions).

- Sayde, C., C. Gregory, M. Gil-Rodriguez, N. Tufillaro, S. Tyler, N. van de Giesen, M. English, R. Cuenca, and J.S. Selker. 2010. Feasibility of soil moisture monitoring with heated fiber optics. *Water Resour. Res.* 46:W06201.
- Schaap, M.G., F.J. Leij, and M.T. van Genuchten. 2001. Rosetta: A computer program for estimating soil hydraulic parameters with hierarchical pedotransfer functions. *J. Hydrol.* 251:163-176.
- Schaefer, G.L., M.H. Cosh, and T.J. Jackson. 2007. The USDA Natural Resources Conservation Service Soil Climate Analysis Network (SCAN). *J. Atmos. Ocean. Tech.* 24:2073-2077.
- Scheffer, M., M. Holmgren, V. Brovkin, and M. Claussen. 2005. Synergy between small- and large-scale feedbacks of vegetation on the water cycle. *Global Change Biology.* 11(7): 1003–1012.
- Schmugge, T., P. Gloersen, T. Wilheit, and F. Geiger. 1974. Remote sensing of soil moisture with microwave radiometers. *J. Geophys. Res.* 79:317-323.
- Schmugge, T., and T. Jackson. 1994. Mapping surface soil moisture with microwave radiometers. *Meteorol Atmos Phys* 54:213-223.
- Schneider, J. M., Fisher, D. K., Elliott, R. L., Brown, G. O., and Bahrmann, C. P., 2003, Spatiotemporal variations in soil water: First results from the ARM SGP CART Network, *J. Hydrometeorology*, 4, 106-120.
- Schroeder, J. L., W. S. Burgett, K. B. Haynie, I. Sonmez, G. D. Skwira, A. L. Doggett, J. W. Lipe, 2005: The West Texas Mesonet: A Technical Overview. *J. Atmos. Oceanic Technol.*, 22, 211–222.
- Schwank, M., J.P. Wigneron, E. Lopez-Baeza, I. Volksch, C. Matzler, and Y.H. Kerr. 2012. L-

band radiative properties of vine vegetation at the MELBEX III SMOS Cal/Val Site. IEEE Trans. Geosci. Remote Sensing 50:1587-1601.

Scott, R. W., E. C. Krug, S. L. Burch, C. R. Mitdarfer, and P. F. Nelson. 2010. Investigations of Soil Moisture Under Sod in of East-Central Illinois. Illinois State Water Survey Report of Investigation 119. Champaign, Illinois. 138 p.

[Scott, B.L., T.E. Ochsner, B.G. Illston, C.A. Fiebrich, J.B. Basara and A.J. Sutherland. in review. New soil property database improves Oklahoma Mesonet soil moisture estimates. J. Atmos. Ocean. Tech.](#)

Selker, J.S., L. Thevenaz, H. Huwald, A. Mallet, W. Luxemburg, N. van de Giesen, M. Stejskal, J. Zeman, M. Westhoff, and M.B. Parlange. 2006. Distributed fiber-optic temperature sensing for hydrologic systems. Water Resour. Res. 42:W12202.

Sellers, P., R. Dickinson, D. Randall, A. Betts, F. Hall, J. Berry, G. Collatz, A. Denning, H. Mooney, and C. Nobre. 1997. Modeling the exchanges of energy, water, and carbon between continents and the atmosphere. Science 275:502-509.

Sellers, P.J., Y. Mintz, Y.C. Sud, and A. Dalcher. 1986. A Simple Biosphere Model (SIB) for Use within General Circulation Models. Journal of the Atmospheric Sciences. 43(6): 505–531.

Seneviratne, Sonia I., Thierry Corti, Edouard L. Davin, Martin Hirschi, Eric B. Jaeger, Irene Lehner, Boris Orlovsky, and Adriaan J. Teuling. 2010. Investigating Soil Moisture–climate Interactions in a Changing Climate: A Review. Earth-Science Reviews 99 (3–4) (May): 125–161. doi:10.1016/j.earscirev.2010.02.004.

Seuffert, G., Wilker, H., Viterbo, P., Drusch, M. and Mahfouf, J.-F. 2004. The usage of screen-level parameters and microwave brightness temperature for soil moisture analysis, Journal

- of Hydrometeorology, 5, 516-531.
- Shao, Yaping, and A. Henderson-Sellers. 1996. Modeling soil moisture: A project for intercomparison of land surface parameterization schemes phase 2(b): GEWEX Continental-Scale International Project (GCIP). *Journal of geophysical research* 101 (D3): 7227-7250.
- Simelton, E., E.G. Fraser, M. Termansen, T. Benton, S. Gosling, A. South, N. Arnell, A. Challinor, A. Dougill, and P. Forster. 2012. The socioeconomics of food crop production and climate change vulnerability: A global scale quantitative analysis of how grain crops are sensitive to drought. *Food Sec.* 4:163-179.
- Simpson, J.A., 2000. The cosmic ray nucleonic component: the invention and scientific uses of the neutron monitor. *Space Science Reviews* 93, 11-32.
- Sitch, S., B. Smith, I.C. Prentice, A. Arneth, A. Bondeau, W. Cramer, J.O. Kaplan, S. Levis, W. Lucht, M.T. Sykes, K. Thonicke, and S. Venevsky. 2003. Evaluation of ecosystem dynamics, plant geography and terrestrial carbon cycling in the LPJ dynamic global vegetation model. *Global Change Biology*. 9(2): 161-185.
- Small, E.E., K.M. Larson, and J.J. Braun. 2010. Sensing vegetation growth with reflected gps signals. *Geophysical Research Letters* 37:L12401.
- Smith, A. B., Walker, J. P., Western, A. W., Young, R. I., Ellett, K. M., Pipunic, R. C., Grayson, R. B., Siriwardena, L., Chiew, F. H. S., and Richter, H. 2012. The Murrumbidgee soil moisture monitoring network data set, *Water Resour. Res.*, 48, W07701, 10.1029/2012wr011976.
- Song, Y., M.B. Kirkham, J.M. Ham, and G.J. Kluitenberg. 1999. Dual probe heat pulse technique for measuring soil water content and sunflower water uptake. *Soil tillage res*

50:345-348.

Sridhar, V., K.G. Hubbard, J. You, and E.D. Hunt. 2008. Development of the soil moisture index to quantify agricultural drought and its user friendliness in severity-area-duration assessment. *Journal of Hydrometeorology* 9:660-676.

Steele-Dunne, S.C., M.M. Rutten, D.M. Krzeminska, M. Hausner, S.W. Tyler, J. Selker, T.A. Bogaard, and N.C. van de Giesen. 2010. Feasibility of soil moisture estimation using passive distributed temperature sensing. *Water Resour. Res.* 46:W03534.

Striegl, A.M., and S.P. Loheide II. 2012. Heated distributed temperature sensing for field scale soil moisture monitoring. *Ground Water* 50:340-347.

Su, Z., Wen, J., Dente, L., van der Velde, R., Wang, L., Ma, Y., Yang, K., and Hu, Z. 2011. The Tibetan Plateau observatory of plateau scale soil moisture and soil temperature (Tibet-Obs) for quantifying uncertainties in coarse resolution satellite and model products, *Hydrol. Earth Syst. Sci.*, 15, 2303-2316, 10.5194/hess-15-2303-2011.

[Sutinen, R., P. Hänninen and A. Venäläinen. 2008. Effect of mild winter events on soil water content beneath snowpack. *Cold Regions Science and Technology* 51: 56-67. doi:<http://dx.doi.org/10.1016/j.coldregions.2007.05.014>.](#)

[Suyker, A.E., S.B. Verma and G.G. Burba. 2003. Interannual variability in net CO₂ exchange of a native tallgrass prairie. *Global Change Biol.* 9: 255-265. doi:10.1046/j.1365-2486.2003.00567.x.](#)

[Svoboda, M., D. LeComte, M. Hayes, R. Heim, K. Gleason, J. Angel, B. Rippey, R. Tinker, M. Palecki, D. Stooksbury, D. Miskus and S. Stephens. 2002. The Drought Monitor. *Bulletin of the American Meteorological Society* 83: 1181-1190.](#)

Tarara, J.M., and J.M. Ham. 1997. Measuring soil water content in the laboratory and field

- with dual-probe heat-capacity sensors. *Agron. J.* 89:535-542.
- Topp, G.C. 2006. TDR reflections: My thoughts and experiences on TDR. *Proc. TDR 2006*. Purdue University, West Lafayette, Indiana, USA. Sept. 2006.
- Topp, G.C., J.L. Davis, and A.P. Annan. 1980. Electromagnetic determination of soil water content: Measurements in coaxial transmission lines. *Water Resour. Res.* 16:574-582.
- Torres, G.M., R.P. Lollato, and T.E. Ochsner. 2013. Comparison of drought probability assessments based on atmospheric water deficit and soil water deficit. *Agron. J.*
- Tyler, S.W., J.S. Selker, M.B. Hausner, C.E. Hatch, T. Torgersen, C.E. Thodal, and S.G. Schladow. 2009. Environmental temperature sensing using raman spectra dts fiber-optic methods. *Water Resour. Res.* 45
- Ulaby, F.T., M.C. Dobson, and D.R. Brunfeldt. 1983. Improvement of moisture estimation accuracy of vegetation-covered soil by combined active/passive microwave remote sensing. *Geoscience and Remote Sensing, IEEE Transactions on GE-21:300-307*.
- VEMAP Members. 1995. Vegetation/Ecosystem Modeling and Analysis Project: Comparing Biogeography and Biogeochemistry Models in a Continental-scale Study of Terrestrial Ecosystem Responses to Climate Change and CO₂ Doubling. *Global Biogeochemical Cycles* 9:407. doi:10.1029/95GB02746.
- Verhoef, A. 1995. Surface energy balance of shrub vegetation in the Sahel. Ph.D. dissertation, Wageningen University, Netherlands, 247 pp.
- Verhoef, A. and Allen, S. J. 2000. A SVAT scheme describing energy and CO₂ fluxes for multi-component vegetation: calibration and test for a Sahelian savannah. *Ecological Modelling*, Vol. 127, pp. 245-267.
- Verhoef, A., Allen, S. J. and Lloyd, C. R. 1999. Seasonal variation of surface energy balance

- over two Sahelian surfaces. *International Journal of Climatology*, Vol. 19, pp. 1267-1277.
- Vinnikov, K.Y., A. Robock, S. Qiu, and J.K. Entin. 1999. Optimal design of surface networks for observation of soil moisture. *J. Geophys. Res.* 104:19743-19749.
- Wagner, W., G. Bloschl, P. Pampaloni, J.C. Calvet, B. Bizzarri, J.P. Wigneron, and Y. Kerr. 2007. Operational readiness of microwave remote sensing of soil moisture for hydrologic applications. *Nord. Hydrol.* 38:1-20.
- [Wagner, W., S. Hahn, R. Kidd, T. Melzer, Z. Bartalis, S. Hasenauer, J. Figa-Saldaña, P. de Rosnay, A. Jann, S. Schneider, J. Komma, G. Kubu, K. Brugger, C. Aubrecht, J. Züger, U. Gangkofner, S. Kienberger, L. Brocca, Y. Wang, G. Blöschl, J. Eitzinger, K. Steinnocher, P. Zeil and F. Rubel. 2013. The ASCAT Soil Moisture Product: A Review of its Specifications, Validation Results, and Emerging Applications. *Meteorologische Zeitschrift* 22: 5-33. doi:10.1127/0941-2948/2013/0399.](#)
- [Wagner, W., G. Lemoine, and H. Rott. 1999. A method for estimating soil moisture from ERS scatterometer and soil data. *Remote Sens. Environ.* 70:191–207.](#)
- Wagner, W., K. Scipal, C. Pathe, D. Gerten, W. Lucht, and B. Rudolf. 2003. Evaluation of the agreement between the first global remotely sensed soil moisture data with model and precipitation data. *J. Geophys. Res.* 108:4611.
- Weinan Pan, R. P. Boyles, J. G. White, and J. L. Heitman. 2012. Characterizing Soil Physical Properties for Soil Moisture Monitoring with the North Carolina Environment and Climate Observing Network, *Journal of Atmospheric and Oceanic Technology*, July 2012, Vol. 29, No. 7 : pp. 933-943 (doi: 10.1175/JTECH-D-11-00104.1)
- Weiss, J.D. 2003. Using fiber optics to detect moisture intrusion into a landfill cap consisting of a vegetative soil barrier. *Journal of the Air & Waste Management Association* 53:1130-

1148.

Western, A.W., and G. Blöschl. 1999. On the spatial scaling of soil moisture. *J. Hydrol.* 217:203-224.

Xu, Liukang, Dennis D. Baldocchi, and Jianwu Tang. 2004. How soil moisture, rain pulses, and growth alter the response of ecosystem respiration to temperature. *Global Biogeochemical Cycles* 18 (4) (October 5): GB4002. doi:10.1029/2004GB002281.

Yang, Hao, Karl Auerswald, Yongfei Bai, and Xingguo Han. 2011. Complementarity in water sources among dominant species in typical steppe ecosystems of Inner Mongolia, China. *Plant and soil* 340 (1-2): 303–313.

Yang, K., T. Koike, I. Kaihotsu, and J. Qin. 2009. Validation of a dual-pass microwave land data assimilation system for estimating surface soil moisture in semiarid regions. *Journal of Hydrometeorology* 10:780-793.10.1175/2008jhm1065.

Zacharias, S., H. Bogen, L. Samaniego, M. Mauder, R. Fuß, T. Pütz, M. Frenzel, M. Schwank, C. Baessler, and K. Butterbach-Bahl. 2011. A network of terrestrial environmental observatories in Germany. *Vadose Zone J.* 10:955-973.

Zavorotny, V., K. Larson, J. Braun, E. Small, E. Gutmann, and A. Bilich, A Physical Model for GPS Multipath Caused by Land Reflections: Toward Bare Soil Moisture Retrievals, *IEEE J. Sel. Topics Appl. Earth Obs. Remote Sens.*, vol. 3, no. 1, pp. 100-110, Mar. 2010.

Zhao, L., K. Yang, J. Qin, Y. Chen, W. Tang, C. Montzka, H. Wu, C. Lin, M. Han, and H. Vereecken. in press. Spatiotemporal analysis of soil moisture observations within a tibetan mesoscale area and its implication to regional soil moisture measurements. *J. Hydrol.* <http://dx.doi.org/10.1016/j.jhydrol.2012.12.033>.

Zreda, M., D. Desilets, T.P.A. Ferré, and R.L. Scott. 2008. Measuring soil moisture content

non-invasively at intermediate spatial scale using cosmic-ray neutrons. *Geophysical Research Letters* 35:10.1029/2008GL035655.

Zreda, M., W. J. Shuttleworth, X. Zeng, C. Zweck, D. Desilets, T. Franz, and R. Rosolem.

2012. COSMOS: the COsmic-ray Soil Moisture Observing System. *Hydrology and Earth System Sciences*, Vol. 16, pp. 4079-4099.

Zreda, M. and 9 others, 2011. Cosmic-ray neutrons, an innovative method for measuring area-average soil moisture. *GEWEX News* 21(3), 6-10.

Zweck, C., Zreda, M. and Desilets, D.. 2011. Empirical confirmation of the sub-kilometer footprint of cosmic-ray soil moisture probes. *Geophysical Research Abstracts* 13, EGU2011-13393.

1425 Table 1. Partial list of large-scale ($>100^2$ km²) in situ soil moisture monitoring networks ordered
 1426 from largest to smallest in areal extent. The areas are enumerated by XX^2 to indicate the length
 1427 of one side of a square of the given area.

Formatted: Superscript

Network Name	Country or State	Site no.	Extent km ²	Density km ² st ⁻¹	Reference
<i>Inside the U.S.-US</i>					
Soil Climate Analysis Network	USA	180	3100 ²	230 ^{2a}	Schaefer et al. (2007)
Climate Reference Network	USA	114	3100 ²	290 ²	Palecki and Groisman (2011)
Cosmic Ray Soil Moisture Observing System	USA	67	3100 ²	380 ²	Zreda et al. (2012)
Plate Boundary Observatory Network	Western US	59	1800 ²	240 ²	Larson et al. (2008)
Automated Weather Data Network	Nebraska	53	450 ²	62 ²	Hubbard et al. (2009)
Oklahoma Mesonet	Oklahoma	108	430 ²	41 ²	Illston et al. (2008)
Automated Environmental Monitoring Network	Georgia	81	390 ²	44 ²	Hoogenboom (1993)
Water & Atmospheric Resources Monitoring Program	Illinois	19	390 ²	89 ²	Scott et al. (2010)
Environment and Climate Observing Network	N. Carolina	37	370 ²	61 ²	Weinan et al. (2012)
West Texas Mesonet	Texas	53	300 ²	41 ²	Schroeder et al. (2005)
ARM-SGP Extended Facilities ^b	OK/KS	13	150 ²	42 ²	Schneider et al. (2003)
<i>Outside the U.S.-US</i>					
Tibet-Obs	China	46	1600 ²	230 ²	Su et al. (2011)
<u>G1K Geological Survey of Finland</u>	<u>Finland</u>	<u>23</u>	<u>580²</u>	<u>121²</u>	<u>Sutinen et al. (2008)</u>
OzNet	Australia	38	290 ²	47 ²	Smith et al. (2012)
SMOSMANIA	France	21	200 ²	44 ²	Calvet et al. (2007)
Gourma Mesoscale Site	Mali	10	170 ²	55 ²	de Rosnay et al. (2009)
Automatic Stations for Soil Hydrology	Mongolia	12	140 ²	40 ²	Yang et al. (2009)
Central Tibetan Plateau SMTMN ^c	China	50	100 ²	14 ²	Zhao et al. (2013)
Umbria Region Hydro-meteorological Network	Italy	15	100 ²	26 ²	www.cfumbria.it

1428 ^a Density is calculated as the ratio of extent to site number. Note 100^2 km² = 10,000 km².

1429 ^b The ARM-SGP Extended Facility network is being restructured. Values listed are projections for summer 2013.

1430 ^c Soil Moisture/Temperature Monitoring Network

1431 Table 2. Selected large-scale hydrologic-atmospheric-remote sensing experiments.

Experiment	Lead Agency	Location	Climatic Regime	Observation Period
HAPEX-MOBILHY	Météo – France	Southwest France	Temperate Forest	Summer, 1986
HAPEX-Sahel	Météo – France	Niger	Tropical Arid	Summer, 1992
BOREAS	NASA	Canada	Boreal Forest	Spr./Fall 1994,1996
IHOP	NSF	KS, OK, TX	Continental	2002
HYMeX	GEWEX	Europe	Mediterranean	2010-2020 (LOP) 2011-2015 (EOP)
CZO	NSF	6 sites	Varies	2007 - Current
AirMOSS	NASA	7 sites	Varies	2011-2015

1432 *LOP – Long-term observation period*1433 *EOP – Enhanced observation period*

1434

1435

1436

1437

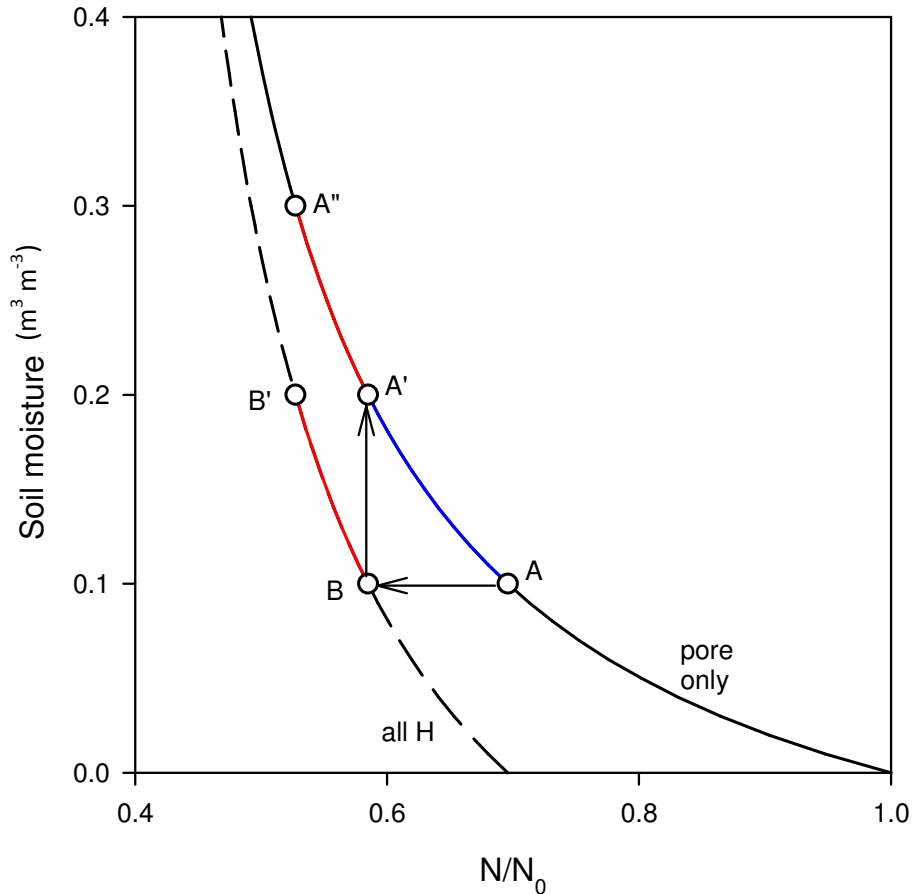
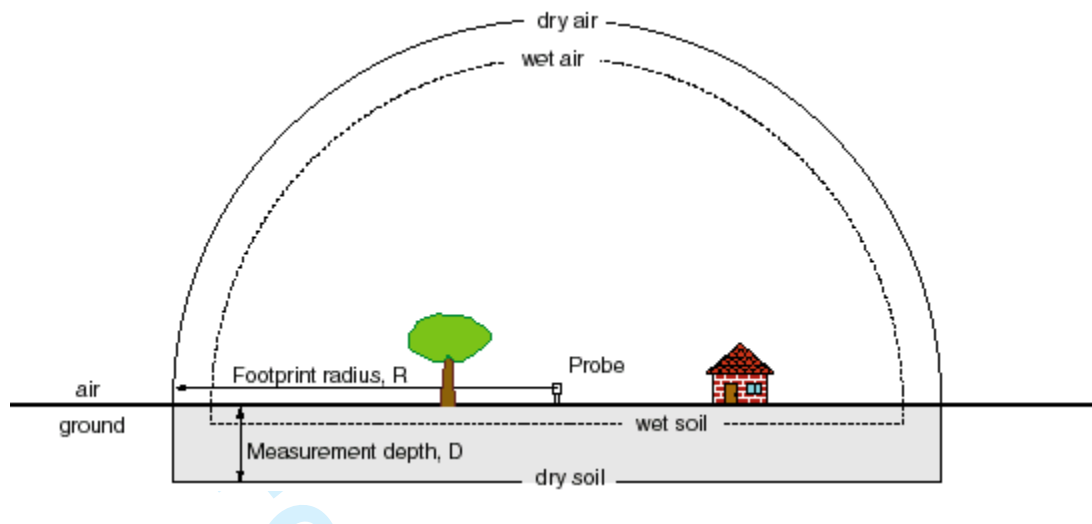


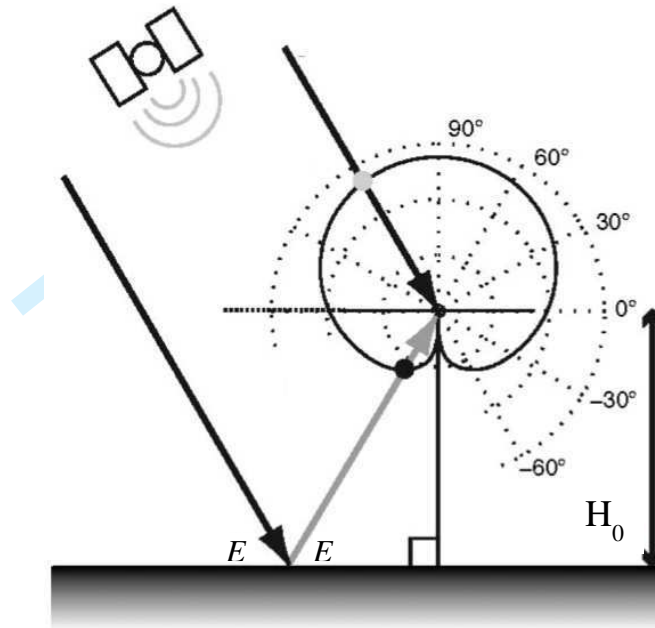
Fig. 1. Response function for cosmic-ray probe for soils with pore water only (solid black line) and those with pore water and other water, such as lattice and organic matter (dashed black line). N is the measured neutron intensity, and N_0 is a calibration parameter representing the neutron intensity above dry soil. The presence of other water shifts the line horizontally from point A to B and A' to B', and the new line is steeper than the original line for the same moisture range (B-B' vs. A-A'). Section B-B' can be placed on the original line by translating it up to fall on section A'-A''. Thus, accounting for additional (non-pore) water does not require a new response function, but merely a translation along the original function by the amount equal to that non-pore water component.



21 Fig. 2. Sensing volume of the cosmic-ray probe comprises a hemisphere in air (of radius R) and a
 22 cylinder in soil (of height D). All hydrogen within the sensing volume is reflected in the
 23 measured neutron intensity. The horizontal footprint, R , depends on air properties: mainly
 24 density and water vapor content. The vertical footprint depends on soil properties: mainly bulk
 25 density and total hydrogen content (pore water, lattice water, organic matter water).

26

27

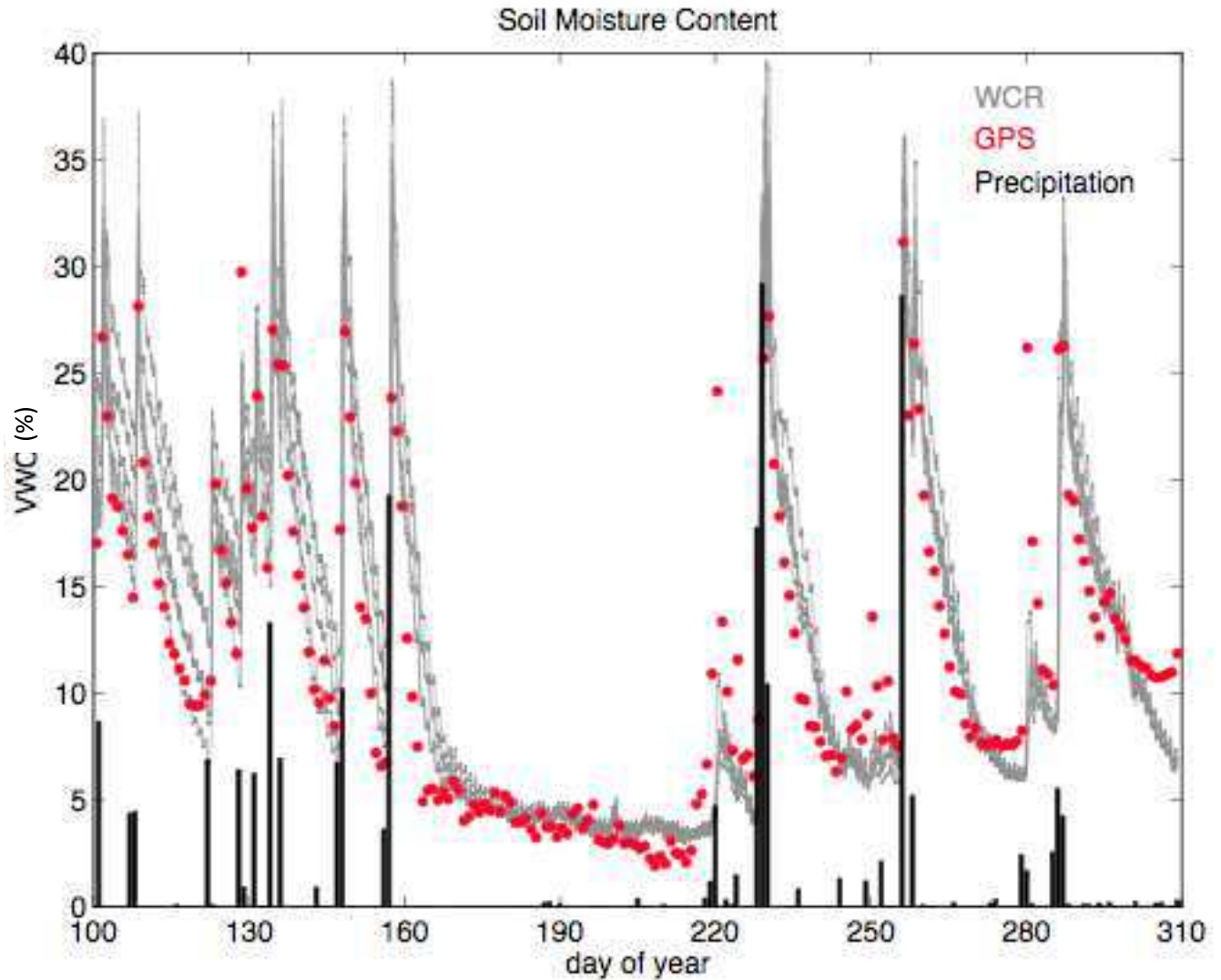


28

29 Fig. 3. Geometry of a multipath signal, for antenna height (H_0) and satellite elevation angle (E).

30 Black lines represent the direct signal transmitted from the satellite. The gray line is the reflected
 31 signal from the ground. The solid line represents the gain pattern of the antenna. Dashed circles
 32 indicate relative power levels of the gain pattern. (Reproduced from Larson et al., 2008)

33

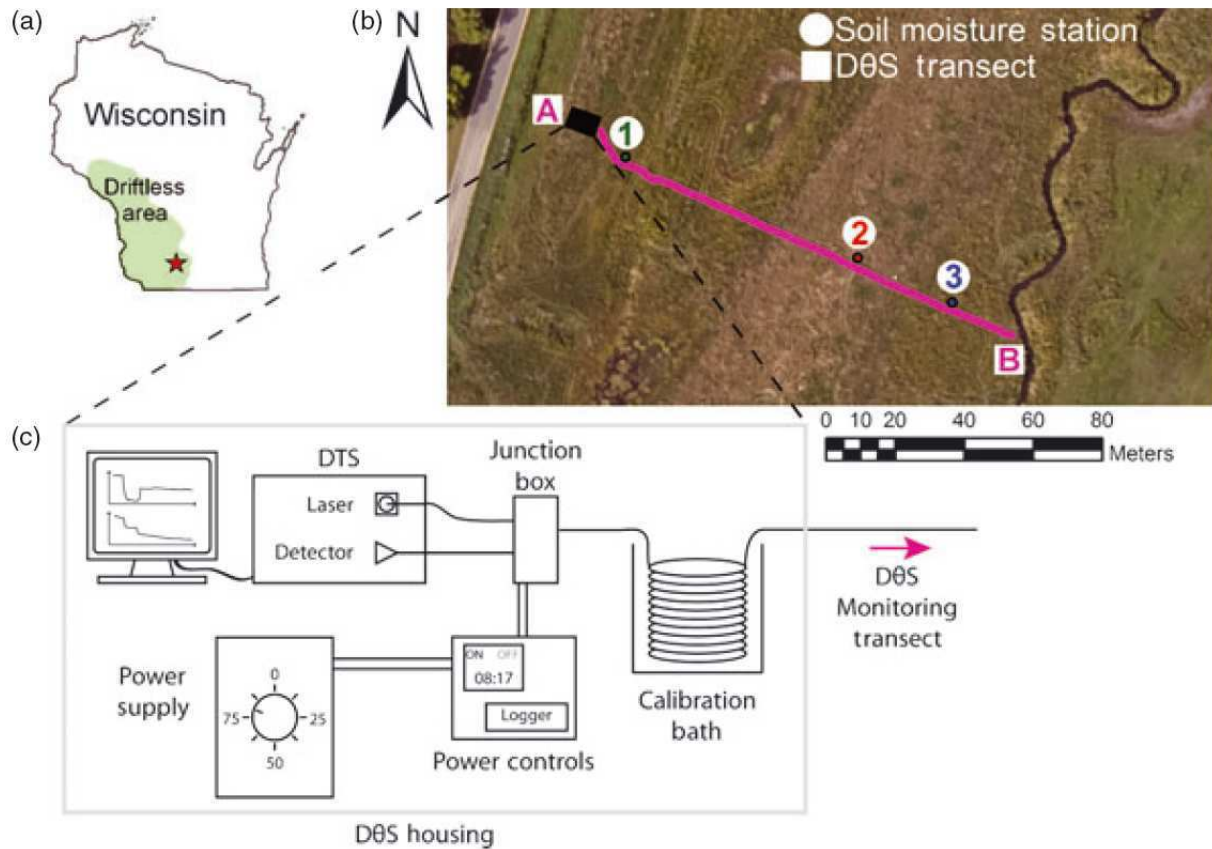


34

35

36 Fig. 4. Soil volumetric water content (VWC, %) measured by five water content reflectometers
37 at 2.5 cm depth (grey lines), soil water content estimated by GPS-Interferometric Reflectometry
38 (circles), and daily precipitation totals (bars) from a site near Marshall, CO, United States.
39 (Adapted from Larson et al., 2010).

40



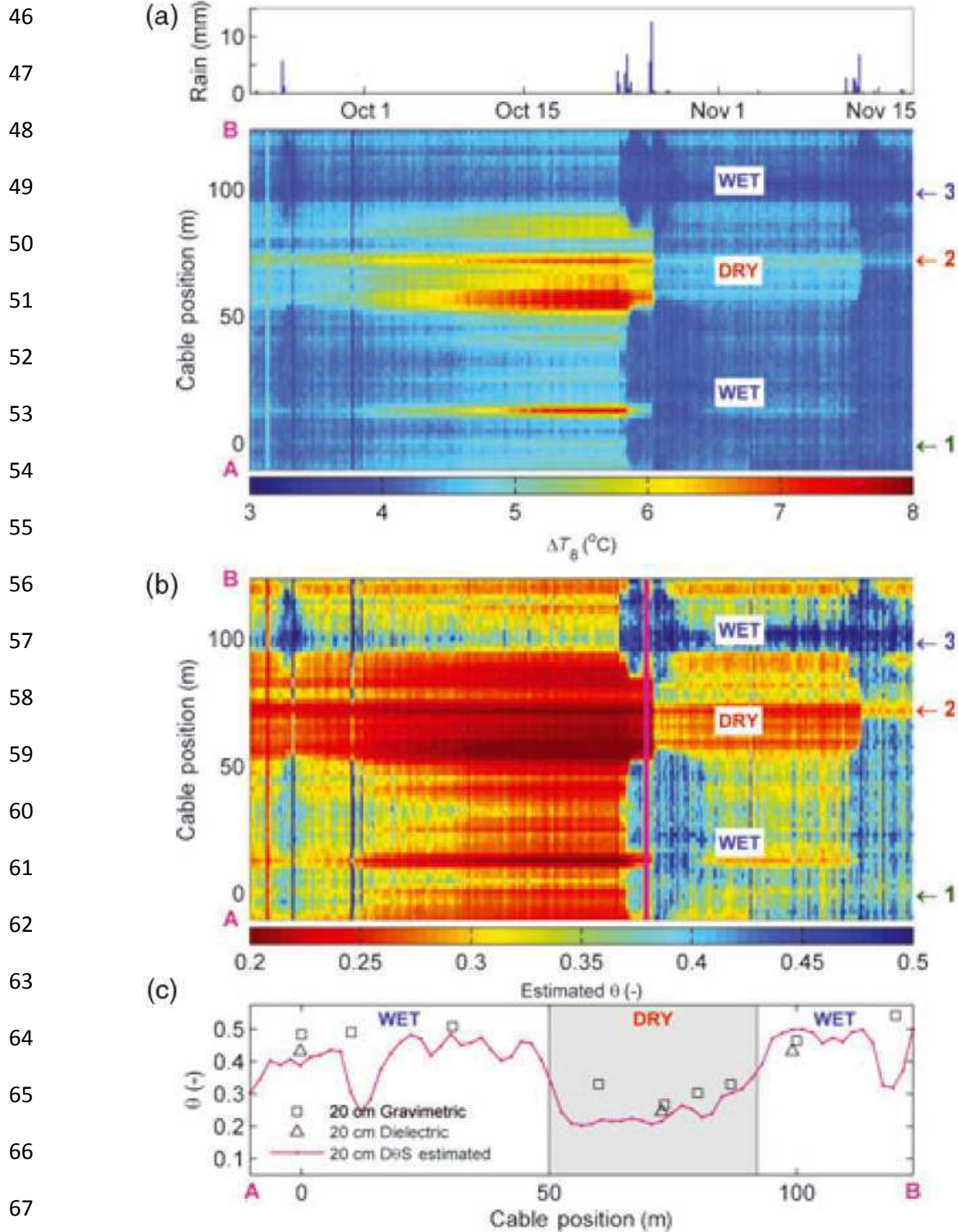
41

42 Fig. 5. Location of study site used by Striegl and Loheide (2012) (a), aerial photo of active DTS

43 transect with three independent soil moisture monitoring stations (b), and schematic diagram of

44 active DTS system components (c). Reproduced from Striegl and Loheide (2012).

45

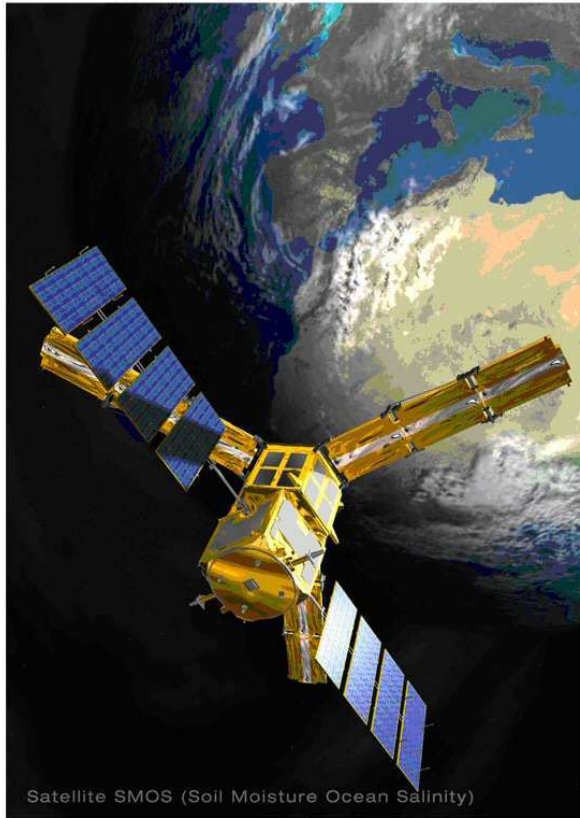


68 Fig. 6. Time series (x-axis) of four hour rainfall totals and DTS measured average temperature
69 rise eight minutes after heating began for each 2-m interval along the 130-m cable transect (a),
70 time series of estimated soil moisture values based on the active DTS data from each 2-m
71 interval along the cable (b), and a plot of active DTS soil moisture estimates and independent
72 soil moisture estimates versus cable position on 25 Oct. 2010 at 16:00 (c).

73

74

75



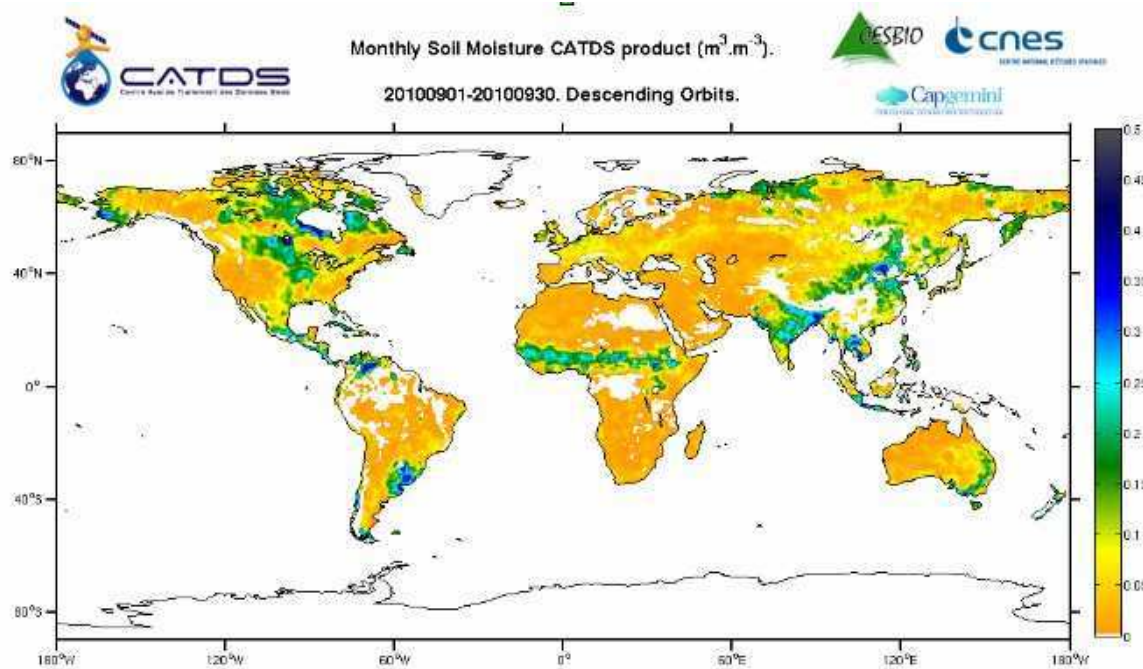
76

77 Fig. 7. Artist's view of the Soil Moisture and Ocean Salinity (SMOS) satellite (Courtesy of

78 Cesbio- Mira).

79

80

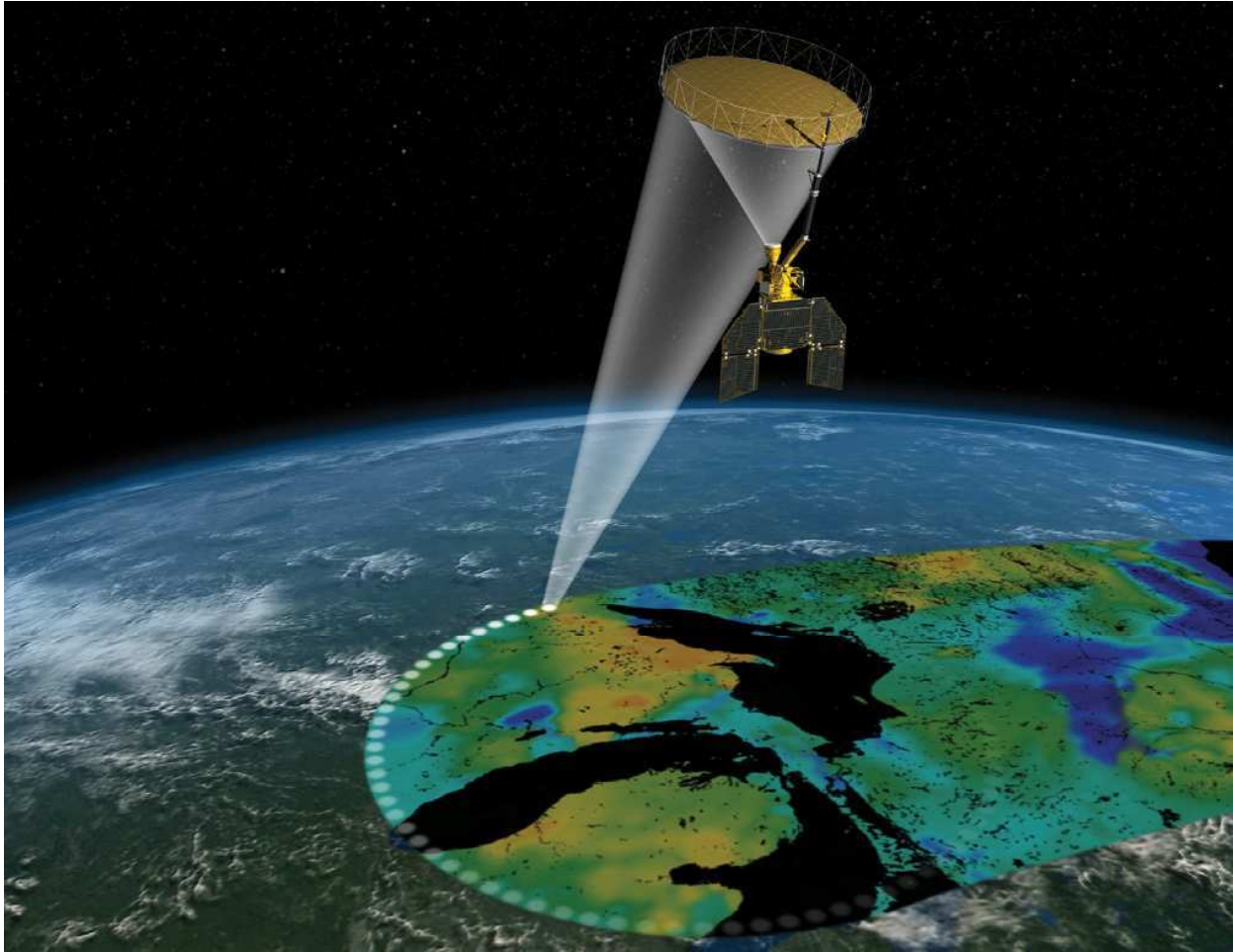


81

82 Fig. 8. Monthly soil moisture product (September 2010) expressed in $\text{m}^3 \text{m}^{-3}$. Note the wet
83 patches in Argentina or the receding Intertropical Convergence Zone influence in Sahel. Where
84 topography is too steep, RFI too important, vegetation too dense (tropical rain forest) or soils are
85 frozen /covered by snow, the retrievals are either not attempted or not represented.

86

87

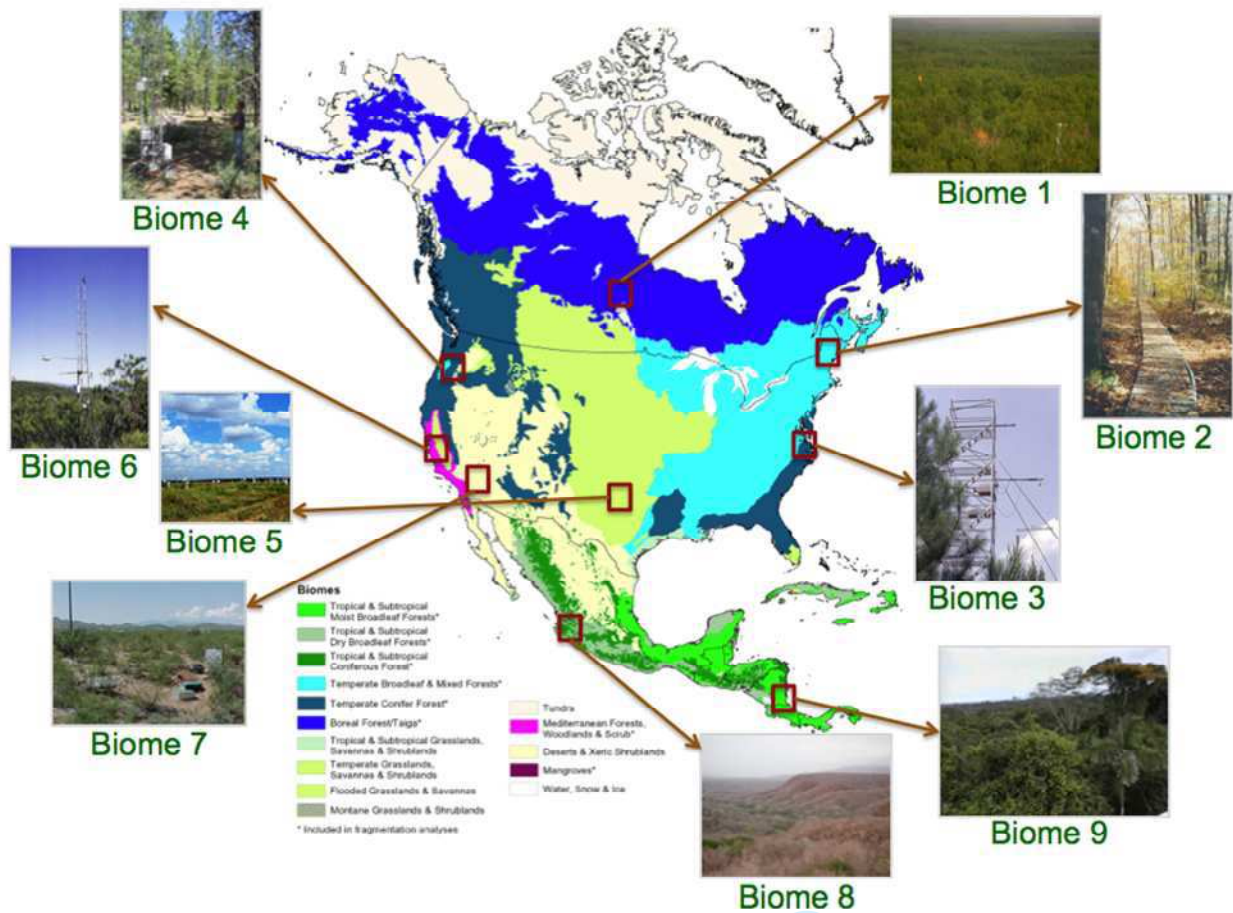


88

89 Fig. 9. Artist's view of the Soil Moisture Active Passive satellite.

90

91

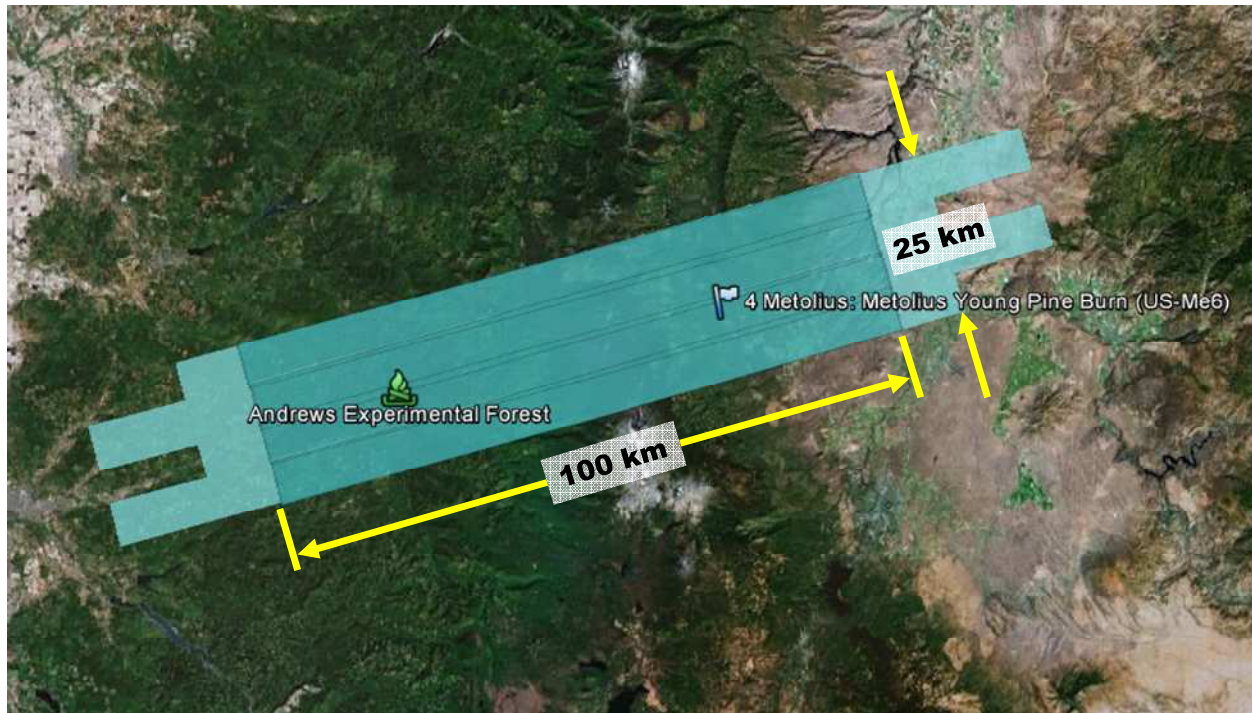


92

93 Fig. 10. Nine AirMOSS flux sites covering major distribution of vegetation types in North
 94 American biomes.

95

96



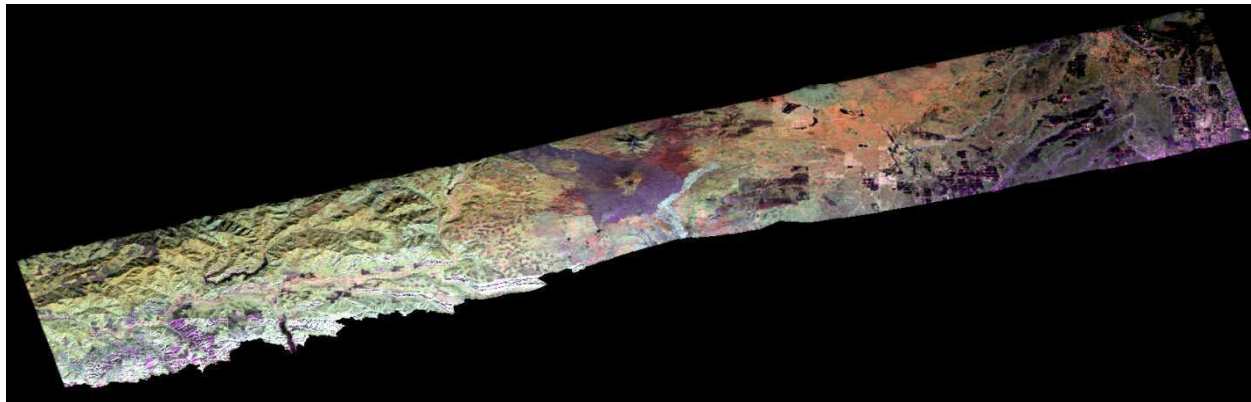
97

98 Fig. 11. AirMOSS flight path made up of four flight lines, Metolius flux site, Cascade

99 Mountains, Oregon.

100

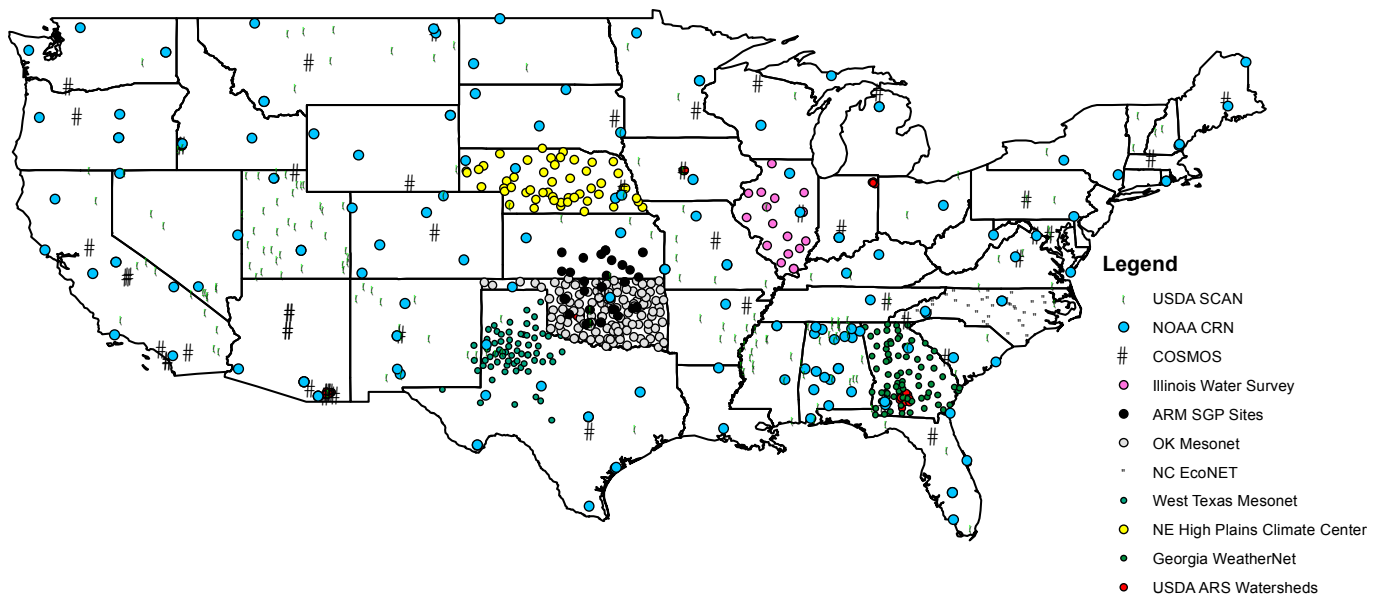
101



102

103 Fig. 12. AirMOSS three band (Red = HH, Green = HV, Blue = VV where H is horizontal
104 polarization and V is vertical polarization) raw data image showing the spatial variation of soil
105 moisture over the Metolius flux site, Cascade Mountains, Oregon along with soil roughness and
106 vegetation effects which have not yet been removed. Volcanic feature in center of image is
107 Black Butte cinder cone.

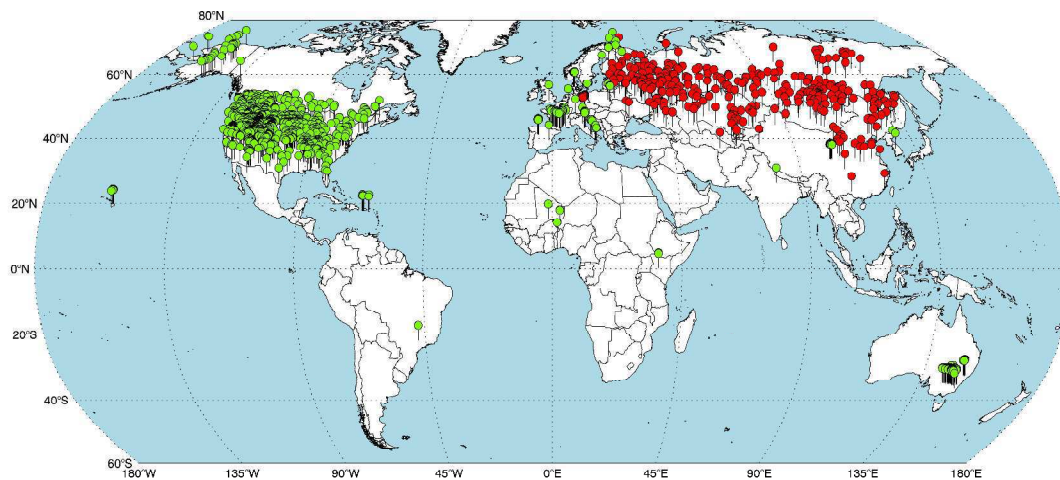
108



121

122 Fig. 13. In situ soil moisture monitoring sites across the Continental U.S.

123



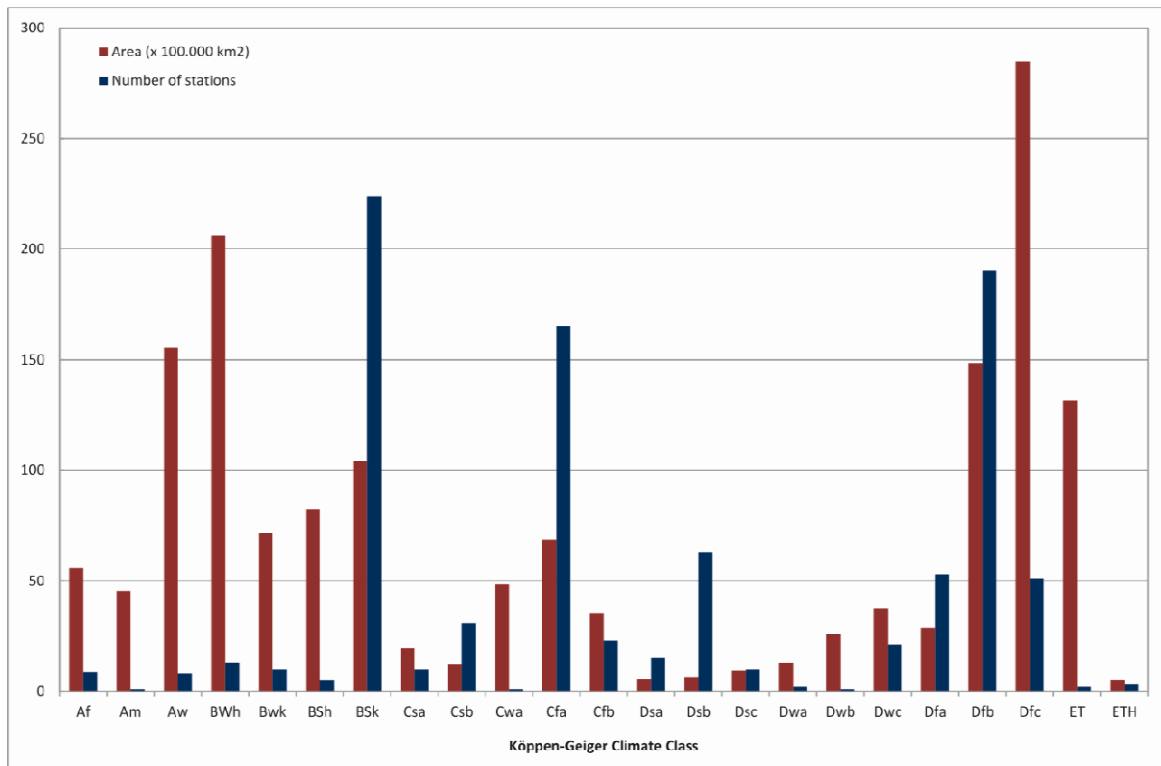
124

125

126 Fig. 14. Overview of soil moisture stations currently contained in the International Soil Moisture
127 Network (ISMN). Green dots show the stations that are still measuring soil moisture, red dots the
128 stations that were imported from the Global Soil Moisture Data Bank.

129

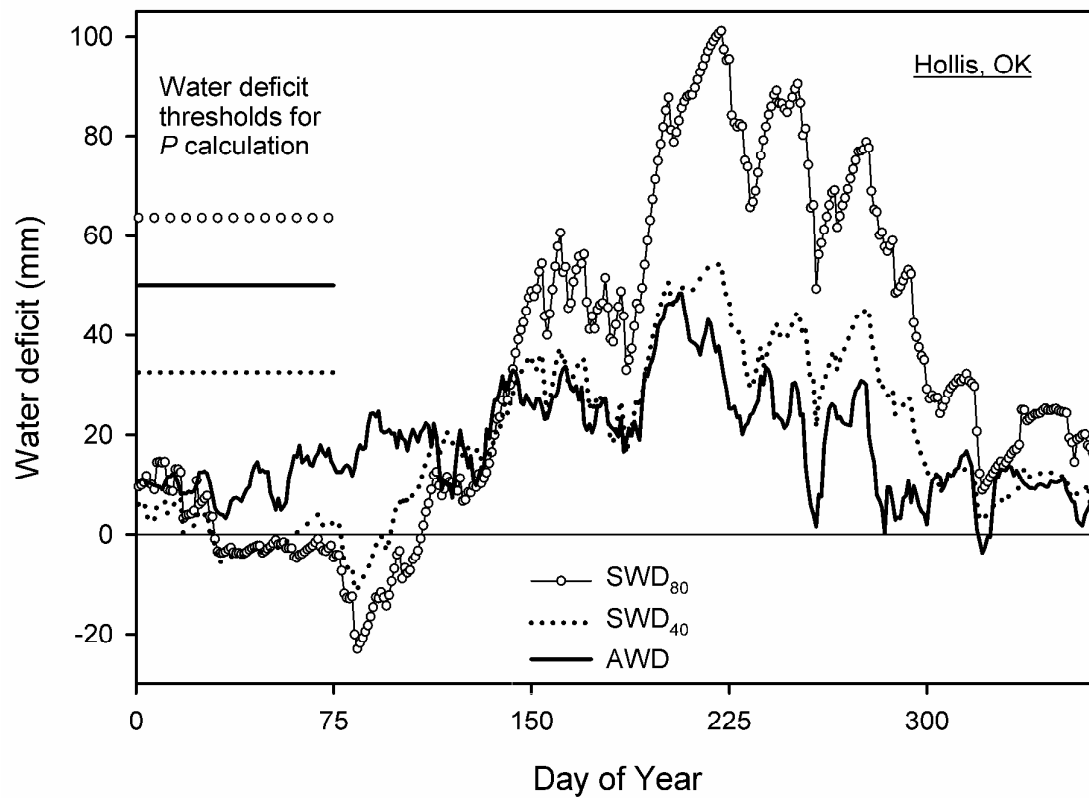
130



131

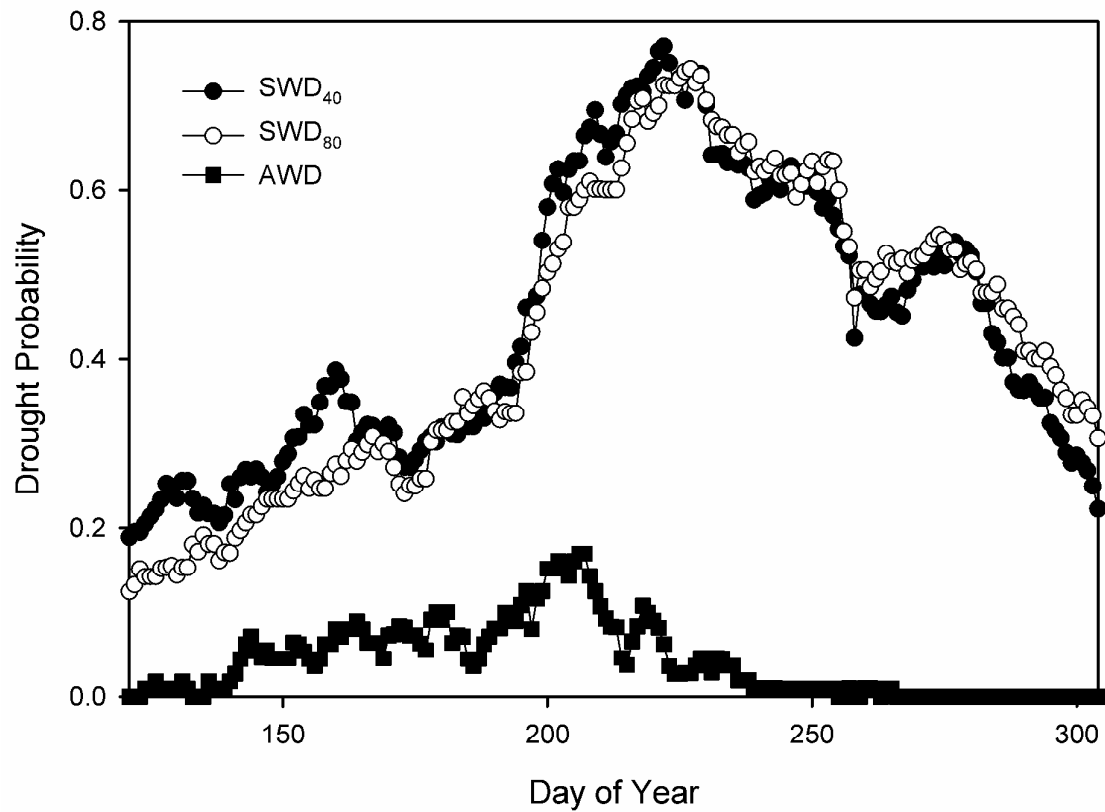
132 Fig. 15. Number of stations found within and area covered by the different Köppen Geiger

133 classes after Peel et al. (2007). For the class legend we refer to the original publication.



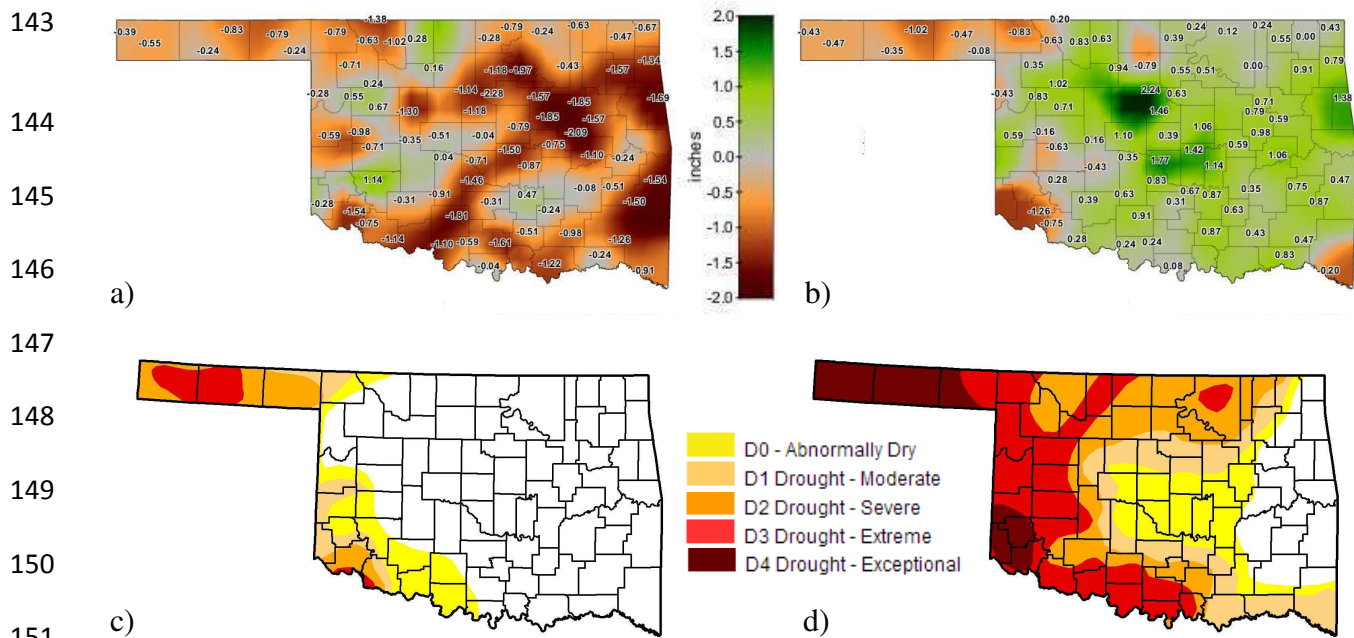
134

135 Fig. 16. Water deficit estimation by the atmospheric water deficit (AWD) method and soil water
 136 deficit methods for the 0- to 40- (SWD₄₀) and 0- to 80-cm depths (SWD₈₀), with corresponding
 137 water deficit thresholds. Averages of 15 yr for Hollis, OK. (Reproduced from Torres et al.,
 138 2013).



139

140 Fig. 17. Drought probabilities estimated by the AWD method and SWD methods for the 0- to 40-
141 (SWD₄₀) and 0- to 80-cm depths (SWD₈₀). Average for 15 yr and eight sites in Oklahoma for
142 May 1 through October 31. (Reproduced from Torres et al., 2013).

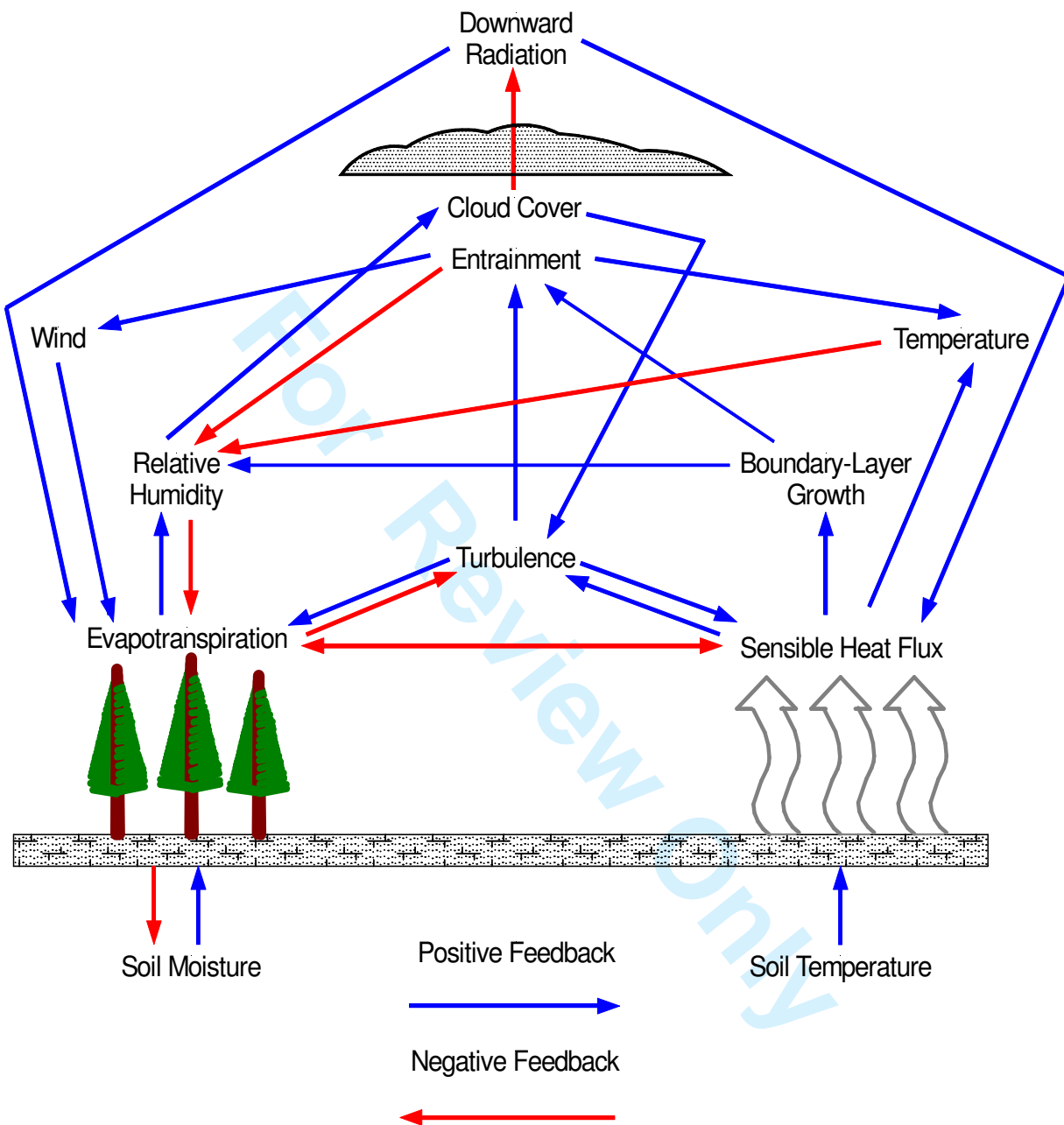


152

153 Fig. 18. Departure from average plant available water (PAW) for the 0-16 inch (40 cm) soil
 154 layer across Oklahoma for May 2012 (a) and May 2013 (b). US Drought Monitor maps for
 155 Oklahoma for May 15, 2012 (c) and May 14, 2013 (d). The PAW maps were adapted from the
 156 Oklahoma Mesonet Long-Term Averages Maps
 157 (http://www.mesonet.org/index.php/weather/mesonet_averages_maps). The Drought Monitor
 158 maps were adapted from the US Drought Monitor Archives
 159 (<http://droughtmonitor.unl.edu/archive.html>).

160

161

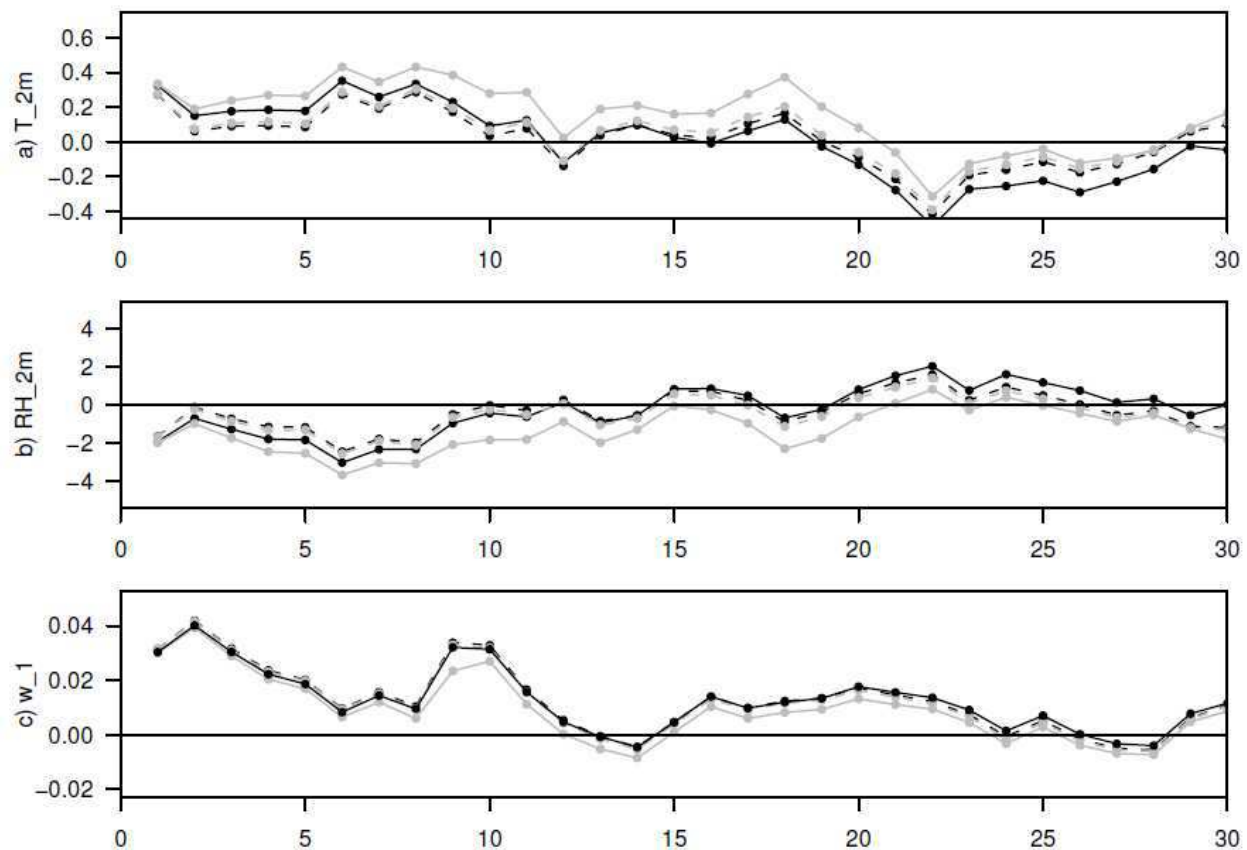


162

163 Fig. 19. Schematic of principle atmospheric boundary layer interactions with the land surface
 164 conditions (modified from Ek and Mahrt, 1994 and Ek, 2005). Note that two consecutive
 165 negative feedbacks result in a positive feedback.

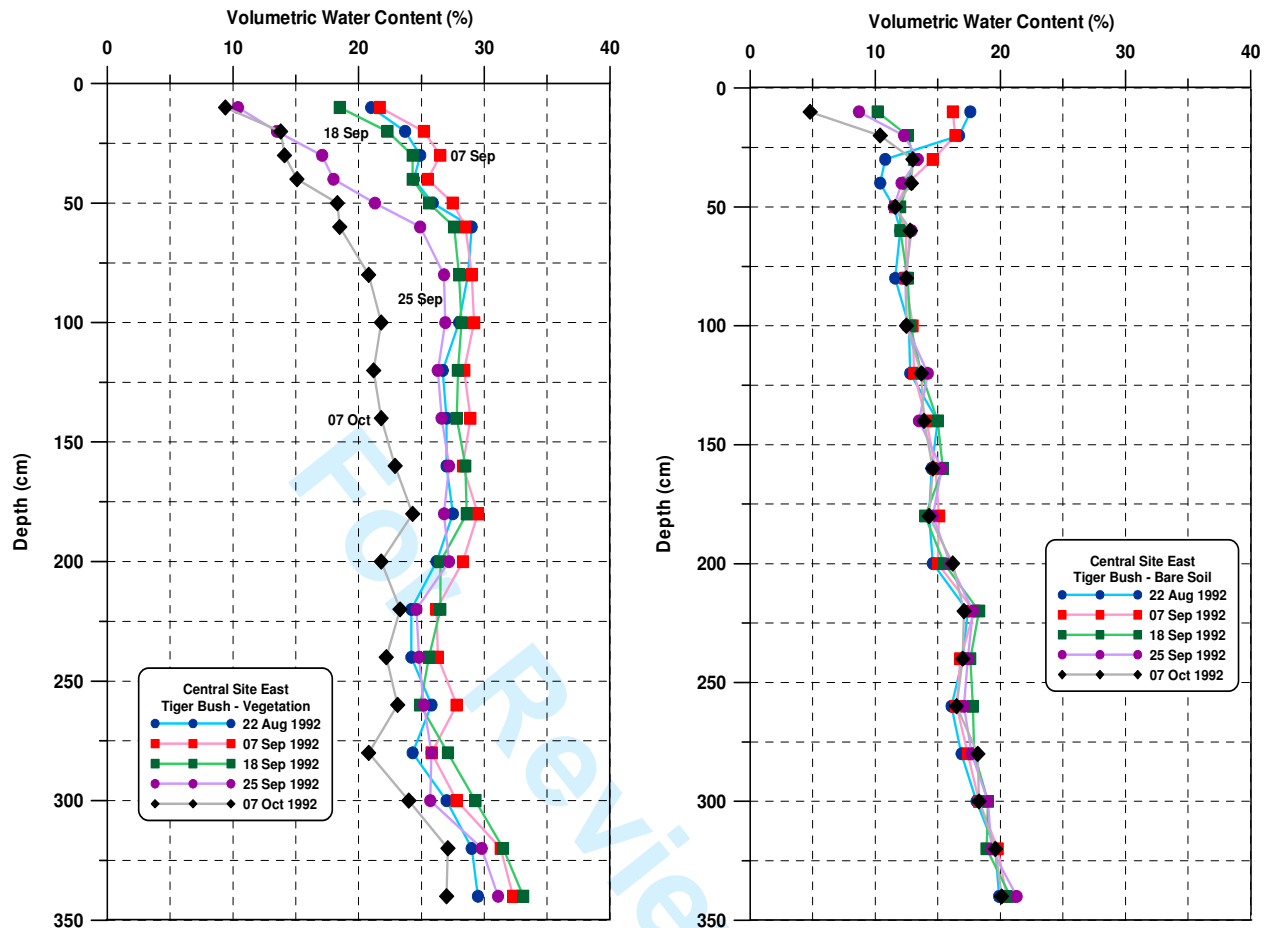
166

167



168

169 Fig. 20. Daily mean for each day in July 2006, averaged over Europe, of the observation minus
 170 6-hour forecast of a) screen-level temperature (K), b) screen-level relative humidity (%), and c)
 171 near-surface soil moisture ($\text{m}^3 \text{m}^{-3}$), from i) no assimilation (black, solid), and assimilation of ii)
 172 screen-level temperature and relative humidity (black, dashed), iii) AMSR-E near-surface soil
 173 moisture (grey, solid), and iv) both (grey, dashed) experiments. The assimilation was performed
 174 with an EKF using Météo -France's ISBA land surface model.



175

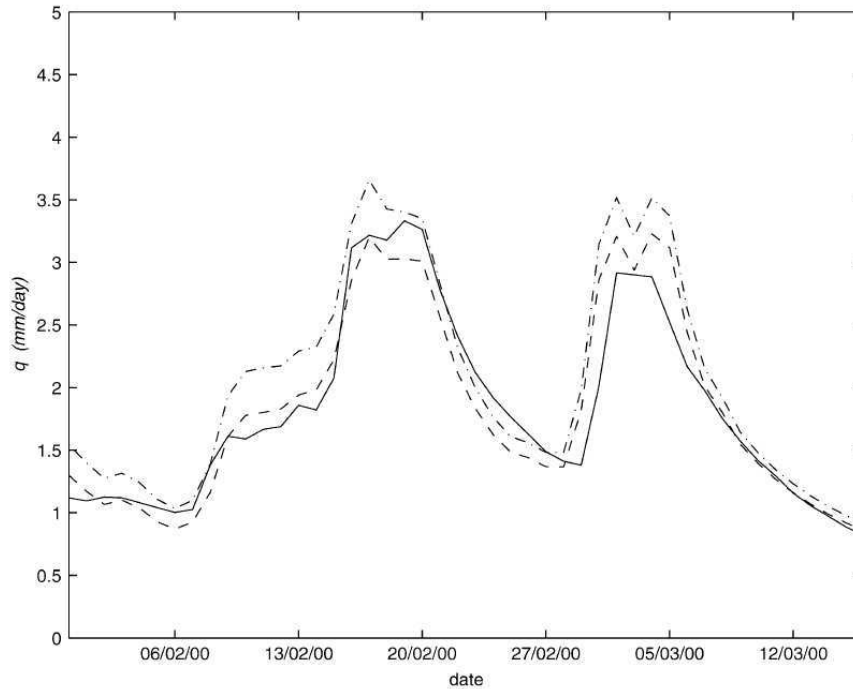
176

177 Fig. 21. Contrasting soil water depletion profiles from Central Site East-Tiger Bush, HAPEX-
 178 Sahel project a) vegetated section and b) bare soil section (modified from Cuenca et al., 1996).

179

180

181



182

183

184 Fig. 22. Time series of streamflow (q) at the outlet of the Serein catchment in the Seine river
185 basin in France for 1 Feb. 2000 to 15 March 2000. Solid line indicates measured streamflow,
186 dash dotted line indicates 1-day streamflow forecast without data assimilation, and dashed line
187 indicated 1-day streamflow forecast with assimilation of streamflow and in situ soil moisture
188 data. (Reproduced from Aubert et al., 2003).

189

190